Functional analysis of some yeast genes

El-Hassi, Mohamed F.

Functional Analysis of Some Yeast Genes

by

Mohamed F. El-Hassi

A thesis submitted to the Department of Biological Sciences, University of Durham in accordance with the requirements for the degree of Doctor of Philosophy

Department of Biological Sciences
University of Durham
U.K.

January 1997

DECLARATION

No part of this thesis has been previously submitted for any other degree in this or any other university. All work was performed by the auther, except where otherwise stated.

Mohamed F. El-Hassi

To the soul of my father

إهداء

إلى والدي المرحوم فرج صالح الحاسي

داعياً المولى سبحانه وتعالى أن يتغمده بواسع رحمته ويسكنه فسيح جناته.

إليك أبتي أهدي ثمرة دراستي التي يرجع الفضل في انجازها إلى الله ثم إلى ما كنت تقدمه من تضحيات ومعاناة طوال حياتك في سبيل تعليمي وتربيتي. لذا سأظل ما بقيت حياً أدعو لك ربي بأن يغفر لك ويدخلك جنةٍ عرضها السموات والأرض.

إلى والدتي الفاضلة أطال الله في عمرها والتي كان لدعائها الفضل بعد الله في تيسير دراستي.

وإلى أشقائي وشقيقاتي الذين كان لهم الفضل اكبير في تشجيعي ومساندتي أثناء دراستي.

الى زوجتي وأبنائي اللذين تحملوا مشاق الغربة من أجل هذه الدراسة وكان لدعمهم الأثر الكبير في انجازها.

Abstract

Mohamed F. El-Hassi B.Sc. MSc. (Garyounis University, Benghazi).

A functional analysis of some yeast genes.

A thesis submitted for a Ph.D. 1997.

A series of mutant strains of the yeast *Saccharomyces cerevisiae* that are sensitive to osmotic stress and also have a defect in vacuolar biogenesis have been isolated (M. Latterich, PhD Thesis 1992). The mutations that cause this pleiotropic phenotype are termed *ssv*, for salt sensitive vacuolar mutants. Complementation analysis has revealed that *ssv* mutations fall into one of 18 complementation groups. A MAP kinase related signal transduction pathway, termed the HOG pathway for High Osmolarity Glycerol, has been identified in yeast. This pathway senses osmotic stress and invokes the cellular response, one aspect of which is the accumulation of intracellular glycerol (Brewster *et. al.*, 1993). Mutations in the HOG pathway often cause an osmosensitive phenotype similar to that shown by *ssv* mutations.

This work sets out to characterise several *ssv* strains for defects in the HOG pathway. These strains were subjected to osmotic stress and the intracellular and extracellular glycerol determined and compared to control strains and conditions. Many of the strains showed reduced, or even elevated in one case, glycerol levels compared to wild-type strains. No correlation could be made between these glycerol levels and the activity of the rate-limiting enzyme, glycerol-3-phosphate dehydrogenase (GPDH) determined in an independent study. Transcription of the GPDH gene is under the control of the HOG pathway.

In a separate study, the nucleotide sequence of a short region of yeast chromosome VII was determined. Approximately 11,000 bases of DNA from the right sub-telomeric region was sequenced. Analysis of the DNA sequence showed four potential open reading frames. One of these encoded the *YOR1* gene and another a protein related to *PAU1*. The remaining two ORFs, termed ORF1 and ORF2, encoded potential proteins of unknown function.

Disruption cassettes containing the *LEU2* selectable marker were constructed for both ORF1 and ORF2. Successful disruption of ORF1 was achieved, but no viable transformants were ever recovered after attempted disruption of ORF2.. ORF1 gene knockouts are viable and show no observable phenotype under a range of growth conditions.

Subsequent analysis of ORF1 and ORF2 after the completion of the Yeast Genome Project, shows that both ORF1 and ORF2 are members of different sub-telomeric associated gene families. ORF2 encodes a putative Y' protein.

ACKNOWLEDGEMENTS

I would like to thank my supervisor Dr Martin D. Watson for his excellent supervision and continuous guidance during the course of this investigation. This work would never have been completed without his continuous encouragement.

Special thanks also due to Dr Bert Popping and Dr Elaine Broomfield for their practical assistance, advice and encouragement.

Thanks are also due to Caroline, Dr Charlie Shaw, Bill, Danita, Eleanor, Natasha, Karen, Matthew, Mark, Ralph, Vicky, Emma , Hassan, Ahmed and Al-Fifi for their assistance and cooperation. John Gilroy for oligonucleotide synthesis, Julia Bartley for automated DNA sequencing, and Terry Gibbons for technical advice and for keeping lab 6 running smoothly.

Thanks are due to the Secretary of Education in Libya for awarding me the scholarship which enabled me to carry this the work.

Thanks are also due to Audrey, Jean, Janice, Gillian and Mike Stacey for their secretarial and administrative assistance and cooperation.

Finally I would like to thank my Wife, children, brothers and sisters for their continued support throughout my education .

ABBREVIATIONS

A_{260} = Absorption at 260 nm

A_{280} = Absorption at 280 nm

ADP = Adenosine Diphosphate

Amp = Ampicillin

ATP = Adenosine triphosphate

BAC =Bacterial Artificial Chromosome

bp = base pair

cAMP = Adenosine 3',5'-Cyclic monophosphate

CPY = Carboxypeptidase Y

dH_2O = Distilled water.

DNA = Deoxyribonucleic acid

λDNA = Lambda DNA

dNTP = Deoxyribonucleoside triphosphate

EDTA = Ethylenediaminetetraacetic acid

EtOH= Ethanol

ExoIII = Exonuclease III

GK= Glycerokinase

GPDH = Glycerol-3-phosphate dehydrogenase

HCl = Hydrochloric acid

HOG = High Osmolarity Glycerol

K^+ = Potassium ion

Kb = Kilobase

KCl = Potassium Chloride

kDa = Kilodalton

LA =Luria Bertani Agar

LB = Luria Bertani Broth

$MgCl_2$ = Magnesium Chloride

MIPS = Martinsreider Institut für Protein Sequenzen

MLY = Martin Latterich Yeast

Na^+ = Sodium ion

NaCl = Sodium Chloride

NaI = Sodium Iodide

NaOH = Sodium Hydroxide

OD_{600} = Optical density (absorbance) at a wavelength of 600nm

PCR = Polymerase Chain Reaction

PDE = Phosphodiesterase

PK= Pyruvate kinase

r.p.m. = revolutions per minute

SDS = Sodium Dodecyl Sulphate

SSC = Saline Sodium Citrate

ssDNA = Single Stranded Salmon Sperm DNA

SSV= Salt Sensitive Vacuole

TAE = Tris-Acetate / EDTA

Tris = 2-Amino-2-(hydroxymethyl)-1,3-propanediol

UV = Ultraviolet

vps = Vacuolar protein sorting

X-Gal = 5-dibromo-4-chloro-3-indoylgalactoside

YMM = Yeast minimal medium

TABLE OF CONTENTS

LIST OF FIGURES

LIST OF TABLES

CHAPTER 1
INTRODUCTION

1.1 General Introduction.

The yeast *Saccharomyces cerevisiae* is recognised as an ideal eukaryotic microorganism for biological studies. Although yeast have greater genetic complexity than bacteria, they share many of the technical advantages that permitted rapid progress in the molecular genetics of prokaryotes and their viruses. Some of the properties that make yeast particularly suitable for biological studies include rapid growth, a budding pattern resulting in dispersed cells, the ease of replica plating and mutant isolation, a well-defined genetic system, and most importantly, a highly versatile DNA transformation system.

All organisms have several complex control mechanisms that allow growth under a range of physiological conditions. Yeast has proven to be a useful model organism for investigating growth responses to different environmental conditions. The aim of the first part of this study is to investigate the cellular response of *Saccharomyces cerevisiae* to osmotic stress. The second part of this study describes the characterisation of part of chromosome VII that was carried out as part of the world-wide effort to sequence the yeast genome.

1.2 General responses to growth under stress conditions.

In response to external stresses such as thermal, nutritional, chemical, oxygen and osmotic a series of stress-response proteins are synthesised. Different but overlapping subsets of these proteins are induced by different stressing agents. Many of these proteins are found in all organisms from bacteria to higher plants and animals.

The best characterised of these stress responses is that for heat-shock which is an inducible system of all living cells. The response to heat-shock is temporary with recovery occurring within a few hours after stress exposure. Furthermore the heat shock response is inhibited in mutants defective in RNA synthesis (Mager and Ferreira,1993). Heat-shock proteins have been implicated in all major growth-related processes such as cell division, DNA synthesis, transcription, translation, protein folding and transport. Induction of heat-shock proteins causes an increased capacity for the cell to resist lethal temperature (an increased thermotolerance) and also causes cross-tolerance to other stresses. The analysis of heat-shock proteins in *Saccharomyces cerevisiae* has so far revealed only a minority of the total proteins involved in this response (Piper,1993).(Fig 1.1).

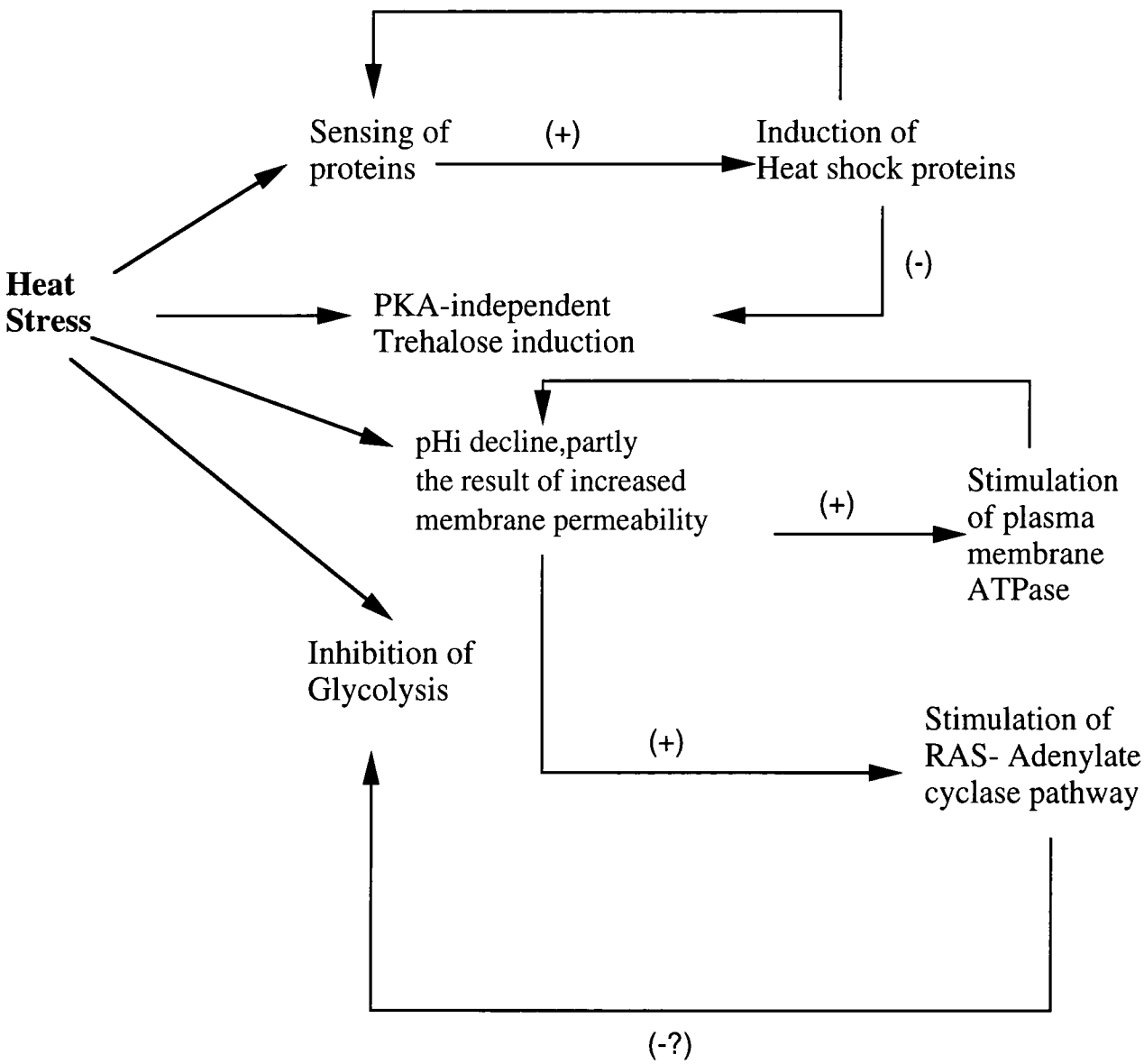

Fig 1.1. The effect of heat stress on cells of *Saccharomyces cerevisiae* (After Piper,1993)

The main classes of stress response proteins are the 25kDa, the 70kDa and the 90kDa heat-shock proteins. The yeast *Saccharomyces cerevisiae* for example, contains eight hsp70-related genes, some of which are transcribed under all conditions whereas the others are expressed only when the cells are exposed to an elevated temperature or other stressed action (Alberts et al, 1989). The hsp70 proteins are involved in a number of cellular processes where protein folding takes place. They facilitate translocation of polypeptides across the endoplasmic reticulum and mitochondrial membrane (Mager and Ferreira,1993). In an ATP driven event they unfold proteins on the cytosolic side and aid refolding on the lumenal side. Thermal stress causes denaturation of proteins. The hsp70 proteins bind to aberrant misfolded proteins and in an ATP dependent manner cause their refolding into a correct conformation.

The low molecular weight hsp proteins of 25kDa are involved in ubiquitin metabolism (Hochstrasser, 1995; Varshavsky, 1992). These include ubiquitin itself, which is covalently attached to lysine residues of misfolded, aberrant or short half-life proteins, and the ubiquitin conjugating enzymes (UBCs). The UBCs have overlapping substrate specificities and cause the ligation of ubiquitin to the target proteins. There are more than 10 UBCs in yeast. The ubiquitinated proteins are then degraded through the action of the 26S proteosome. The ubiquitin is released from the degraded polypeptides by ubiquitin processing proteases (UBPs) of which there at least 14 in yeast.

1.3. Osmohomeostasis

When a cell culture of *Saccharomyces cerevisiae* is transferred into high osmotic strength medium (1.4M NaCl) there is a drop in cell viability which is less severe if the cells are pre-treated in 0.7M NaCl (Blomberg and Adler, 1989) . Adaptation to osmotic stress is associated with an accumulation of glycerol as a compatible osmolyte. During osmotic conditioning with 0.7M NaCl the rate of formation of glycerol is increased (Blomberg and Adler, 1989) . The activities of glycerol-3-phosphate dehydrogenase (GPDH) and phosphofructokinase are elevated in cells subjected to osmotic stress (Edgley and Brown, 1983) allowing a shift in the metabolic flux to favour glycerol production. The glycerol accumulation in response to osmotic stress will be discussed in more detail in section 1.4.2.

Before yeast cells can adjust their intracellular glycerol levels they must first recognise a change in extracellular osmolarity and initiate signals that cause the cell to respond to that change. Signal transduction in response to salt stress occurs through the High Osmolarity Glycerol response pathway (Brewster *et al.*, 1993) and other less well defined pathways.

The HOG pathway enhances intracellular glycerol concentration by increasing the transcription of GPDH (Albertyn *et al.*, 1994) .

To maintain osmohomeostasis, yeast must also be able to respond to a decrease in extracellular osmolarity. Mutants of the PKC1 (protein kinase C1, or C-kinase) pathway have previously been described as having a cell lysis defect which can be stabilised by a high osmolarity medium (Lee and Levin, 1992; Levin and Bartlett-Heubusch, 1992; Paravicini *et al.*, 1992) suggesting a role for the pathway in cell integrity. There is now evidence that the PKC1 pathway is involved in recognising decreases in extracellular osmolarity (Davenport *et al.*, 1995) and thus acts as a second osmosensing signal transduction pathway. The role of the HOG pathway and the PKC1 pathway in maintaining osmohomeostasis will be discussed more fully in section 1.4.

An important function in osmohomeostasis is removing toxic ions such as Na^+ from the cytoplasm. A gene with enhanced activity during salt stress is the *ENA1* gene (Marquez and Serrano, 1996) . *ENA1* is the first gene of a tandem array encoding ion transporters of the P-type ATPase family (Haro *et al.*, 1991; Garciadeblas *et al.*, 1993). Ena1p can function as either a Li^+ or a Na^+ transporter and is particularly important for excluding Na^+ ions during salt stress. Although the *ENA* genes are partially functionally redundant, the Δ*ena1* mutation confers osmosensitivity suggesting a particular role for the *ENA1* gene in recovery from osmotic shock. Signalling through the HOG pathway enhances *ENA1* transcription at 0.3M NaCl but at higher salt concentrations, e.g. 0.8M, *ENA1* transcription can be enhanced even in the absence of functional Hog1p (Marquez and Serrano, 1996) . The phosphatase calcineurin was found to be necessary for this HOG-independent response. The phosphatases Ppz1p and Ppz2p also have an effect on salt exclusion (Posas *et al.*, 1995) . The Δ*ppz1* mutation increases tolerance to Na^+ and Li^+ ions and the expression of *ENA1* is enhanced in Δ*ppz1* Δ*ppz2* mutant cells. Thus Ppz1p and Ppz2p limit salt exclusion through effects on *ENA1*.

One approach to the study of osmohomeostasis is the investigation of genes which, when overexpressed, confer a greater osmotolerance to a strain. It was using this approach that the *HAL* genes (for halotolerance) were characterised. *HAL1* is induced by osmotic stress and the Δ*hal1* strain has a reduced salt tolerance (Gaxiola *et al.*, 1992) . Overexpression of *HAL1* increases K^+ accumulation suggesting that Hal1p may interact with the K^+ transport machinery. *HAL3* is also involved in ion transport but its effects are specific for Na^+ and Li^+ (Ferrando *et al.*, 1995) . *HAL3* overexpression results in increased expression of *ENA1* and, conversely, *ENA1* overexpression can suppress the osmosensitivity of Δ*hal3*. The exact roles

of Hal1p and Hal3p in ion homeostasis have yet to be elucidated. *HAL2* is apparently unrelated to *HAL1* and *HAL3* as it encodes an inositol phosphatase with a role in methionine biosynthesis (Glaser *et al.*, 1993) . The ability of this gene, when overexpressed, to confer a greater osmotolerance suggests that the methionine biosynthetic machinery may be particularly sensitive to fluctuations in osmolarity. Supplementing the growth media with methionine can have the same growth effect as overexpression of *HAL2* for salt-stressed yeast.

A mutant strain has now been described which has an enhanced salt tolerance (Gaxiola *et al.*, 1996) . The study of this strain underlines again the importance of intracellular cation concentrations to osmohomeostasis. This strain has half as much Na^+ and 60% more K^+ than its 'wild-type' parental strain and thus a greatly reduced Na^+/K^+ ratio. This improves its osmotolerance as it withstands concentrations of 2M NaCl.

A role for actin in osmohomeostasis was proposed after the discovery that increasing the osmotic strength of the medium decreased the temperature sensitivity of a collection of actin mutants (Novick and Botstein, 1985) . On exposure to high osmotic stress, the actin cytoskeleton undergoes a rapid and reversible disassembly (Chowdhury *et al.*, 1992) . This disassembly is most obvious in cells with small buds or in cells about to bud and occurs within the first minute of an increase in extracellular osmolarity. Reassembly of the cytoskeleton during recovery from osmotic shock was found to require an actin binding protein, Rah3p (Chowdhury *et al.*, 1992) .

Many mutations causing defects in vacuolar protein sorting also cause osmosensitivity (Banta *et al.*, 1988; Latterich, 1992) . The initial response to increased osmolarity may involve a flow of solute from the vacuole (as suggested by Mager and Varela (1993)). The vacuole may also play a role in osmohomeostasis by reducing the cytoplasmic Na^+ concentration via the Na^+/H^+ antiporter (as discussed by Haro *et al.*, (1993)). The role of the vacuole in osmohomeostasis will be discussed more fully in section 1.5.

Some of the reactions in osmohomeostasis may form part of the general stress response. For example the cytoplasmic catalase T gene (*CTT1*) is under the control of many stress response pathways, including the HOG pathway, which act through an upstream activation sequence named STRE (for stress response element) (Marchler *et al.*, 1993; Schuller *et al.*, 1994) . Induction of certain heat shock genes has also been observed during salt stress (e.g. Hsp12p; Hirayama *et al.*, 1995; Varela *et al.*, 1992) . Ubiquitin metabolism may play a role during salt stress as part of a general stress response.

The ubiquitination pathway is important for stress-induced proteolysis (see Hilt and Wolf, 1992 for a review). The polyubiquitin gene, *UBI4*, is positively regulated by heat stress and is essential for resistance to high temperature and nitrogen starvation (Finley *et al.*, 1987) . In such conditions it is likely that *UBI4* provides a valuable pool of ubiquitin to allow a rapid turnover of proteins - either to remove heat-damaged proteins or to provide a means for altered metabolism. The nature of the ubiquitin-ubiquitin linkage is important to the stress response as mutations that disrupt a particular type of link are no longer able to survive heat and canavanine stress (Arnason and Ellison, 1994) . Although a role for ubiquitin processing in response to osmotic stress is not well characterised, the *DOA4* gene, which encodes one of many ubiquitin-processing enzymes (Papa and Hochstrasser, 1993) was isolated through its ability to complement a mutation conferring salt-sensitivity (Latterich, 1992; R. Baker, personal communication). The *DOA4* gene has since been implicated in the co-ordination of DNA replication to produce one copy of the genome per cell cycle (Singer *et al.*, 1996) . The effects of *doa4* deletion seem to be two-fold. The temperature-sensitivity of a *doa4* strain can be rescued by overexpression of *UBI4* showing the importance of Doa4p in maintaining a free ubiquitin pool. However, the effects on DNA replication are not suppressed by *UBI4* overexpression indicating a separate role for Doa4p. Singer *et al* (1996) did not examine the effects of overexpression of *UBI4* on the salt-sensitivity of the D*doa4* strain so it is not yet known if it is the need for a free ubiquitin pool during stress conditions that links osmohomeostasis to the ubiquitin pathway.

The involvement of all of the above cell processes in osmohomeostasis underlines the complexity of the osmostress response. Osmosensitivity can be indicative of a defect in one of many processes, not restricted to osmosensing signal transduction or glycerol accumulation. The transcription levels of many proteins can be altered with salt stress (see (Mager and Varela, 1993) for a review) and the study of genes with enhanced or depressed activities in changing osmotic conditions will lead to a greater understanding of osmohomeostasis.

1.4. The High Osmolarity Glycerol (HOG) Response Pathway

1.4.1. Osmosensing signal transduction

An increase in intracellular glycerol concentration in response to an increase in extracellular osmolarity requires signalling through the High Osmolarity Glycerol (HOG) response

pathway (Brewster *et al.*, 1993) . Two components of the pathway, *HOG1* and *HOG4*, were identified by complementation cloning of osmosensitive mutants which showed a reduced glycerol accumulation after addition of salt (Brewster *et al.*, 1993) . Sequence analysis revealed that *HOG1* is a member of the MAP (mitogen-activated protein) kinase (MAPK) family with significant sequence homology to the pheromone response pathway gene, *FUS3* (Elion *et al.*, 1990) . It was discovered that *HOG4* is identical to *PBS2* and is related to MAP kinase kinases (Boguslawski and Polazzi, 1987) . A linear kinase cascade was proposed based on the observation that Hog1p is tyrosine-phosphorylated in response to salt stress and that this phosphorylation requires functional Pbs2p (Brewster *et al.*, 1993) .

When the HOG pathway was first described (Brewster *et al.*, 1993) , little was known about other components of the pathway. The discovery of an upstream regulator came through the study of tyrosine phosphatases (Maeda *et al.*, 1994) . Maeda *et al* (1994) studied mutants that require *PTP2* tyrosine phosphatase for survival. One gene identified in their study was identical to the previously described *SLN1* gene (Ota and Varshavsky, 1993) . *SLN1* has homology to bacterial two-component regulators that are involved in a variety of cellular processes, including osmoregulation . Sln1p consists of a histidine kinase domain and a potential extracellular sensor domain. Maeda *et al.* (1994) demonstrated that *SLN1* is an upstream regulator of the HOG pathway by using recessive mutations of *hog1* or *pbs2* to suppress Δ*sln1* lethality. This implies that the deletion of *SLN1* causes inappropriate signalling through the HOG pathway, and therefore that *SLN1* is a negative regulator of the HOG pathway. It is likely that the requirement for overexpression of *PTP2* to suppress the Δ*sln1* mutation is for dephosphorylation of the inappropriately activated Hog1p and thus down-regulation of the response.

The study of recessive suppressors of the Δ*sln1* mutation led to the identification of *SSK1* (for suppressor of sensor kinase). Ssk1p has homology to the receiver domain of bacterial response regulator molecules. Expression of *SSK1* in the absence of *SLN1* induces tyrosine phosphorylation of Hog1p. Ssk1p is probably unphosphorylated in Δ*sln1* cells suggesting unphosphorylated Ssk1p is the active form (Maeda *et al.*, 1994) . Although *SSK1* clearly has a role in the HOG signal transduction pathway, the Δ*ssk1* mutation does not itself confer osmosensitivity. This implies that other receptors for osmotic stress also feed into the HOG pathway.

In a separate report, Maeda *et al.* (1995) describe another *ssk* gene, *SSK2*, which has homology to MAPK kinase kinases. Ssk2p is not solely responsible for activation of the HOG pathway and a related gene, *SSK22* was isolated by DNA hybridisation techniques.

Deletion of the N-terminal non-catalytic domain of either *SSK2* or *SSK22* (leading to their constitutive activation) results in tyrosine phosphorylation of Hog1p in a Pbs2p-dependent manner. Such N-terminal deletions are lethal, with lethality rescued by deletions in either *PBS2* or *HOG1* but not *SSK1*. Two-hybrid analysis revealed that both Ssk2p and Ssk22p can interact with Ssk1p. On the basis of this evidence it was suggested that Ssk2p and Ssk22p act between Ssk1p and Pbs2p in the signal transduction pathway.

Ssk2p and Ssk22p are not however the only means of inducing tyrosine phosphorylation of Hog1p and Δ*ssk2* Δ*ssk22* double mutants are not osmosensitive (Maeda *et al.*, 1995) . A search for a mutagenized gene that would confer osmosensitivity in a Δ*ssk2* Δ*ssk22* strain led to identification of *SHO1* (for synthetic, high-osmolarity sensitive). Sequence analysis of *SHO1* suggests that it encodes four transmembrane segments and an SH3-domain. SH3-domains have been described as important for protein interactions in a variety of processes (see Cohen *et al.*, 1995 for a review). Two-hybrid analysis showed that the SH3-domain of Sho1p can interact with the proline-rich domain of Pbs2p. This interaction does not appear to require Ssk2p or Ssk22p suggesting Pbs2p can receive signals from two different branches of the HOG pathway (Maeda *et al.*, 1995) . A model for osmosensing signal transduction based on a scheme proposed by Maeda *et al.* (1995) is shown in figure 1.2.

Although the HOG pathway is required for the induction of various genes involved in the osmostress response, for example *GPD1* (Albertyn *et al.*, 1994) and *CTT1* (Schuller *et al.*, 1994) , the downstream targets of Hog1p which mediate this induction have yet to be discovered.

The HOG pathway is one of several MAP kinase pathways described for the yeast *Saccharomyces cerevisiae* (see Herskowitz, 1995 for a review). These pathways all have a central core of kinases which act in a cascade to transduce a signal. The MAP kinase itself is phosphorylated by MAP kinase kinase (MAPKK, also known as ERK kinase, or MEK) which is phosphorylated by MAPKK kinase (MAPKKK, also known as MERK, or MEKK).

The pheromone signalling pathway is a particularly well-characterised MAP kinase pathway in *Saccharomyces cerevisiae*. The pheromone binds to its receptor and consequently activates a trimeric G protein which causes a series of phosphorylation events (Zhou *et al.*, 1993) . Ste11p (a MAPKKK homologue) phosphorylates, and thereby activates, Ste7p (a MAPKK homologue; Teague *et al.*, 1986) which in turn phosphorylates the MAPK homologues, Fus3p and Kss1p (Errede *et al.*, 1993; Neiman and Herskowitz, 1994) . Fus3p activation and

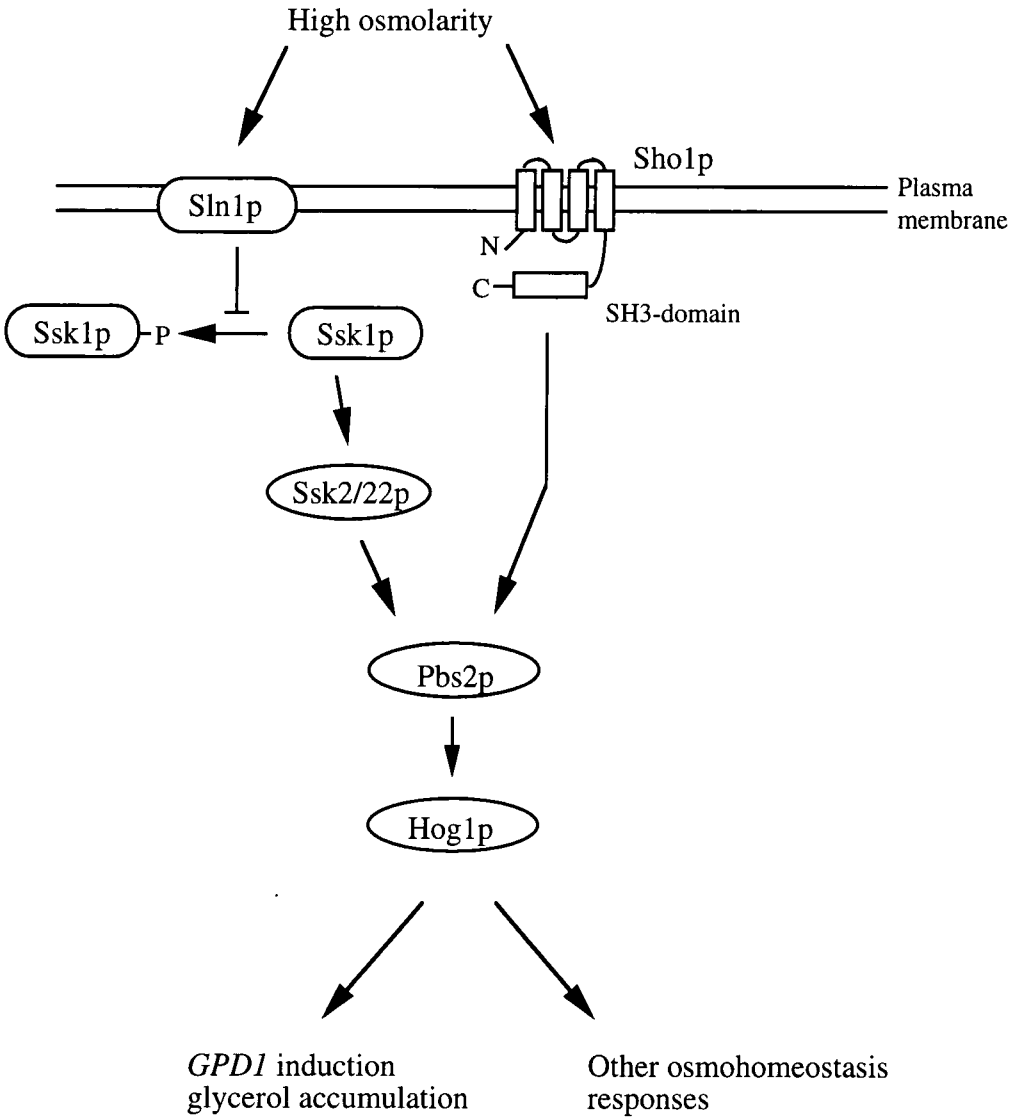

Fig 1.2 The HOG pathway
Increasing osmolarity causes tyrosine phosphorylation of Hogl p by Pbs. Pbs2p activation requires either phosphorylation by the Ssk2/22p kinases or interaction with the SH3-domain of Sholp. Ssk2/22p is itself activated by unphosphorylated Sskl p. Sskl p is phosphorylated by Sln lp in the absence of osmotic stress.

the cellular response to pheromone require Ste11p- and Ste7p-dependent phosphorylation of Fus3p on both threonine and tyrosine residues (Gartner *et al.*, 1992) . Fus3p phosphorylates many components involved in the mating response, including Far1p (which results in cell cycle arrest) and the transcription factor Ste12p (Elion *et al.*, 1993) .

Ste11p, Ste7p and Fus3p (or Kss1p) are brought into contact with each other by Ste5p (Choi *et al.*, 1994; Marcus *et al.*, 1994; Printen and Sprague, 1994) which acts as a scaffold for protein interaction. It is possible that Ste5p regulates the actions of the kinases it interacts with to prevent inappropriate signalling through the pathway and inappropriate cross-reactions with other MAP kinase cascades (Printen and Sprague, 1994) . This would explain the observation that purified Ste11p is constitutively active *in vitro* and yet *in vivo* is apparently only involved in signalling in response to pheromone (Neiman and Herskowitz, 1994) . However, mutational activation of Ste5p can constitutively activate the pheromone response pathway but cannot suppress mutations in *STE7*, *STE11*, *FUS3* or *KSS1* suggesting that Ste5p also acts upstream of Ste11p in the cascade (Hasson *et al.*, 1994) . This pathway is summarised in figure 1.3.

Other MAP kinase pathways include the PKC1 pathway. As mentioned in section 1.3, this pathway is involved in cell integrity and growth. Mutations in components of the PKC1 pathway lead to a cell lysis defect which is recovered by adding osmotic stabilisers to the medium (Lee and Levin, 1992; Levin and Bartlett-Heubusch, 1992; Paravicini *et al.*, 1992) . Pkc1p regulates β-glucanase activity linking the PKC1 pathway directly with cell wall maintenance (Shimizu *et al.*, 1994) . The PKC1 pathway has also been discovered to be an osmosensing signal transduction pathway but in contrast to the HOG pathway it responds to a *decrease* in extracellular osmolarity (Davenport *et al.*, 1995) .

MAPK, MAPKK and MAPKKK homologues in the PKC1 pathway were identified by their ability, when mutationally activated or present in multicopy, to overcome the requirement for *PKC1*. *BCK1* encodes a MAPKKK homologue with 45% identity to Ste11p (Lee and Levin, 1992) . The functionally redundant Mkk1p and Mkk2p kinases act downstream of Bck1p. *MKK1* and *MKK2* are highly homologous to each other and also share homology with the MAPKK homologue *STE7* (Irie *et al.*, 1993) . The MAP kinase homologue, Mpk1p, was found to be the previously identified Slt2p and Δ*mpk1* confers the cell lysis defect characteristic of mutations in other components of the pathway (Lee *et al.*, 1993) . Genetic evidence confirms that the order of activity in the pathway is Pkc1p -> Bck1p -> Mkk1p/Mkk2p -> Mpk1p (Irie *et al.*, 1993; Watanabe *et al.*, 1995).

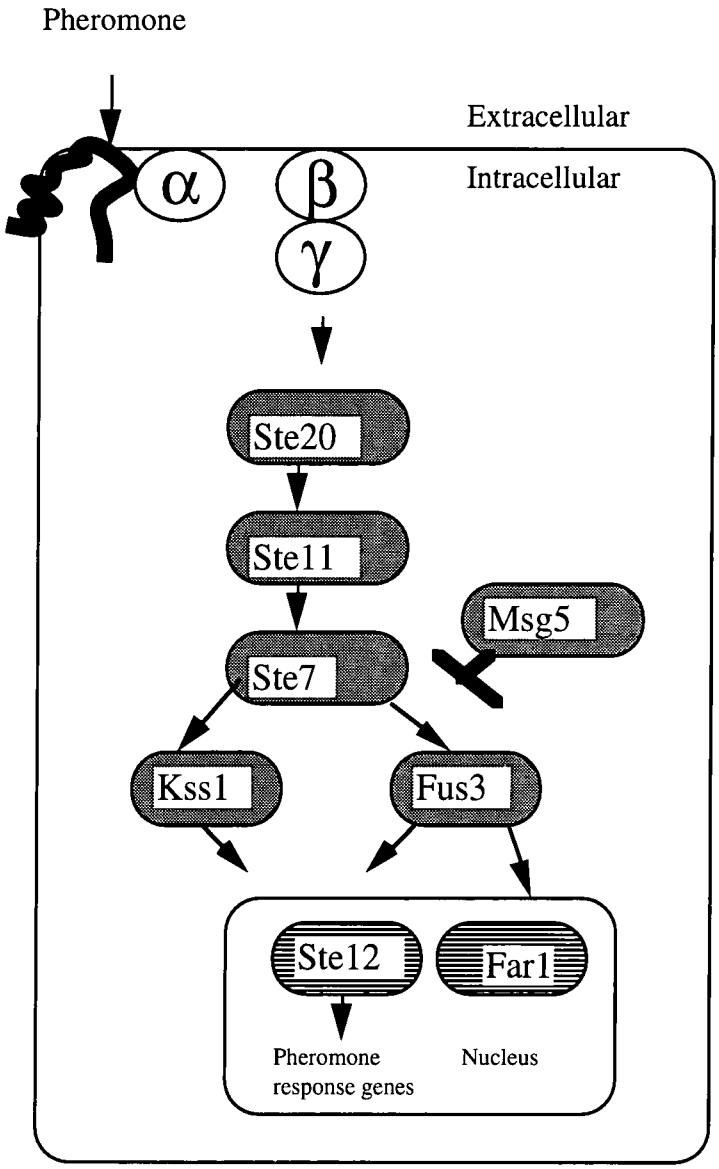

Fig. 1.3 Pheromone response signal transduction pathway components. Pheromone binds a cell surface receptor, causing dissociation of a heterotrimeric G protein to generate an activated complex. The signal is transmitted through a series of kinases, activating the transcription of pheromone-response genes through Ste12p and causing cell cycle arrest through Far1p. Protein interactions that result in positive activation are indicated by arrows and the tined bar indicates inhibition. The molecular connection between βγ and Ste20p is not known. (After Schultz *et al*, 1995).

The two phosphatases Ppz1p and Ppz2p are required for the maintenance of cell size and integrity in response to hypo-osmotic stress (Hughes *et al.*, 1993) and mutations in *PPZ1* and *PPZ2* confer a cell lysis defect with similarities to defects in the PKC1 pathway. Overexpression of *PPZ1* or *PPZ2* can suppress *mpk1* deletion (Lee *et al.*, 1993) suggesting a direct relationship between the phosphatases and the PKC1 pathway. The Msg5p phosphatase can also interact with the PKC1 pathway as overexpression of *MSG5* can suppress the growth defect of a constitutively active *MKK1* allele (Watanabe *et al.*, 1995) . How the dephosphorylation by Ppz1/2p or Msg5p can act co-operatively with, or even by-pass the need for, the phosphorylation events of the PKC1 pathway is not yet known.

Two downstream targets of Mpk1p, the DNA-binding proteins Nhp6Ap and Nhp6Bp, have been identified by their ability to act as high copy suppressors of the Δ*mkk1* mutation (Costigan *et al.*, 1994) . There is no evidence for a direct interaction between Mpk1p and Nhp6p suggesting more components of the pathway are yet to be revealed. Δ*nhp6A/B* strains display very similar but less severe phenotypes compared to the Δ*mpk1* mutant (Costigan *et al.*, 1994) which implies that activated Mpk1p may also elicit Nhp6p-independent functions. The DNA binding protein Rlm1p may be involved in such Nhp6p-independent functions as mutations in *RLM1* can suppress a constitutively active *MKK1* allele (Watanabe *et al.*, 1995) . As was the case for the Δ*nhp6* strain, Δ*rlm1* confers similar but less severe growth phenotypes than Δ*bck1* or Δ*mpk1*.

Figure 1.4 shows the pattern of components of these signal transduction pathways in relation to a basic MAP kinase model.

1.4.2. Glycerol accumulation

Cytoplasmic GPDH activity is elevated during salt stress (Andre *et al.*, 1991; Blomberg and Adler, 1989) and recovery from salt stress requires protein synthesis (Albertyn *et al.*, 1994a; Blomberg and Adler, 1989) . The transcription of the gene *GPD1*, encoding cytoplasmic GPDH, is increased in response to salt stress in a Hog1p-dependent manner and Δ*gpd1* cells are osmosensitive (Albertyn *et al.*, 1994) . Δ*gpd1* cells show some residual glycerol accumulation and a second gene, *GPD2*, encoding an isoenzyme of cytoplasmic GPDH has been identified (Eriksson *et al.*, 1995) . *GPD2* is not induced by salt stress and Δ*gpd2* does not confer osmosensitivity.

GPDH uses the substrate dihydroxyacetone phosphate (DHAP) to produce glycerol-3-phosphate which is then converted to glycerol (Gancedo *et al.*, 1968) . This reaction is in

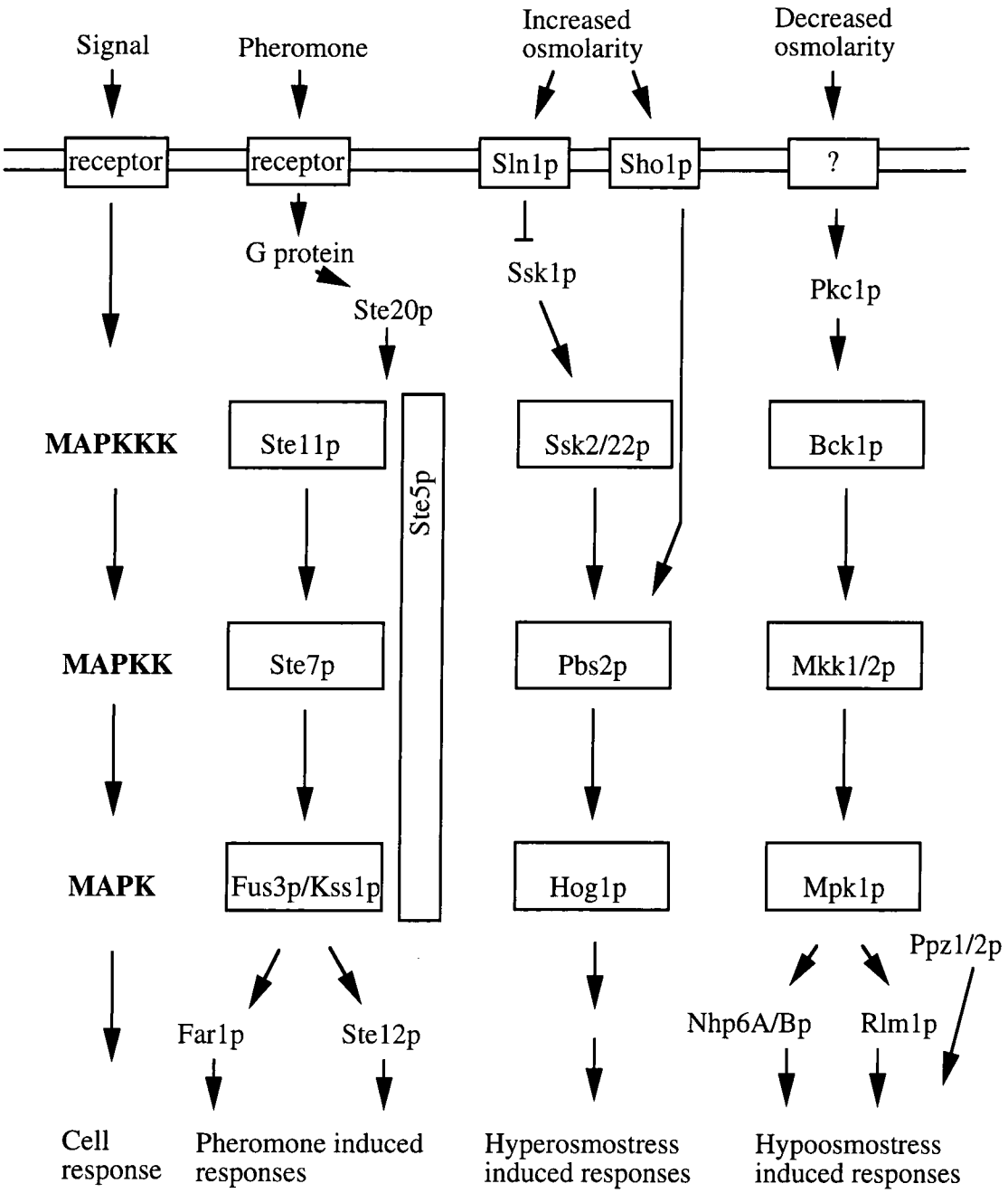

Fig. 1.4. MAP kinase cascades in *Saccharomyces cerevisiae*

contrast to the glycerol utilisation pathway that occurs in mitochondria. The mitochondrial glycerol-3-phosphate dehydrogenase, encoded by *GUT2*, was identified by the study of mutants unable to grow on glycerol as the major carbon source (Sprague and Cronan, 1977). The *GUT2* gene contains a mitochondrial pre-sequence and a potential FAD-binding site (Ronnow and Kielland-Brandt, 1993) whereas the cytoplasmic GPDH has a specificity for NADH (Albertyn *et al.*, 1992; Gancedo *et al.*, 1968). The highest levels of glycerol accumulation in response to salt stress were observed in a *gut2* strain (Albertyn *et al.*, 1994a). Intracellular glycerol concentration is therefore dependent on the relative activities of glycerol metabolism and glycerol utilisation and the availability of substrates. A scheme for glycerol metabolism is shown in figure 1.5.

For some time it was considered that the conversion of glycerol-3-phosphate to glycerol was catalysed by a non-specific phosphatase (e.g. Gancedo *et al.*, 1968). However Norbeck *et al.* (1996) have recently reported the identification of two isoenzymes of glycerol-3-phosphatase. The expression of one of the corresponding genes, *GPP2*, is regulated by the HOG pathway. The osmotic induction of Gpp2p again implies the importance of glycerol accumulation to yeast in the response to osmotic stress.

Glycerol accumulation is also affected by the rate at which glycerol can be lost to the extracellular medium. Although glycerol is able to diffuse across the membrane, facilitated diffusion by a glycerol channel, Fps1p, has also been described (Luyten *et al.*, 1995). In the absence of osmotic stress, Δ*fps1* mutants have higher intracellular and lower extracellular glycerol concentrations than the equivalent 'wild-type' strain. However, the glycerol accumulation during stress is not significantly different for the Δ*fps1* strain and kinetics of diffusion suggest that the Fps1p channel is inactive during osmotic stress. The inactivation of facilitated diffusion through Fps1p during osmotic stress is independent of Hog1p activity (Luyten *et al.*, 1995).

The metabolic shift to produce glycerol in osmotically stressed cells may be aided by the elevated activities of genes encoding proteins involved in the uptake of glucose. The study of hyperosmolarity responsive (*HOR*) genes showed enhanced transcription of glucokinase (Glk1p) and hexose transporter (Hxt1p) with osmotic stress (Hirayama *et al.*, 1995).

1.4.3. Interactions between the HOG pathway and other cell processes

Elevating intracellular glycerol is not the sole outcome of high-osmolarity signal transduction. As mentioned before, the HOG pathway enhances the transcription of the

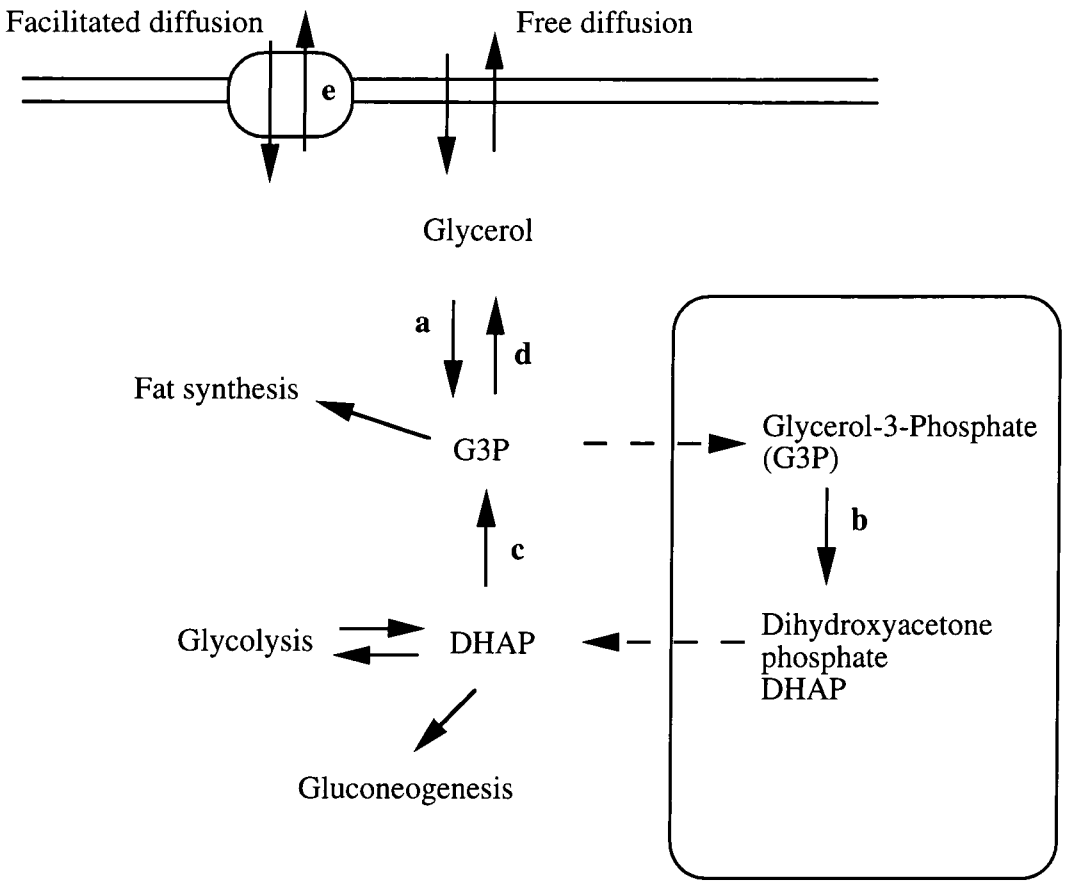

Fig. 1.5. A scheme for glycerol metabolism in *S. cerevisiae*

The enzymes involved in glycerol metabolism:

Reaction	Enzyme	Gene	Notes
a	Glycerol kinase	*GUT1*	
b	Glycerol 3-phosphate dehydrogenase	*GUT2*	mitochondrial; FAD-dependent
c	Glycerol 3-phosphate dehydrogenase	*GPD1* / *GPD2*	osmostress-inducible (*GPD1* only); NADH-dependent
d	Glycerol-3-phosphate phosphatase	*GPP1* / *GPP2*	osmostress-inducible (*GPP2* only)
e	Glycerol channel	*FPS1*	inactive during osmostress

ENA1 gene involved in sodium exclusion (Marquez and Serrano, 1996) in addition to the glycerol synthesis genes *GPD1* (Albertyn *et al.*, 1994) and *GPP2* (Norbeck *et al.*, 1996). The HOG pathway can also enhance the transcription of genes known to be responsive to oxidative stress (Krems *et al.*, 1995) , heat shock (Varela *et al.*, 1992) , and nutrient starvation (Marchler *et al.*, 1993) . This suggests that some gene products may be involved in a general stress response.

The precise mechanism by which active Hog1p brings about enhanced transcription of stress responsive genes is not yet known. The induction of the *CTT1* gene in response to salt stress is mediated via the STRE which is also required for the action of other stresses (Schuller *et al.*, 1994) . The transcription factor(s) which can bind to this element have not yet been described so it is not yet known whether there are a) several transcription factors, each responding to a different kind of stress; or b) one transcription factor that responds to several stresses. The *GPD1* gene does not appear to have an upstream STRE of the same nature as *CTT1*. Therefore a model could be proposed where there is both a general transcription factor which responds to a variety of stresses (and exerts action through the STRE) and a specific transcription factor which responds only to the HOG pathway. There is evidence that MAP kinases can be found in both the nucleus and the cytoplasm (Chen *et al.*, 1992) and it is possible that Hog1p enters the nucleus and phosphorylates certain transcription factors in response to salt stress.

The HOG pathway also plays a role in bud site selection (Brewster and Gustin, 1994) . In cells subjected to osmotic stress there is a temporary growth arrest and rapid dissociation of the actin cytoskeleton (Chowdhury *et al.*, 1992) . On recovery from osmotic shock the actin cables reassemble and bud growth resumes in the same location. However, Δ*hog1* cells fail to resume bud growth at the same site and instead initiate a new bud site (Brewster and Gustin, 1994) . Thus it would appear that the HOG pathway is required for retention of spatial information when the actin cytoskeleton disassembles. Both disassembly of the cytoskeleton and tyrosine phosphorylation of Hog1p occur within one minute of application of salt stress (Brewster and Gustin, 1994; Chowdhury *et al.*, 1992) . The independence of the actin response from Hog1p raises the intriguing possibility that actin may interact with upstream components of the osmosensing signal transduction pathway. There are other possible causes for the actin response that cannot be ruled out however. For example, the immediate solute loss due to changes in osmolarity may cause a mechanical response which triggers reorganisation of the cytoskeleton. Temperature stress and changes in carbon source can cause a similar actin disassembly (Chowdhury *et al.*, 1992) but in these conditions Hog1p is not required to redirect growth to the original bud site. It is clear that the HOG

pathway does play a role in regulating cell morphogenesis but apparently only in response to salt.

It is interesting that the other osmosensing signal transduction pathway, the PKC1 pathway, has also been implicated in regulation of growth from the bud. A mutant allele of *BCK1* (*slk1*) was isolated by its requirement for the bud formation protein, Spa2p, for growth (Costigan *et al.*, 1992) . Other evidence for the involvement of this pathway in the regulation of budding comes from a mutant *mpk1* allele which causes delocalization of chitin deposition and actin cortical spots (Mazzoni *et al.*, 1993) . Thus it would appear that both the HOG pathway and the PKC1 pathway can effect the organisation of the cytoskeleton and growth at the bud. The study of protein-protein interactions at the bud during different physiological conditions may reveal further information about how these two pathways exert control over cell morphogenesis.

An interaction between the HOG pathway and another stress-responsive cell process may occur through the function of Sln1p. A strain containing a mutant allele of *SLN1* was first identified by its requirement for the ubiquitin N-end rule for degradation (Ota and Varshavsky, 1992; for a review of the N-end rule see Varshavsky, 1992). The lethality of the *Δsln1 Δubr1* double mutation (deleted for both Sln1p activity and the recognition component of the N-end rule) was suppressed by high copy expression of the *PTP2* gene which encodes protein tyrosine phosphatase. As the *Δsln1* mutation can cause constitutive activation of the HOG pathway it seems likely that high copy Ptp2p can suppress the lethality by dephosphorylating and thereby deactivating Hog1p (Maeda *et al.*, 1994) . The role of the N-end rule pathway is unclear but it is possible that it allows for tight regulation of the amount of protein in the HOG pathway. A model that would be consistent with the phenotypes observed would be that the N-end rule could be required for rapid turnover of Ssk1p. Ssk1p is apparently inactivated by phosphorylation by Sln1p. The constitutive activation of Ssk1p caused by loss of Sln1p activity could be counteracted by enhanced turnover of Ssk1p, thereby removing inappropriate signalling through the HOG pathway or, as mentioned before, by enhanced phosphatase activity down-regulating active Hog1p. *PTP2* is induced by heat and is required for certain aspects of thermotolerance (Ota and Varshavsky, 1992) suggesting another point of interaction between the HOG pathway and other stress responses.

Sln1p is also involved in Hog1p-independent cellular activity (Yu *et al.*, 1995) . Deletion of *SLN1* severely reduces the activity of the transcription factor Mcm1p, and certain alleles of *sln1* can enhance Mcm1p-mediated transcriptional activation. These responses were unaltered

by deletion of *HOG1* showing that Sln1p can control functions independently of its role in osmoregulation.

It is apparent that Hog1p can bring about osmostress-induced changes at the level of both transcription and post-translational modification and as such is likely to phosphorylate an array of substrates.

1.5. The Vacuole and Osmohomeostasis

The vacuole could play a variety of roles in osmohomeostasis. It could help maintain the intracellular Na^+/K^+ ion ratio, the importance of which was discussed in section 1.2. The vacuole may also be involved in osmohomeostasis by degrading proteins that are not required in a particular physiological state.

Of the vacuolar protein sorting (*vps*) mutant strains described as being osmosensitive, three, namely *vps1*, *vps15* and *vps34* (isolated as *vpt26*, *vpt15* and *vpt29* respectively; Banta *et al.*, 1988) , are involved in the early stages of vacuolar protein sorting from the Golgi. Vps15p and Vps34p form a complex that regulates trafficking (Stack *et al.*, 1993) . *vps15* and *vps34* mutations both confer class D morphology which is a segregation defect (Raymond *et al.*, 1992) . Vps1p is also involved in transport from the Golgi. It has GTPase activity (Vater *et al.*, 1992) , and is required for retention of Golgi proteins, such as Kex2p (Wilsbach and Payne, 1993) . The reason for the osmosensitivity displayed by *vps1*, *vps15* and *vps34* strains is not known. It is possible that the stage of sorting from the Golgi is particularly sensitive to fluctuations in ion concentration.

All four *vps* strains with class C vacuole morphology (a total lack of a visible vacuole), *vps11*, *vps16*, *vps18* and *vps33* (Banta *et al.*, 1988) have an associated osmosensitive phenotype. This implies that a coherent vacuolar structure is required for some aspect of osmohomeostasis. Vps33p is a cytoplasmic ATPase (Banta *et al.*, 1990) . A temperature-sensitive *vps33* strain which contains a vacuole was found to be defective in vacuolar inheritance. This suggests the protein has a function common to both vacuole segregation and integrity. A defect in vacuole inheritance does not always confer osmosensitivity. For example, D*vac1* is not osmosensitive, so it is more likely that it is the structural defect caused by *vps33* that disrupts osmohomeostasis.

The degradation of proteins in the vacuole may play a general role in homeostasis in a variety of conditions. Endocytosis and degradation of plasma membrane proteins can require

ubiquitin-protein ligase, a functional actin cytoskeleton and mature vacuolar proteins (Galan *et al.*, 1996) . If the vacuole is the route of degradation for proteins involved in metabolism and homeostasis, then disruptions in vacuolar integrity or transport to the vacuole could have pleiotropic effects on osmosensitivity. A link between vacuole function and metabolism has been demonstrated. Defects in *gut1* and *aro7*, encoding glycerol kinase and chorismate mutase, have an associated CPY secretion phenotype (Latterich *et al.*, 1993) . Mutations in *aro7* also confer osmosensitivity.

1.6 Yeast Genome Project.

Projects to sequence the entire genome of several model organisms have recently been initiated. This includes several prokaryotes such as *Escherichia coli* (Sofia et al., 1994), *Bacillus subtilis, Mycobacterium leprae* (Bergh and Cole,1994) and *Mycoplasma genitalium* (Peterson et al., 1993). The genomes of *Mycobacterium leprae*, *Mycoplasma genitalium* and *Haemophilus influenzae* have all sequenced in their entirety. This makes these the first living organisms to be completely characterised at the genome level. The first eukaryotic genome was completely sequenced by the end of 1996, this was for the yeast *Saccharomyces cerevisiae* (Oliver et al., 1992; Vassarotti & Goffeau, 1992; Dujon et al., 1994). The genome sequencing of the three other model organisms is presently being determined by a world-wide consortium of laboratories. The European effort is funded and coordinated by the European Union. The organisms are *Schizosaccharomyces pombe*, *Arabidopsis thaliana* (Magnien et al., 1992) and *B. subtilis* (Glaser et al., 1993; Sorokin et al., 1993; Azevedo et al., 1993., Daniel & Errington,1993; Scotti et al., 1993).

The yeast genome sequencing project was initiated in January 1989. This was undertaken for several reasons, firstly yeast is the best characterised of all eukaryotic organisms and is the only one in which there is any hope of a complete genetic, biochemical and physiological description. Secondly, as a prelude to the human genome project by working up the technology. Lastly to show that a distributed network of laboratories could function efficiently and in a cost effective manner. This resulted in the successful sequencing of the first entire chromosome from any organism. This was chromosome III, one of the smallest in yeast (Oliver *et al,* 1992). The sequencing of chromosome III has led to the identification of about 100 new genes never described before.

The systematic sequencing of the yeast genome opens the door to the identification of the basic biological mechanisms which have not so far been accessible through classical approaches. Moreover, yeast is an industrial microorganism widely used in the

pharmaceutical, food and beverage industries as well as for the production of industrial enzymes. The sequence information generated is therefore bound to stimulate further applied developments.

The major advantages of such a systematic characterisation of yeast is that it combines the intracellular structure and organisation of a eukaryote with the simplicity of handling of a single celled organism. Hence yeast gene sequences can be reliably used to identify and ascribe a function to the corresponding gene sequences in higher and more important eukaryotes.

1.6.1 Summary of the sequencing of individual chromosomes.

Chromosome I. (230kb).
Coordinator: H Bussey, McGill University, Canada. This sequence has been published (Bussey *et al,* 1995). The chromosome contains 75 ORFS on the right arm and 68 on the left.

Chromosome II.(813kb)
Coordinator: H Feldman, Munich, Germany.. This sequence has been published (Feldman *et al,* 1994). The chromosome contains 302 ORFS on the right arm and 113 on the left.

Chromosome III. (315kb)
Coordinator: S. Oliver, UMIST, UK. This sequence was the first ever complete chromosome of a eukaryote to be published (Oliver *et al,* 1992). The chromosome contains 107 ORFS on the right arm and 76 on the left.

Chromosome IV.(1532).
Coordinators: C. Jacq, Paris, France for the EU, B. Barrell, Cambridge, for the Sanger Centre, R Davis and D. Botstein, Stanford, USA and M. Johnson, St. Louis, USA. This is the largest chromosome and contains 545 ORFS on the right arm and 248 on the left.

Chromosome V. (577kb)
Coordinators: R Davis and D. Botstein, Stanford University, USA. The chromosome contains 190 ORFS on the right arm and 77 on the left.

Chromosome VI. (270kb)

Coordinator: Y. Murakami, Riken, Japan. This sequence has been published (Murakami *et al,* 1995). The chromosome contains 57 ORFS on the right arm and 68 on the left.

Chromosome VII. (1091kb)

Coordinators: A. Goffeau and H. Tettelin, Louvain-la-Neuve, Belgium. The chromosome contains 296 ORFS on the right arm and 263 on the left.

Chromosome VIII. (562kb)

Coordinator: M. Johnston, St .Louis, USA. This sequence has been published (Johnston et al., 1994). The sequence was determined from a set of 23 cosmid clones and has revealed 269 ORFs of which 210 represent novel genes; 59 ORFs correspond to previously identified genes.

Chromosome IX. (440kb)

Coordinator B. Barrell, Sanger Centre, Cambridge, UK. The chromosome contains 44 ORFS on the right arm and 177 on the left.

Chromosome X. (745kb).

Coordinator: F. Galibert, Rennes, France. This sequence has been published (Galibert *et al,* 1996). The chromosome contains 162 ORFS on the right arm and 225 on the left.

Chromosome XI. (666kb)

Coordinator: B. Dujon, Paris, France. This sequence has been published (Dujon *et al,* 1994). The chromosome contains 106 ORFS on the right arm and 225 on the left.

Chromosome XII. (1078kb)

Coordinators: M. Johnston, St .Louis, USA and J. Hoheisel, Heidelberg, Germany for the EU. The chromosome contains 467 ORFS on the right arm and 67 on the left.

Chromosome XIII. (924kb)

Coordinator B. Barrell, Sanger Centre, Cambridge, UK. The chromosome contains 326 ORFS on the right arm and 113 on the left.

Chromosome XIV. (784kb)

Coordinator: P Philippsen, Basel, Switzerland. The chromosome contains 77 ORFS on the right arm and 339 on the left.

Chromosome XV. (1091kb).
Coordinator: B.Dujon, Paris, France. The chromosome contains 395 ORFS on the right arm and 166 on the left.

Chromosome XVI. (948kb)
Coordinators: B. Barrell, Sanger Centre, Cambridge, UK; M. Johnston, St .Louis, USA; A. Goffeau, Louvain-la-Neuve, Belgium for the EU; R Davis and D. Botstein, Stanford University, USA; and H. Bussey, McGill University, Canada. The chromosome contains 204 ORFS on the right arm and 283 on the left.

Of the 6130 ORFS that have been putatively identified, over one third correspond to previously identified genes, over one third show similarity to previously identified genes either in yeast or in other organisms and one quarter have no known function and represent completely new genes.

1.7. Aims of Project

The initial aim of this project was to characterise *ssv* strains from the laboratory collection of mutants (Latterich, 1992) . These mutants were isolated by their lack of growth on media containing 1.5M NaCl. The vacuolar morphology and protein sorting defects for the strains were tested previously. This part of the project was dedicated to screening the strains for phenotypes which may signify a defect in osmosensing signal transduction. This screen was to test some of the strains for glycerol accumulation.

The second part of the project was to determine the sequence of the right sub-telomeric region of chromosome VII. This region was approximately 11kb in size. The last part of the project was to initiate a functional analysis of some of the predicted genes that were uncovered in this region.

CHAPTER 2

MATERIALS AND METHODS

2.1. Materials.

2.1.1. Reagents and Suppliers.

All chemicals were of AnalaR quality and were from BDH Chemicals Ltd., Poole, Dorset, U.K. or Sigma Chemicals Plc., Poole, Dorset, U.K. unless otherwise specified.

Yeast extract was from Oxoid Ltd., Basingstoke, Hants., U.K..

Trypticase Peptone was from BBL, Cockeysville, U.S.A..

Bacto Peptone and Yeast Nitrogen Base without Amino Acids were from Difco Laboratories, Detroit, MI, U.S.A..

Select agar and agarose were from Gibco BRL, Gaithersburg, U.S.A..

Restriction endonucleases and buffers, T4 DNA ligase, Klenow enzyme, 5-bromo-4-chloro-3-indolyl-β-D-galactoside (X-gal) and wild-type λ DNA were from NBL, Cramlington, Northumberland, U.K., Boehringer Mannheim (U.K.) Ltd., Lewes., U.K., or New England Biolabs, CP Labs Ltd., Bishop's Stortford, Hertfordshire, U.K..

Filter paper (3MM) and laboratory sealing film were from Whatman International Ltd., Maidstone, U.K..

Nitrocellulose was from Bio-Rad Laboratories Ltd., Hemel Hempstead, U.K..

Polaroid film was from Polaroid (U.K.) Ltd., St. Albans, Hertfordshire, U.K..

2.1.2. Buffers and Stock Solutions (Listed in Alphabetical Order).

Amino Acid Stock Solutions

Stock solutions of individual amino acids and nucleotide bases were prepared at 2mg/ml and then autoclaved. They were used at a final concentration of 20μg/ml as supplements of yeast minimal medium as required.

Antibiotic Stock Solutions

Ampicillin was prepared as a 50mg/ml stock solution in 70% ethanol, and used at a final concentration of 50µg/ml. Kanamycin was prepared as a 20mg/ml stock solution in dH_2O, filter sterilised and used at final concentration of 20µg/ml.

Vitamin Stock Solutions

A stock solution of 1mg /ml thiamine was prepared. It was used at a final concentration 10µg/ml.

6x Agarose Gel Loading Buffer

Bromophenol Blue	25mg
Xylene Cyanol	25mg
Sucrose	4g

in 10ml dH_2O.

20x SSC

NaCl	175.3g
Sodium Citrate	88.2g

in 1l dH_2O. The solution was adjusted to pH7.0 with 10M NaOH.

50x TAE Buffer

Tris.HCl	242g
EDTA	18.5g
Glacial Acetic Acid	57.1ml

in 1l dH_2O.

TE Buffer pH 8.0 (10mM Tris.HCl, 1mM EDTA)

1M Tris.HCl pH 8.0	10ml
250mM EDTA pH 8.0	4ml

in 1l dH_2O.

Prehybridization buffer

20x SSC	15 ml
0% SDS	2.5ml
5x Denhardts solution	5.0 ml
Denatured salmon sperm DNA (100 µl / ml)	200 µl

Hybridization buffer

This has the same components as prehybridization buffer in addition to 0.01M EDTA.

Nucleotide Mixture Solution

15 µ l of 10 mM of ATP, GTP, CTP and UTP were mixed and the volume completed to 100 µl by sterile water.

Sodium Iodide Solution.

NaI	98.5g
Na_2CO_3	1.5g

in 100 ml dH_20. Stored in the dark at 4 °C

STET buffer (Sodium chloride , Tris, EDTA, Triton)

Sucrose (w/v)	8.0%
Triton x100 (v/v)	0.5%
50 mM EDTA (pH 8.0)	
10mM Tris- HCl (pH 8.0)	

2.1.3. Growth Media (Listed in Alphabetical Order).

All growth media described below can be used as liquid media or can be solidified by the addition of 2% agar.

Luria-Bertani Broth (L-Broth)

Trypticase Peptone	10g
Yeast Extract	5g
NaCl	5g
in 1l dH_2O.	

Sporulation Agar

Yeast Extract	1g
Glucose	0.5g
Potassium Acetate	10g
Agar	20g

in 1l dH_2O. Required amino acids were added to a final concentration of 20µg/ml.

Yeast Minimal Medium (YMM)

Yeast Nitrogen Base without Amino Acids	6.7g
Glucose	20g

in 1l d H_2O. Required amino acids were added to a final concentration of 20µg/ml.

YPD(A)

Yeast Extract	10g
Bacto Peptone	20g
Glucose	20g
(Adenine	20mg)

in 1l dH_2O.

M9 (Minimal medium)

Na_2HPO4	0.6g
KH_2PO4	0.3g
NaCl	50mg
NH_4Cl	0.1g
dH_2O	90 ml

These components were mixed, autoclaved, cooled to room temperature then added

1M Mg SO_4	0.2ml
20% Glucose	1.0 ml
1M $CaCl_2$	0.01ml
H_2O complete to	100 ml
Agar	1.5g
Thiamine	1ml
Tryptophan (20mg to 20 ml of dH_2O)	1 ml
Ampicillin	1ml

2.2. Strains and Plasmids.

2.2.1. Bacterial Strains.

The bacterial strain used in this study was *Escherichia coli*, and strains are listed in table 2.1.. All strains represent laboratory stocks.

E. coli strains were cultured in L-Broth at 37°C. Cultures of bacteria containing plasmids were grown in media containing the appropriate antibiotic selection. Strains were maintained for short periods of time on L-Agar and stocks of all bacteria were maintained in 15% glycerol at -80°C.

Strain	Genotype	Source
DH5∝	*supE44 ΔlacU169(ϕ80 lacZΔM15)hsdR17 recAI endAI gyrA96 thi-1 rel A1*	Laboratory stock
JA221	*recA1 leuB6 trpΔE5 hsdR⁻ hsdM⁺ lacY*	Laboratory stock

Table 2.1. Bacterial strains used in this study.

2.2.2. Plasmids.

All plasmids used in this study were maintained in DH5α. Plasmids and their prominent features are listed in table 2.2.. The plasmid pL2 was kindly supplied by T. H. Stevens and C. R. Raymond, Oregon .

Plasmid	Genotype	Reference
pUCI9	amp^R	[Yanisch-Perron, 1985 #]
pL2	amp^R, *LEU2*	Laboratory Stock
pBlueScript KS+	mp^R	Laboratory Stock

Table 2.2. Plasmids used in this study.

2.2.3. Yeast Strains.

Saccharomyces cerevisiae strains used in this study are listed in table 2.3.. MLY *ssv* strains are laboratory strains derived from the parental strains SEY6210 and SEY6211 [Latterich, 1992]. MLY strains which are MATα are derived from SEY6210 and have the genotype *leu2-3,112 ura3-Δ52 his3-Δ200 trp1-Δ901 lys2-801 suc2-Δ9 GAL.* MLY strains which are MATa are derived from SEY6211 and have the genotype *leu2-3,112 ura3-Δ52 his3-Δ200 trp1-Δ901 ade2-101 suc2-Δ9 GAL.*
Stocks of all yeast strains were kept in 40% glycerol at -80°C.

2.3. General Methods.

2.3.1. Sterile Working Practices.

Sterile working practices were maintained throughout. All media and materials were autoclaved at 15 p.s.i. for 15 minutes, unless heat sensitive, in which case they were filter sterilised by passing through a 0.22μm nitrocellulose membrane filter. Heat sensitive plastic ware was sterilised by leaving overnight in 70% ethanol then washing in sterile dH_2O.

All bottles necks were flamed before and after use, and caps were replaced on all containers as soon as possible . Culture plates were sterilised after pouring by flaming the surface of the molten agar with a roaring Bunsen flame.

Strain	Genotype	Reference
SEY6210	*MATα leu2-3,112 ura3-Δ52 his3-Δ200 trp1-Δ901lys2-801 suc2-Δ9 GAL*	[Robinson,1988]
SEY6211	*MATa leu2-3,112 ura3-Δ52 his3-Δ200 trp1-Δ901 ade2-101 suc2-Δ9 GAL*	[Robinson,1988]
MLY0103	*MATα ssv 10-1*	[Latterich,, 1992]
MLY0106	*MATα ssv1-2*	[Latterich,, 1992]
MLY0111	*MAT α ssv2-2*	[Latterich,199 2]
MLY0124	*MAT α ssv11-1*	[Latterich ,1992]
MLY0126	*MAT α ssv4-1*	[Latterich ,1992]
MLY0134	*MAT α ssv8-1*	[Latterich, 1992]
MLY0307	*MAT a ssv 1-7*	[Latterich, 1992]
MLY0310	*MAT a ssv 9-1*	[Latterich,1992]
MLY0419	*MAT a ssv17-100*	[Latterich,1992]
MLY0524	*MAT a ssv 5-1*	[Latterich,1992]
MLY0527	*MAT a ssv 6-1*	[Latterich ,1992]
MLY1311	*MAT a ssv9-7*	[Latterich ,1992]
MLY1156	*MAT a ssv 16-1*	[Latterich ,1992]
MLY1514	*MAT a ssv3-1*	[Latterich , 199]
MLY1517	*MAT a ssv7-1*	[Latterich ,1992]
MLY1520	*MAT α ssv12-1*	[Latterich ,1992]
MLY1521	*MAT α ssv14-1*	[Latterich ,1992]
MLY1522	*MLY α ssv 13-1*	[Latterich ,1992]
CEN. PK2	*a / α ura3-52/ura3-52 trp1-289/trp1-289 leu2-3,112/leu2-3,112/leu his 3Δ1 / his 3Δ1*	[Laboratory Stock]

Table 2.3. Yeast strains used in this study.

2.3.2 Measurements of Yeast Growth.

Total cell counts of yeast cultures were determine with a Coulter Multisizer II fitted with a 37 μm aperture. The window was adjusted to take account of all particles between 0.748 and 10.00 μm . A sample of the yeast culture was diluted 100 times with Isoton electrolyte solution and two counts were made per sample, subtracting the blank. The cell number could be calculated as follows:

Total Cell Count /ml (for 200 μl)x40x Dilution Factor.

2.3.3 Measurements of Bacterial Growth.

Bacterial growth was either determined spectrophotometrically by measuring the OD 600 if a correlation between the number of bacteria and the optical density was known, or by viable cell counts. For the later, a known volume of the culture was diluted down in 1xPBS in decimal steps, and 100μl of each dilution was plated out in duplicates onto Luria agar plates under the correct selective conditions. The plates were incubated at 37°C for 12 hours, and the plates showing between 15 and 200 colonies were used for the assessment of the number of bacteria present in the original culture.

2.3.4 Maintenance of Stock Cultures (Bacterial Strains).

Strains carrying no plasmids or selectable marker were cultured in Luria Bertani broth or Luria Bertani agar plates without antibiotics. Strains containing plasmids and or selectable markers were grown in the medium under selective conditions. A master stock was maintained in 40% (v/v) glycerol at -80°C. for glycerol stocks, 10 ml Luria Bertani broth was inoculated with a colony from the respective strains and incubated at 37°C overnight with continuous shaking . The culture was centrifuged for 5 minutes, the pellets resuspended in 1 ml Luria Bertani Broth and transferred to a 2 ml glass vial containing 1 ml 80% (v/v) sterile glycerol. The vial was frozen in liquid nitrogen and placed in a freezer at -80 °C.

2.3.5 Maintenance of Stock Cultures (Yeast Strains).

A stock culture of all yeast strains was maintained in glycerol at -80°C. A single colony of each yeast strain was used to inoculate 10 ml YPDA. The culture was grown to saturation at 30°C with shaking for 24 to 48 hours, depending on the growth rate of the strain concerned. The cells were sedimented by centrifugation for 10 minutes, resuspended in 0.75 ml YPDA and added to 1.25 ml 80% (v/v) glycerol in a 2.5 ml glass vial.

2.3.6 Preparation of Competent *E.coli* Cells.

Method for preparing competent *E.coli* cells by calcium chloride treatment.

Cells of the required strains were grown up as discrete colonies on an agar plate (no antibiotics were added). A single colony was then picked from the plate and used to

inoculate 5 ml of sterile LB (Luria-Bertani) broth . After incubation at 37°C overnight 1 ml of this fresh overnight culture was then used to inoculate a further 50 ml of LB broth which was incubated at 37°C for 2 to 3 hours until an absorbance at 550 nm of 0.4-0.5 was reached. After incubation, the culture was first chilled by swirling in an ice water bath, and then subjected to a centrifugation step (5000 r.p.m for 5 minutes at 4°C) to sediment the cells. The supernatant was decanted and the cells resuspended in 25 ml of sterile ice -cold 0.1 M calcium chloride and left on ice for 30 minutes. Centrifugation at 5000 r.p.m for 10 minutes at 4°C was again used to sediment the cells. The supernatant was discarded and the pellet resuspended in 5 ml of sterile ice -cold 0.1 M calcium chloride solution. At this point the cells were either used directly or stored for later use. To store the cells, 3 ml of 80% glycerol was first added to the suspension. The cells were then aliquoted in to 400 µl portions and frozen in liquid nitrogen. These frozen cells can be stored at -80°C .

2.3.7 Extraction of Glycerol.

10ml of the mutant cells were grown in YPDA broth overnight at 30°C, and then 5 ml of these cells added to 5 ml of fresh YPDA broth. The remaining 5ml of cells were added to 5ml of YPDA with 1.8 M NaCl. The cells were incubated overnight at 30°C with continuous shaking and counted in the Coulter counter. 1.5ml of cells were centrifuged for 1 min and the supernatant frozen until needed for the extracelluar glycerol determination. Another 1.5ml of cells were centrifuged for 1 min and the supernatant discarded. The pellet was washed in either distilled water or 0.09 M NaCl (according to the growth condition of the cells). The cell pellet was resuspended in 10 ml 80% ethanol for 21h, centrifuged and the supernatant retained. The supernatant fractions were pooled and evaporated to dryness at 54°C in a rotary evaporator for 30 min. The residue was resuspended in 0.5 ml water, for intracellular glycerol determination.
Glycerol concentration was determined enzymically using a standard diagnostic kit (BCL) and is expressed as mg glycerol / 10^7 cells.

2.4. Transformation Methods.

2.4.1. Transformation of *E. coli* - Heat Shock.

Transformation of *E. coli* by heat shock was based on the method of Mandel and Higa (1970).

Frozen cells were thawed on ice before transformation . DNA in TE buffer or a ligation mixture (typically 200ng of DNA in a volume of 5ml) was added to a 0.2ml aliquot of cells and mixed gently by inversion before incubation on ice for 30-60 minutes. The cells were heat-shocked for 2 minutes at 42°C before the addition of 1ml L-broth. The tube

was then incubated at 37°C in a heating block for 1 hour before appropriate aliquots were spread on selective agar plates.

2.4.2. Transformation of *S. cerevisiae* - Electroporation.

Transformation of *S. cerevisiae* by electroporation was based on a method from B. Stevenson (personal communication).

10ml YPDA were inoculated with a colony of the yeast strain to be transformed and incubated overnight with agitation at 30°C. 100ml were used to inoculate 100ml of YPDA and incubated as above until a cell density of approximately $1x10^7$ cells/ml was reached (16-18 hours). The culture was then centrifuged at 2400g for 5 minutes and the pellet resuspended in 20ml ice-cold dH_2O. The cells were washed twice in ice-cold 1M sorbitol by resuspending the pellet and centrifuging the cells as above, before resuspending the final pellet in 0.3-0.5ml of 1M sorbitol and storing on ice until transformation. Up to 5ml of DNA solution were pre-mixed with 1mg of carrier DNA (single-stranded Salmon sperm DNA). 100ml of cells were added to the DNA, mixed and transferred into a cold Genepulser cuvette (Bio-Rad 0.2cm electrode gap). The cells were pulsed at 1.5kV (7.5kV/cm), 25mF, 200W for about 4.8ms 300ml 1M sorbitol was added to the transformation mixture and 100ml aliquots plated out onto selective media. The plates were incubated at 30°C for at least 4 days.

2.5. DNA Manipulations.

2.5.1. Precipitation of DNA with Ethanol.

0.1 volume of 3M sodium acetate (pH5.2) and 2.5 volumes of 100% ethanol were added to the DNA containing solution, mixed and stored at -80°C for at least 30 minutes. DNA was pelleted by centrifugation at 12 000 g for 10 minutes. Pellets were washed in ice-cold 70% ethanol, the supernatant removed and the pellet allowed to dry before resuspension in TE buffer.

2.5.2. Spectrophotometric Quantification of DNA.

The DNA sample was diluted 1:50 or 1:100 with TE to give final volume of 0.1ml. This was put into a quartz cuvette and the absorbance of the solution at 260 and 280nm measured with a UV spectrophotometer (LKB) using TE as a blank. A pure DNA sample has an $A_{260/280}$ ratio of 1.8. An A_{260} value of 1.0 is equivalent to a concentration of $50mgml^{-1}$ of double stranded DNA or $20mgml^{-1}$ of single stranded oligonucleotides.

2.5.3. Plasmid DNA Preparation from *E. coli* - Silica Fines Preps.

A method for the isolation of small amounts of plasmid DNA (4 to 10μg) from *E. coli* using silica fines was employed throughout (Amersham).

5 ml Luria broth containing the appropriate antibiotics were inoculated with a single bacterial colony, and incubated at 37°C overnight with vigorous agitation (200 r.p.m). 1.5 ml of the culture was transferred into an eppendorf and centrifuged for 1 minute at 12,000 g in a microcentrifuge. The supernatant was removed by aspiration leaving the bacterial pellet as dry as possible. The pellet was resuspended in 350 µl of STET buffer (8% sucrose, 0.5% (v/v) Triton X-100, 50mM EDTA, 10mM Tris. HCl pH8.0.), 25µl of a freshly prepared lysozyme solution (10mg/ml lysozyme in TE buffer) was added, and the tube vortexed for 3 seconds. The tube was incubated in a boiling water bath for exactly 90 seconds and immediately centrifuged at room temperature for 10 minutes. The pellet was removed from the tube with a sterile toothpick and 0.7 ml NaI solution was added to the supernatant. 5µl of resuspended acid washed silica fines (silica 325 mesh, 50% (v/v) in water) were added to the tube, mixed by inversion and the plasmid DNA bound to the glass by incubation at room temperature for 30 minutes. The tubes were centrifuged for 15 seconds at 12,000 g and the supernatant removed by aspiration. The pellet was washed in 1 ml 70% (v/v) ethanol 30% (v/v) TE buffer, centrifuged and the ethanol removed leaving the pellet as dry as possible. The fines were resuspended in 50 µl TE buffer and the DNA eluted by incubation at 37°C for 10 minutes. The fines were pellet by centrifugation as before and the plasmid DNA containing supernatant was transferred to a fresh tube. The DNA was now ready for digestion with any restriction endonuclease or transformation without any further purification.

2.5.4. Plasmid DNA Preparation from *E. coli* - High Purity.

Plasmids to be sequenced or required in high concentration were prepared by a modified alkaline lysis method using the Promega Wizard Minipreps (DNA Purification System) kit according to the manufacturer's instructions.

2.5.5. Sonication of DNA

Fragmentation of the DNA by sonication is a reliable methods. It can be used to break large target DNA into segments that are optimal in size for random sequencing and yields a collection of overlapping fragments. The DNA of interest was sonicated (Soniprep 150 MSE) for 10 seconds. After sonication 410 µl of TE was added, followed by 50 µl of 3M sodium acetate and 1 ml of ethanol . This solution was precipitated overnight at -20 °C, centrifuged at 4 °C for 15 minutes and the pellet washed with 70% ethanol. The pellet was resuspended in 30 µl TE and stored at -20°C.

2.5.6. Restriction Digests.

Restriction digests were carried out using commercial sources of enzymes and their corresponding buffers, as supplied by the manufacturer. Restriction enzymes used at least 1 unit enzyme per mg of DNA to be digested. Digests were carried out for a minimum of

2 hours at 37°C. Manufacturer's guidelines were followed for the most appropriate buffer to use in digests involving more than one enzyme. If digestions were to be analysed by gel electrophoresis, 0.2 volumes of 6x gel loading buffer were added. If the digestion was to be used in further subcloning steps, the digestion was stopped by removing the restriction enzyme(s) using Promega Wizard Clean Up System spin-columns according to the manufacturer's instructions (or the DNA was purified by fragment isolation as described in section 2.5.10.).

2.5.7. Ligation Reactions.

T4 DNA ligase was used to ligate DNA fragments with compatible cohesive or blunt-ended termini. The insert and vector DNA were mixed so that there was an excess of insert, typically a ratio of 3:1 (insert:vector) for cohesive and 10:1 (insert:vector) for blunt-end ligations. 5x ligase buffer containing ATP (supplied with the enzyme) and 1 unit of DNA ligase were added and the ligation mix incubated overnight at 15°C. 1 to 10ml of the ligation reaction were used in transformations of competent *E. coli*..

2.5.8. DNA Molecular Weight Markers.

DNA molecular weight markers were prepared by digestion of phage lDNA with *Pst*I completion. A typical preparative digest was performed in the following reaction:

l DNA (300µg/ml)	100µl
dH_2O	780µl
l DNA (300mg/ml)	100ml
dH_2O	780ml
10x Restriction Enzyme Buffer	100ml
Restriction Enzyme (10U/ml)	20ml

Digestion was carried out for 7 hours at 37°C. 200ml 6x loading buffer were added, and the markers stored at -20°C. 15ml were loaded onto agarose gels as a size standard.
A l*Pst*I digest produces DNA fragments of the following sizes (in kb):
14.05, 11.49, 5.07, 4.75, 4.51, 2.84, [2.56, 2.46, 2.44], 2.14, 1.99, 1.70, 1.16, 1.09, 0.81, 0.52, 0.47, 0.45, 0.34.
The fragments in brackets run together on an agarose gel.

2.5.9. Agarose Gel Electrophoresis.

Agarose gel electrophoresis was performed in an Appligene or Bio-Rad mini-gel system for mini gels or in a Scotlab gel system for larger gels. Agarose was added to a measured quantity of 1x TAE buffer, usually to a concentration of 0.7% (w/v) which efficiently separated linear DNA between 10-0.8 kb. The agarose was dissolved by microwaving the mixture. After cooling, ethidium bromide was added to a final concentration of 0.5mg/ml and the agarose poured into the mould with a well comb in place. Once the agarose had

set, the gel was placed into the tank and covered with 1x TAE buffer containing 0.5mg/ml ethidium bromide. DNA samples in loading buffer were loaded and electrophoresis performed, usually at 80mV, until the marker dyes had migrated to appropriate distances. The gel was then placed onto a UV illumination apparatus and photographed using a red-filter and a Polaroid camera.

2.5.10. DNA Fragment Isolation.(Modified By Martin Watson).

DNA fragments were isolated from agarose gels using the QIAGEN QIAquick Gel Extraction Kit according to the manufacturer's instructions. The DNA was with 50µl eluted of sterile water and then used for subsequent reactions.

2.5.11. Filling in 3'-Recessed Termini.

The DNA fragment (maximum of 500ng) was resuspended in 10-15 µl of sterile distilled water following isolation from an agarose gel. A 1 µl solution containing all 4 dNTPs (each at 1mM) was added to the DNA. 2 µl of Klenow buffer(10x) was added (supplied with the enzyme) and the reaction buffer made up to 20 µl with sterile distilled water plus 1 µl (1 unit) of Klenow fragment. The reaction mixture was left at room temperature for 30 minutes and then the Klenow fragment inactivated by incubating at 70°C for 5 minutes.

.

2.5.12. Polymerase Chain Reaction (PCR).

PCR reactions were performed in a thermal cycler (PHC-3, Techne). Typically reactions contained 80pmoles of each primer, 20nmol of each dNTP, PCR buffer (provided with the enzyme) and 1 unit of *Taq* DNA Polymerase (Gibco-BRL) in a final volume of 100ml in a 0.5ml microcentrifuge tube. The quantity of template and $MgCl_2$ in each reaction and the cycling conditions varied according to what was to be amplified and are therefore described where individual PCR reactions appear in the results chapters. *Taq* polymerase was the last component to be added to the reaction before mixing by brief centrifugation. The reaction mixture was then overlaid with sterile mineral oil (100ml) to prevent evaporation during the heat cycles.

After completion of the PCR, samples were kept at 4°C until analysis by gel electrophoresis. PCR products could then be purified by band fragment isolation as described in section 2.5.10.

2.5.13. Exonuclease /III Mung Bean Nuclease Deletions.

Nested deletions were generated using the Pharmacia kit exactly as described in the technical information. In outline, restricted DNA was treated with Exonuclease III in the presence of 75mM NaCl at 30°C. Aliguots were taken every 90 seconds which should correspond to deletions at about 300bp. Samples were then treated with Mung Bean

Nuclease to remove single stranded DNA. Blunt-ended linear DNA was then recircularised by overnight ligation and then transformed into *E.coli* DH5a. After overnight growth on L- Ampicillin at 37°C, colonies were purified and then plasmid DNA extracted by "mini-preparations". The extent at digestion was determined by electrophoresing undigested plasmid DNA on 0.7% agarose gels and comparing the migration to that of known size samples.

2.6. DNA Hybridisation Procedures.

2.6.1. Labelling DNA Fragments.

DNA fragments were labelled for use as probes in hybridisations using the Boehringer Mannheim DIG DNA Labelling and Detection Kit. A 15ml aliquot of 200ng of DNA was boiled for 10 minutes to denature the DNA and then cooled rapidly on ice-water to prevent re-annealing of the strands. dNTPs, hexanucleotides and Klenow enzyme were added according to the manufacturer's instructions and the sample was incubated overnight at 37°C. 1ml of 0.5M EDTA was added to stop the reaction and the DNA was ethanol precipitated. The DNA was washed in ice-cold 70% ethanol, dried and then resuspended in 100ml TE.

The probe was denatured by boiling and rapid cooling on ice before use in hybridisation reactions.

2.6.2. Southern Blotting.

Southern blotting and hybridisation reactions were based on the method of Southern, 1975.

DNA for hybridisation was separated on an agarose gel, visualised under UV illumination and photographed. The DNA was depurinated by soaking the gel in 0.25M HCl for 7 minutes with shaking. The gel was then rinsed twice with dH_2O before being soaked in denaturing solution (0.5M NaOH, 1.5MNaCl) for 20 minutes again with shaking. The gel was rinsed and neutralised in 0.5M Tris.HCl, 3.0M NaCl, pH7.0 for two times 15 minutes. A DNA blot transfer system was assembled as described in [Sambrook, 1989]. The gel was placed, wells uppermost, on a long piece of 3MM paper that was soaked in 20xSSC and positioned over a glass plate with its ends dipped in a reservoir of 20xSSC. A nylon or nitrocellulose membrane cut to the same size as the gel was pre-wetted with dH_2O, put on top of the gel and any air bubbles were removed. The transfer membrane was covered with 3 pieces of 3MM paper soaked in 20xSSC followed by 2 layers of disposable nappies and these were covered with a glass plate with a 1kg weight placed on top. Care was taken that everything placed on top of the filter was cut to the same size as the gel and nothing touched the bottom layer of 3MM paper. After

2-16 hours (usually overnight) the system was disassembled and the membrane rinsed in 2xSSC for 5 minutes. The membrane was air dried for 1 hour before fixing of the DNA by baking for 45 minutes in a vacuum oven at 80°C. The membrane could then be used in hybridisation reactions.

2.6.3. Hybridisation of Labelled Probes to Southern Blots.

Hybridisation reactions were carried out using Techne Hybridisation tubes in a Techne Hybridiser HB-1 oven. Southern blot membranes were pre-hybridised at 68°C for 30 minutes in 50ml of a pre-hybridisation solution consisting of 6xSSC, 5x Denhardt's solution (100x: 2% (w/v) bovine serum albumin, 2% (w/v) Ficoll, 2% (w/v) polyvinylpyrollidone), 0.5% (w/v) SDS and 100mg/ml of 10mg/ml single-stranded salmon sperm DNA (denatured at 95°C for 10 minutes and placed on ice immediately). Denatured, labelled probe was added and the membranes were incubated overnight with rotation at 68°C for hybridisation. To remove non-specifically bound probe the membrane was washed at room temperature in 2x SSC, 0.5% (w/v) SDS for 5 minutes and then in 2x SSC, 0.1% (w/v) SDS for 15 minutes. The final wash was in 0.1x SSC, 0.5% (w/v) SDS at 68°C for 60 minutes. The filters could then be used in the detection procedure described below.

2.6.4. Detection of Hybridising Probes.

Anti-digoxigenin antibody conjugated to alkaline phosphatase (Boehringer) was used to detect the labelled probe. All incubations for this procedure were at room temperature. The hybridised membrane was first rinsed in Tris-salt (0.15M NaCl, 1.5mM KCl, 25mM Tris.HCl pH7.4) for 5 minutes and then blocked in 50ml of fresh blocking solution (Tris-salt, 1.5% dried milk powder, 0.2% Tween-20) for 30 minutes. The membrane was transferred into fresh blocking solution with 5ml of anti-digoxigenin antibody and incubated for 4 hours to allow the antibody to bind to the attached probe. The membrane was washed twice in Tris-salt + 0.2% Tween-20 for 5 minutes each time and then in Tris-salt (no Tween-20) for another 5 minutes to remove all the unbound antibody.

Antibody binding was visualised using solutions provided in the DIG DNA Labelling and Detection Kit. The filter was rinsed in alkaline phosphatase buffer (100mM NaCl, 50mM $MgCl_2$, 0.1M Tris pH9.5) and then placed in a clean petri dish. Alkaline phosphatase buffer was added until the liquid just covered the membrane and 15ml XP and 15ml NBT were added. Alkaline phophatase cleaves the XP resulting in a colour change. Membranes were stored in the dark during signal development (10 minutes - 15 hours depending on the strength of the signal) and care was taken not to agitate the solutions. The colour development was stopped by the addition of 0.5M EDTA and the membranes were rinsed, dried and stored in the dark.

2.7. Yeast Methods.

2.7.1. Sporulation of Diploids.

Diploids of the cells to be sporulated were patched onto YPDA agar, incubated overnight at 30°C and then replica plated onto sporulation agar. Spore plates were incubated at room temperature for 6 to 8 days, until tetrads had formed as detected by light microscopy. A loopful of the sporulated diploids (about the size of a match head) was resuspended in 100ml 1:10 dilution of b-glucuronidase. The suspension was incubated at room temperature for 5 minutes and 5-10ml were streaked along one side of a YPDA plate. The plate was inverted over the microscope on a specially designed plate holder. Spores were visualised under a Nikon Labophot-2 microscope (Nikon, Japan) using a 20x objective lens and 10x eyepieces. The spores were dissected by picking up a tetrad on a needle mounted in a micromanipulator (Narishige Co., Ltd, Tokyo, Japan. Model MO-202). The four spores were separated and plated at 5mm intervals across the plate. The plate was incubated at 30°C for 2-3 days until small colonies appeared. These haploids were picked and tested for various markers.

2.8. DNA Sequencing.

2.8.1. DNA sequencing.

Double stranded DNA was prepared using a high purity preparation method (see section 2.5.4.).

DNA sequencing was always carried out using the departmental sequencing service with an Applied Biosystems 373A DNA Sequencer using double stranded DNA templates. Usually fluorescently labelled universal M13 primers from the Applied Biosystems PRISM™ Ready Reaction Dye Primer Cycle Sequencing Kit were used, according to the manufacturer's instructions. Occasionally custom-synthesised primers (synthesised on an Applied Biosystems 381A DNA Synthesiser) were used in conjunction with the Applied Biosystems Taq DyeDeoxy™ Terminator Cycle Sequencing Kit.

2.8.2. DNA Sequence Analysis.

The DNA sequence generated were initially analysed using the Macintosh computer programmes DNA Strider™1.2 (Marck, 1988) and Sequencher. Primary DNA sequence analysis involved aligning DNA fragments, analysing restriction sites, creating graphical maps of the sequenced fragments, and translating all six hypothetical reading frames.

CHAPTER 3

GLYCEROL ACCUMULATION IN OSMOSENSITIVE YEAST STRAINS.

3.1.INTRODUCTION.

All living cells, whether eukaryotic or prokaryotic, show a rapid molecular response to changes in environmental condition (Mager and Ferreira, 1993). Many similarities between prokaryotic and certain eukaryotic organisms have been found with respect to their cellular response to osmotic stress. Both groups accumulate cytoplasmic compounds on exposure to hyperosmolarity. These organisms can actively counteract the osmotic stress by increasing their intracellular osmotic potential (Csonka, 1989). Microorganisms display differing levels of osmotolerance (Brown,1978). Eukaryotic cells, such as yeast , are more resistant to osmotic stress than prokaryotic cells. Specific environmental conditions can cause changes in the internal osmotic potential e.g through the accumulation of glycerol (Singh and Norton,1991). Osmoregulation, which is defined as the active processes carried out by an organism to adapt to osmotic stress (Csonka,1989) takes place via accumulation of compatible solutes such as polyols or amino acids (Latterich, et al 1993). The yeast *Saccharomyces cerevisiae* responds to osmotic stress, i.e an increase in osmolarity of the growth medium, by enhanced production and intracellular accumulation of glycerol as a compatible solute (Blomberg and Adler,1989 and Albertyn et al, 1994). The production of this polyol to counteract osmotic stress occurs through specific changes to the biochemical processes inside the cell (Brown and Edgley, 1980). The intracellular and extracellular accumulation of glycerol during growth of both wild-type and mutant strains of *Debaryomyces hansenii* in medium containing high concentrations of NaCl has been determined by Adler, et al (1985). Both the mutant and wild-type strains responded similarly in that the glycerol content of the cells increased with an increase in external salinity. In wild-type strains the extracellular glycerol was rapidly salvaged.

The aim of this chapter is to characterise *ssv* mutant strains with respect to the osmotic-pressure responsive signal transduction pathway. This will be accomplished by the determination of internal and external accumulation of glycerol during osmotic stress by 0.9M NaCl.

3.2. RESULTS.

The intracellular and extracellular glycerol accumulation under NaCl stressed and non-stressed conditions was determined for wild-type and selected *ssv* mutant strains. The strains used are listed in Table 3.1 Glycerol accumulation was determined as described in section 2.3.7. In outline, 100ml YPDA cultures were grown to mid-log phase in shake flasks at 30°C. The culture was then divided into two, one half was mixed with an equal volume of pre-warmed YPDA and the other with an equal volume of YPDA containing 1.8M NaCl. Growth was continued for a further 21 hours and the cells harvested. The culture supernatant was also retained for the determination of extracellular glycerol accumulation. Glycerol concentration was determined enzymatically, using a diagnostic kit which acts as follows:

Glycerol is phosphorylated by adenosine-5-triphosphate (ATP) to L-glycerol-3-phosphate in the reaction catalyzed by glycerokinase (GK).

$$\text{Glycerol} + \text{ATP} \xrightarrow[\text{Glycerokinase}]{} \text{L-Glycerol-3-phosphate} + \text{ADP}$$

The adenosine-5-diphosphate (ADP) formed in the above reaction is converted by phosphoenolpyruvate (PEP) with the aid of pyruvate kinase (PK) into ATP with the formation of pyruvate.

$$\text{ADP} + \text{PEP} \xrightarrow[\text{Pyruvate kinase}]{} \text{ATP} + \text{Pyruvate}$$

In the presence of the enzyme lactate dehydrogenase (LDH) pyruvate is reduced to L-lactate by reduced nicotinamide-adenine dinucleotide (NADH) with the oxidation of NADH to NAD.

$$\text{Pyruvate} + \text{NADH} + \text{H}^+ \xrightarrow[\text{Lactate dehydrogenase}]{} \text{L-Lactate} + \text{NAD}^+$$

The conversion of NADH to NAD is directly proportional to glycerol concentration. This is followed by measuring the absorbance of NADH at 340nm.

The results for extracellular glycerol accumulation are presented in Figures 3.1A and 3.1 B. This figure shows the steady state level of extracellular glycerol accumulation. Some cells (e.g. MLY1311) show over twice the amount of glycerol accumulation compared to the wild-type SEY 6210. In general all of the mutant strains show a higher glycerol accumulation than the wild-type strains. Wild-type cells show an almost three-fold increase in glycerol accumulation after osmotic stress. The level observed is about the same as that observed for many of the mutant strains under non-stressed conditions. However, most of the mutant strains do not show any increase in glycerol accumulation. This is with the notable exceptions of MLY0106 *(ssv1-2)* and MLY0524 *(ssv5-1)*, the latter showing particularly high levels of glycerol accumulation, but this is only comparable to wild-type with the degree of induction.

The results for intracellular glycerol accumulation in nonstressed and stressed cells are presented in Figures 3.2 A and 3.2 B.

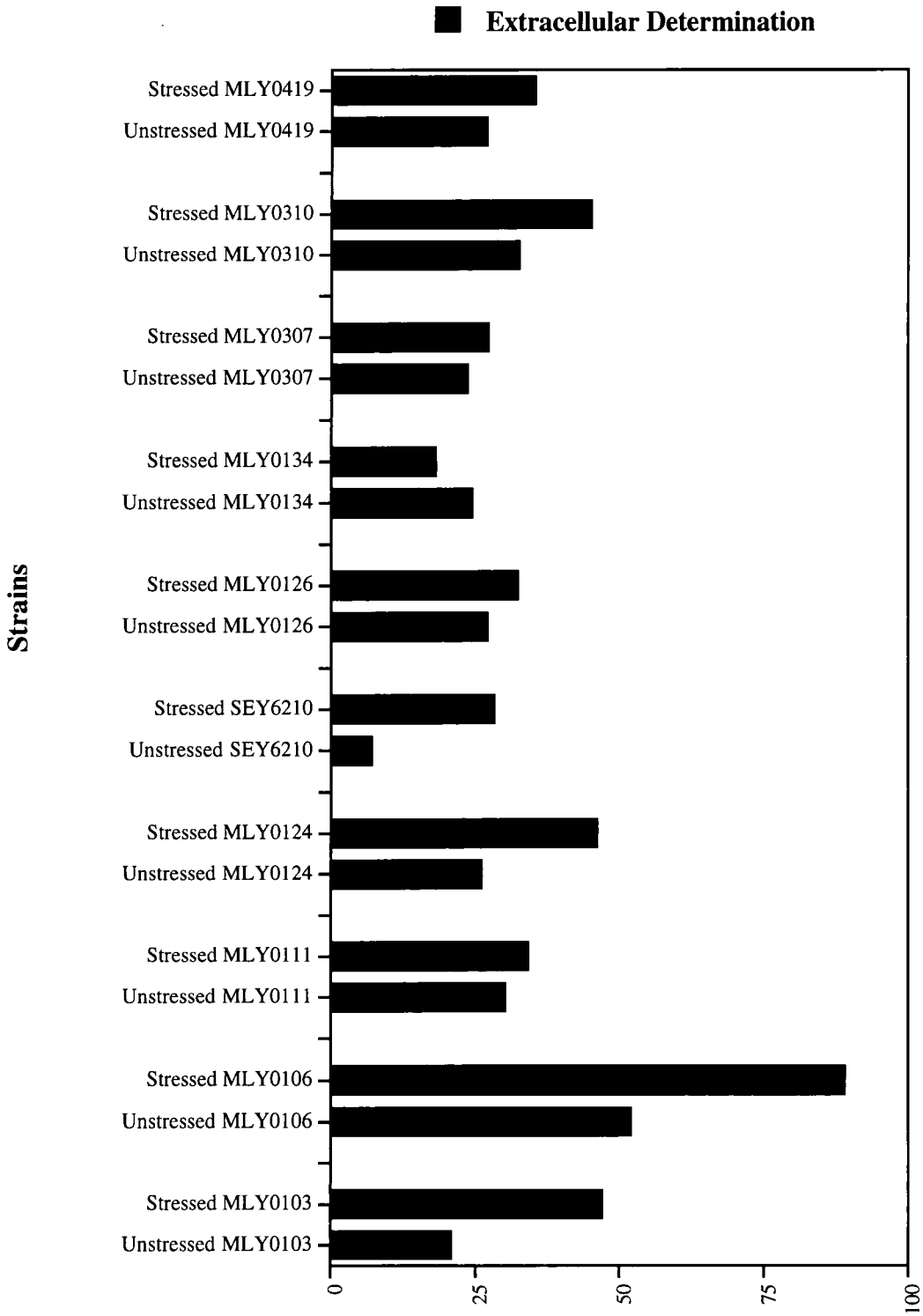

Fig 3.1. A Extracellular Determination of Glycerol under Stressed and Nonstressed conditions

(Units are μg glycerol /10^7 cells)

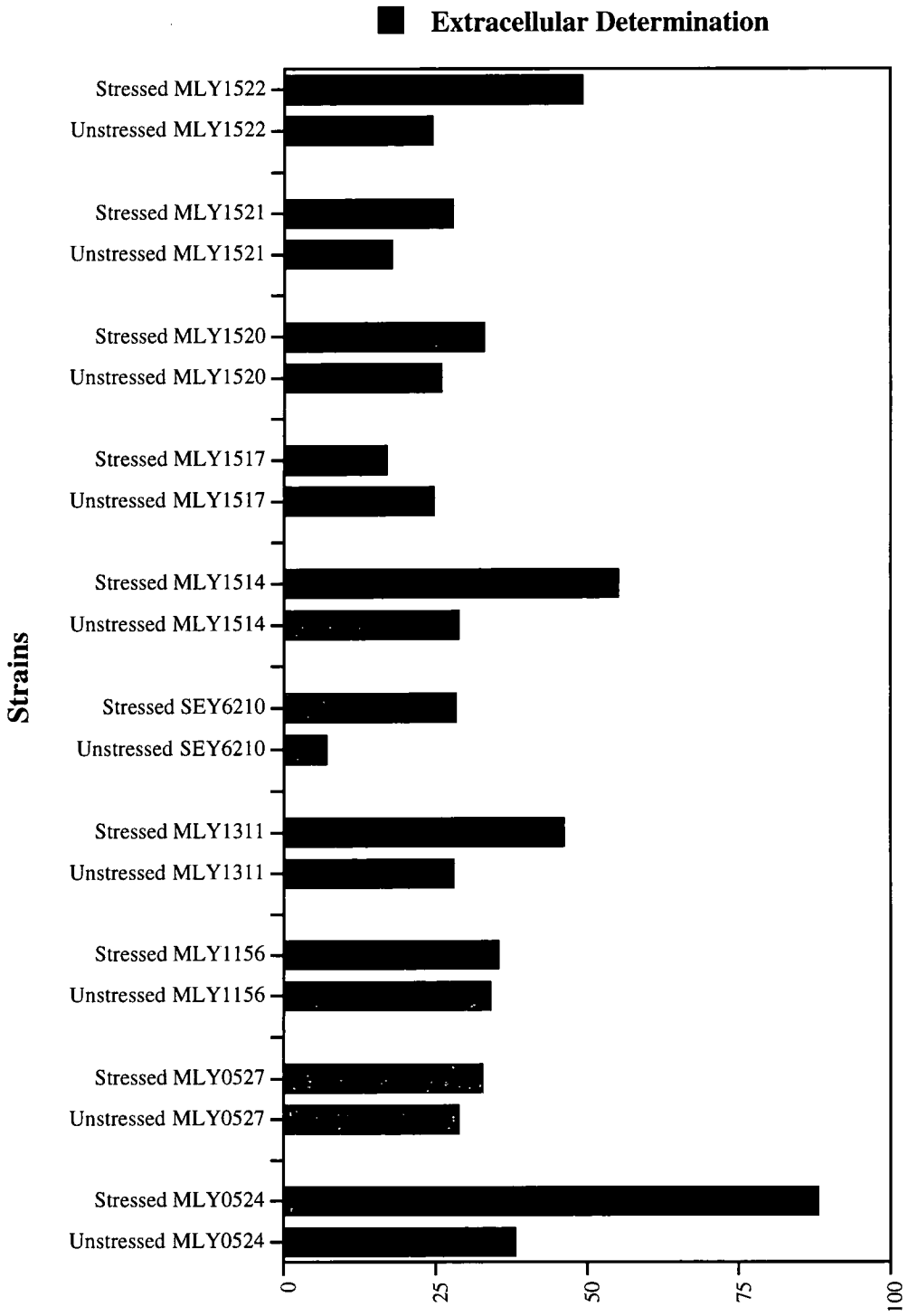

Fig 3.1 B.Extracellular Determination of Glycerol under Stressed and Nonstressed conditions

(Units are μg glycerol / 10^7 cells)

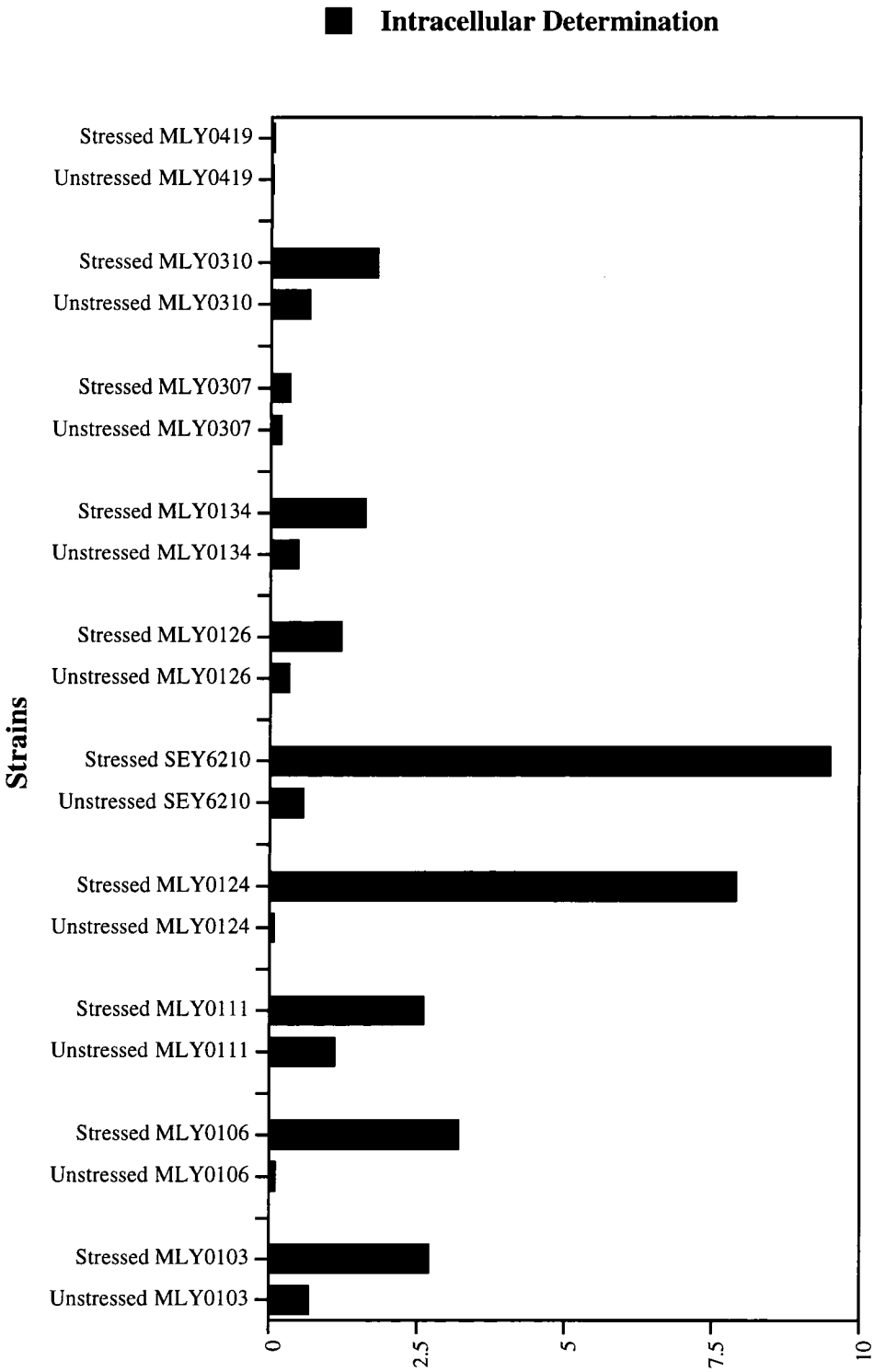

Fig 3.2 A Intracellular Determination of Glycerol under Stressed and Nonstressed conditions

(Units are μg glycerol / 10^7 cells)

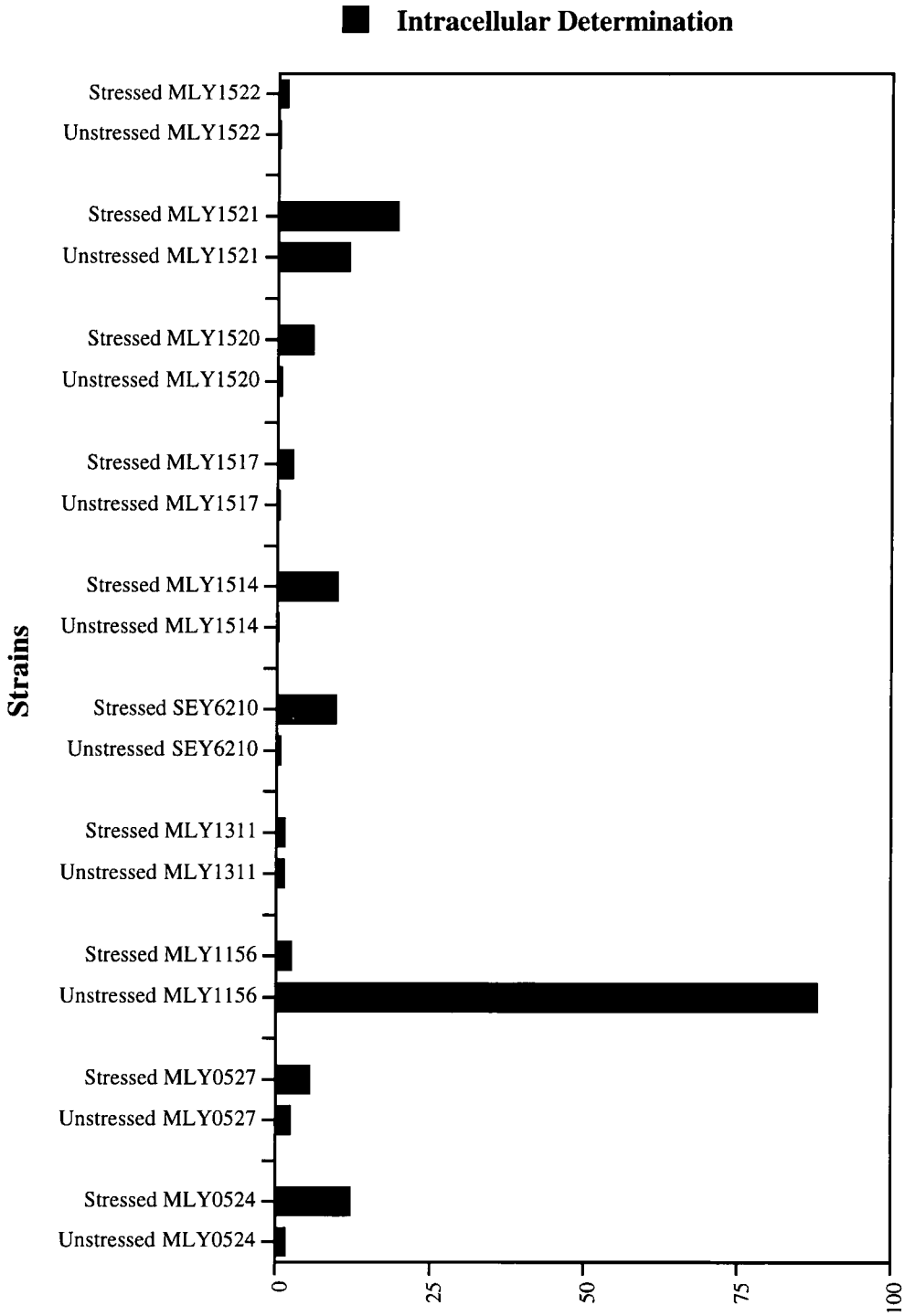

Fig 3.2 B Intracellular Determination of Glycerol under Stressed and Nonstressed conditions

(Units are μg glycerol/ 10^7 cells)

Strains	SSV Group	Mating Type
SEY6210	Wild-type	
MLY0103	*ssv10-1*	α
MLY0106	*ssv1-2*	α
MLY0111	*ssv2-2*	α
MLY0124	*ssv11-1*	α
MLY0126	*ssv4-1*	α
MLY0134	*ssv8-1*	α
MLY0307	*ssv1-7*	a
MLY0310	*ssv9-1*	a
MLY0419	*ssv17-100*	a
MLY0524	*ssv5-1*	a
MLY0527	*ssv6-1*	a
MLY1156	*ssv16-1*	a
MLY1311	*ssv9-7*	a
MLY1514	*ssv3-1*	a
MLY1517	*ssv7-1*	a
MLY1520	*ssv12-1*	α
MLY1521	*ssv14-1*	α
MLY1522	*ssv13-1*	α

Table 3.1 Yeast strains used in the determination of glycerol accumulation.

3.3 DISCUSSION.

The mutant strains of yeast involved in this investigation, of intracellular and extracellular accumulation of glycerol under normal and NaCl stressed conditions are shown in Table 3.1. The levels of glycerol accumulation vary markedly from one strain to another. The results presented here indicate that many of the *ssv* mutant strains are capable of accumulating elevated levels of internal glycerol when subjected to salt stress (Fig 3.2). This shows that in these strains the osmosensitive phenotype is not due to a deficiency in glycerol metabolism.

The *ssv* mutant strains that exhibit levels of internal glycerol accumulation upon osmotic stress similar to the wild-type strain SEY6210 are MLY0524, MLY0527, MLY0124, MLY1514, MLY1520 and MLY1521. Several strains show slight induction of internal glycerol accumulation but the levels are much lower than that found in SEY6210. These strains are MLY0103, MLY0106, MLY0111, MLY0126, MLY0134, MLY0310, MLY1517 and MLY1522. Two strains show reduced levels of internal glycerol accumulation with no induction upon salt stress. These are MLY0307 and MLY1311. The two remaining strains show unusual glycerol accumulation patterns. MLY0419 shows almost no glycerol accumulation with or without salt stress. MLY1156 shows extreme elevation of glycerol accumulation upon salt stress, almost four times the levels displayed by any other strain.

The analysis of the extracellular accumulation is more complex, either with or without comparison with the intracellular levels. Most of the strains show some degree of enhanced glycerol accumulation upon salt-stress. Strains that are similar to wild-type in their behaviour are MLY0103, MLY0124 and MLY0310. Strains MLY0106, MLY0524, MLY1311, MLY1514 and MLY1522 all show increased glycerol accumulation upon salt-stress, however, the basal levels are much higher than in the wild-type strain. This particularly noticeable with MLY0106 and MLY0524. The remaining strains show almost no increase in extracellular glycerol accumulation upon salt-stress. However, it should be noted that in all these strains the basal level is higher than that found in the wild-type strain, often as high as the wild-type stressed level.

Glycerol accumulation is regulated by a number of proteins. Most important amongst these are cytoplasmic glycerol-3-phosphate dehydrogenase (GPDH) and the action of a glycerol channel that mediates transport across the plasma membrane. Glycerol is in fact freely diffusible across the plasma-membrane, but export is greatly enhanced by the channel. This is encoded by the *FPS1* gene and facilitates the rapid loss of glycerol when osmotic stress has been relieved (Luyten *et al*,1995). Fps1p is rapidly inactivated upon

salt stress. GPDG is encoded by the *GPD1* gene. Mutations in *GPD1* cause an osmosensitive phenotype (Albertyn *et. al,* 1994). The activity of glycerol-3-phosphate dehydrogenase (GPDH) which links glycerol formation to glycolysis, is enhanced in cells growing under osmotic stress (Blomberg and Alder ,1989). *GPD1* expression is induced by salt-stress under the control of the High Osmolarity Glycerol (HOG) signal transduction pathway.

In a parallel study to the experiments described here the levels of GPDH activity were determined in other *ssv* strains under normal and salt-stressed conditions (Eleanor Harwood, personal communication). Only one of these strains, MLY0419, was the same as those investigated here. This is a particularly interesting strain as it accumulates almost no internal glycerol. A possible reason for this could be a lack of GPDH. This, however, seems unlikely if the external glycerol accumulation is considered where the levels seem almost normal, although no induction under salt-stress is observed. The presence of functional GPDH in MLY0419 is confirmed by the enzyme assays in Harwood's experiments. The levels of enzyme activity are normal under non-stressed conditions but are elevated five-fold by osmotic stress. These data present a paradox. The glycerol accumulation data suggests some defect in glycerol metabolism, but the enzyme data would suggest that glycerol accumulation should be elevated.

Such conflicting results appear to be normal for the *ssv* strains, GPDH enzyme levels do not correlate in any consistent way with glycerol accumulation. Both the enzyme assays and glycerol data are reproducible. The enzyme assays were performed in triplicate on independent cultures and the glycerol accumulation data reproduced by others (B. Popping, personal communication). There is one other factor affecting the data that cannot be excluded and that is in the experimental design itself. In the measurement of intracellular glycerol, concentrations are expressed as μg glycerol per 10^8 cells. However, as cells are subjected to salt-stress there is an immediate cell shrinkage followed by a recovery period where the original cell volume is restored (Albertyn *et al*, 1994). It is possible that some of the salt-sensitive strains are unable to recover their original cell volume or may have unusually large cells and these discrepancies could lead to a natural variation in glycerol concentrations. The intracellular glycerol concentration per ml of cytosol could be the same for two strains but if the cell volumes are different glycerol concentration per cell number will also be different. Therefore some of the cells with low or high intracellular glycerol concentrations may be behaving in the same way as the parent strain in terms of glycerol production but have an abnormal cell size or morphology.

The low levels of glycerol produced after salt-stress may reflect defects in the osmosensing signal transduction pathway (HOG pathway) or alternatively may be due to

the inhibitory effects of Na^+ ions on the metabolic processes of the yeast cells (Singh and Norton, 1991). The Na^+ ions could have a direct affect on the activity of enzymes involved in glycerol synthesis. The activity of glycerol-3-phosphate dehydrogenase in the closely related yeast *Saccharomyces carlsbergensis* is known to be inhibited by Na^+. The excess Na^+ ions may perturb the ability of the cell to maintain a correct intracellular Na^+ concentration thus causing the inhibition of glycerol accumulation. It has been reported that K^+ has an inhibitory effect on GPDH activity (Gancedo et al, 1968; Meikle et al, 1991) but that this is not normally of physiological significance because the majority of intracellular K^+ is located in the vacuole. Vacuole biogenesis mutants investigated by Latterich and Watson (1991) showed that *ssv* and *vps* strains show defects in the osmoregulation response. This may be correlated with the abnormal vacuolar morphology displayed by many of these strains. Indeed all of the osmosensitive *vps* mutants have aberrant or even absent vacuoles. These may be altered in K^+ ion storage and thus have less than optimal GPDH activity.

The events that occur during osmotic stress of *S. cerevisiae* can be compared with those that occur in the halotolerant yeast *Zygosaccharomyces rouxi.* This organism is capable of growth on 4M NaCl. During the exposure of *Z. rouxi* to salt the levels of cAMP rise quickly and reach a maximum within 10 min and then decline. The maximum levels are about 4.6 times higher than the initial intracellular levels. Adenylate cyclase activity increases immediately after exposure of cells to salt. However, the activity of phosphodiesterase (PDE), which hydrolyses cAMP to AMP increases more slowly after salt stress and reaches a maximum level at 25min. The increase in PDE activity results in a decrease in the cAMP content of cells (Nishi, et al 1993). This result links the increase in the cAMP content of cells to the intracellular and extracellular accumulation of glycerol and to the activity of a plasma membrane ATPase during salt stress. The basal levels of glycerol content is much higher in *Z. rouxii* and increases proportionally less than *S. cerevisiae* during salt-stress.

These studies show the difficulties in measuring glycerol accumulation as a measure of defects in the HOG pathway. Although this has been successfully used by Schuller et al (1994) to identify the *HOG1* and *PBS2 (=HOG4)* genes it is not a reliable method for determining activation of the signal transduction pathway. A more reliable method would be the construction of a good reporter gene system such as *GPD1::lacZ* or *GPD1::GFP* fusions. Other people in the laboratory have attempted to construct a usable *GPD1::lacZ* system (E. Harwood, personal communication).

CHAPTER 4

SEQUENCE DETERMINATION OF THE RIGHT SUBTELOMERIC REGION OF CHROMOSOME VII

4.1 Introduction.

The sequencing of the entire genome of the budding yeast *Saccharomyces cerevisiae* has been successfully completed by a world-wide consortium of laboratories. About 12 kb of the right end of chromosome VII has been sequenced successfully in our laboratory. The region of interest was the immediate sub-telomeric sequences at the far - right hand end of chromosome VII. In the context of this study, I determined the nucleotide sequence of several restriction fragments from within cosmid pEGH344. The complete nucleotide sequence of 12,226 bp was achieved by using an appropriate directed sequencing strategy in combination with automated DNA sequencing.

The aim of this chapter is to describe the subcloning and sequencing of the 4.6 and 9.2kb EcoRI fragments from pEGH344.

4.2. Sequencing of the 4.6 kb EcoRI Fragment.

4.2.1 Isolation and Cloning of the 4.6kb EcoRI fragment.

The right sub-telomeric region of chromosome VII was determined to lie within cosmid pEGH344 (Tettelin, personal communication). pEGH344 is the rightmost of a series of overlapping cosmids that cover all of chromosome VII. The left neighbour of pEGH344 is cosmid pEGH452, whose sequence was determined by Volckaert and colleagues. It was determined by the chromosome VII coordinator (Tettelin) that the 4.6kb EcoRI fragment of pEGH344 was the rightmost and this was adjacent to a 9.2kb EcoRI fragment that partially overlaps pEGH452 (Fig 4.1). The aim of this work was to sequence the entire 4.6kb fragment and about 7kb of the 9.2kb fragment to overlap pEGH452 by approximately 500bp.

pEGH344 DNA was purified and digested with EcoRI. The fragments were separated by agarose gel electrophoresis and visualised by UV light (Fig 4.2). The 4.6 kb fragment was excised, purified and ligated with EcoRI cut Bluescript pSK$^+$. *Escherichia coli* DH5α cells were transformed with the ligation mixture. The transformed cells were plated onto L- agar plus ampicillin and X-gal. A few white colonies were picked, purified and then used to inoculate individual 10 ml of LB broth plus ampicillin cultures. The cells were allowed to propagate overnight at 37°C with continuous shaking. Wizard minipreps were carried out in order to isolate the plasmid DNA. 5µl samples of each miniprep was mixed with EcoRI, incubated for 3-4 hours at 37°C and then mixed with

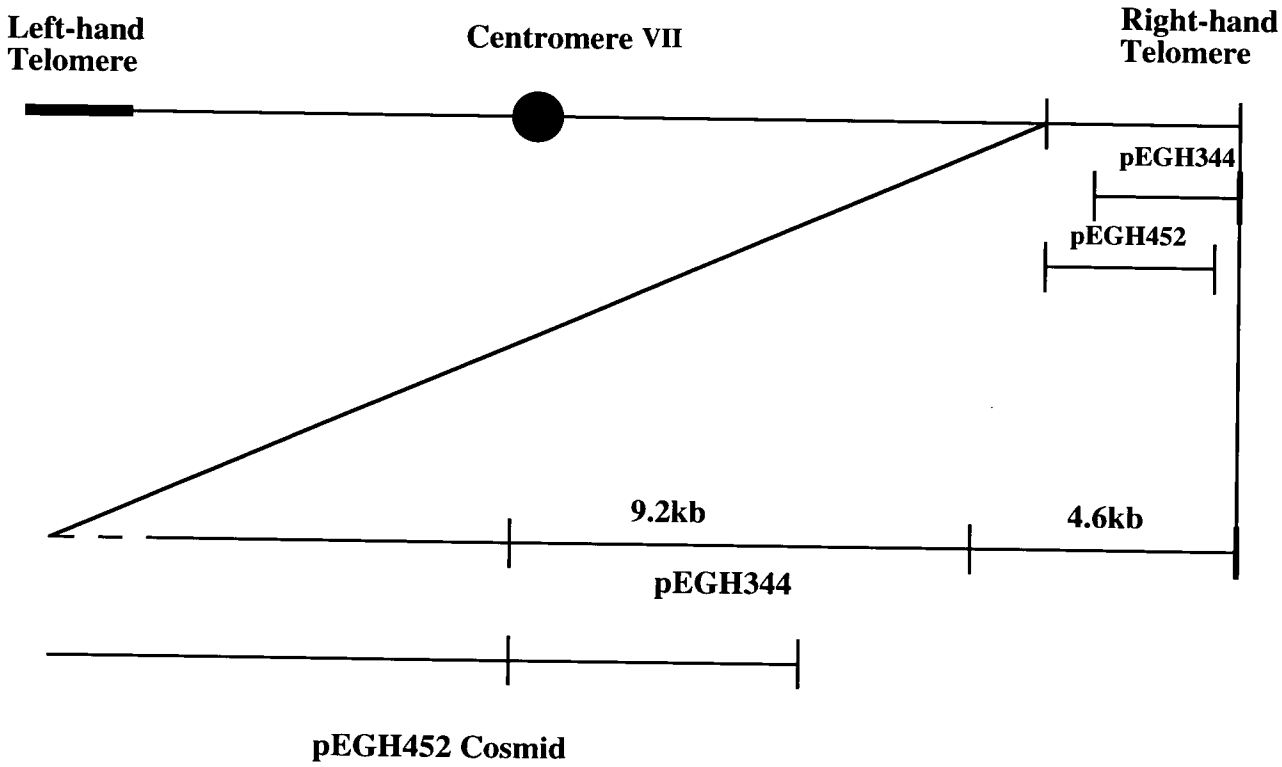

Fig 4.1. The overlapping cosmids at the right end of Chromosome VII.
Cosmid pEGH344 at the extreme right end is adjacent to cosmid pEGH452.

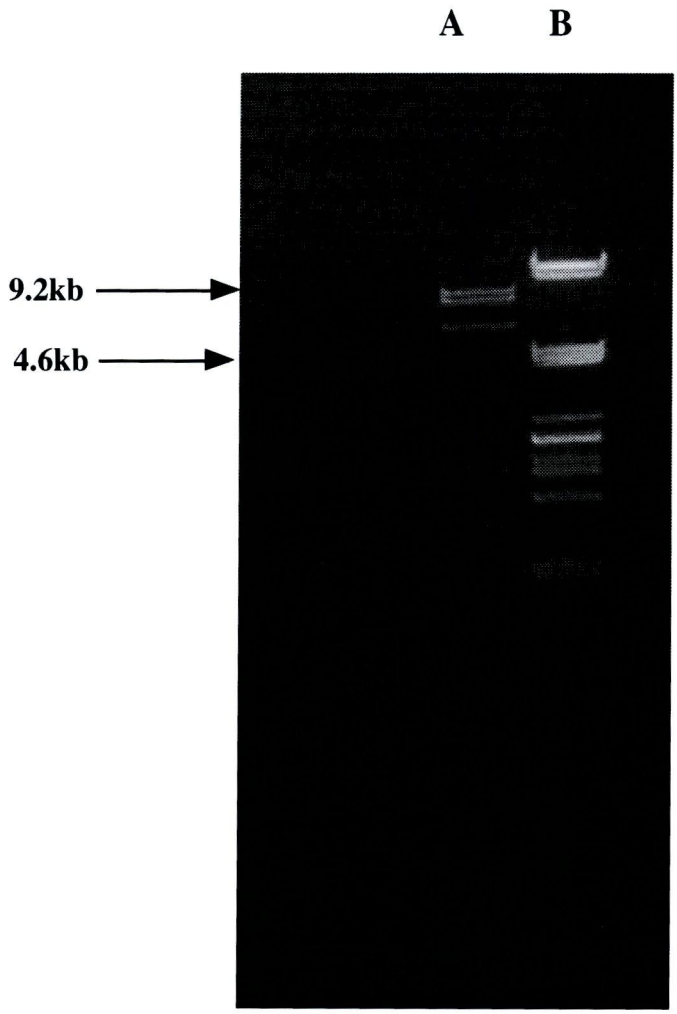

Fig .4.2. EcoRI digestion of cosmid pEGH344.
Lane A is cosmid pEGH344. Lane B lis λ PstI size marker

loading dye and analysed by 0.7% agarose gel electrophoresis. Fig 4.3 shows the digestion of plasmid DNA from one of these cultures. It clearly shows the presence of 4.6kb EcoRI fragment. This plasmid was named pECY2. The sequence of the 4.6kb fragment ends was determined by sequencing pECY2 with normal forward and reverse primers.

4.2.2 Restriction mapping and subcloning of pECY2.

Using restriction enzymes BamHI EcoRI PstI and Xbal, a partial restriction map of pECY2 was constructed (Fig 4.4). To generate deletions of pECY2, 5 µl of DNA was digested separately using 2 µl of each restriction enzyme. After gel electrophoresis the largest fragment for each restriction digest (Fig 4.5) was isolated and purified using the silica fines method. The fragments were then self-ligated to recover the appropriate deletion derivative. See figure 4.6 for a schematic showing the generation of the BamHI deletion. The principle is the same for the other enzymes. High purity DNA was prepared from transformed bacteria using the Wizard minipreps protocol. The plasmid DNA was sequenced in both directions using standard forward and reverse primers.

4.2.3 Shotgun sequencing of pECY2.

There are three strategies available for sequencing large DNA fragments, firstly shotgun sequencing, secondly nested-deletions and lastly primer walking. The first two of these methods were tried with pECY2. This section describes the first of these. Random cloning and sequencing known as shotgun sequencing is often the method of choice for determining the nucleotide sequencing of large fragments of DNA. In this method random short DNA fragments are generated and then cloned. Individual clones are then sequenced. In this investigation the random fragments were produced by sonication.

Four sets of 20µl of pECY2 and 430µl TE were mixed in an eppendorf tube. The DNA was sonicated at maximum power for 10, 20, 30 or 40 seconds and then ethanol precipitated overnight. The DNA was washed and resuspended in 10µl TE. The sonicated fragments were separated by agarose gel electrophoresis (Fig 4.7). Fragments from 0.52-1.09kb were excised, purified and then repaired by T4 DNA polymerase. The repaired fragments were ligated into pUC19 cut with HindII and then transformed into DH5α. After growth on L-agar plus ampicillin and X-gal, the white colonies that were formed were picked and purified. Wizard minipreps were made of each plasmid and the sequence of each was determined using forward and reverse primers.

4.2.4 Nested deletions of pECY2D.

The generation of ordered nested-deletions is the most efficient method for the rapid sequencing of medium size (< 10kb) DNA fragments. For its successful operation two unique restriction sites are required adjacent to one end of the fragment to be sequenced.

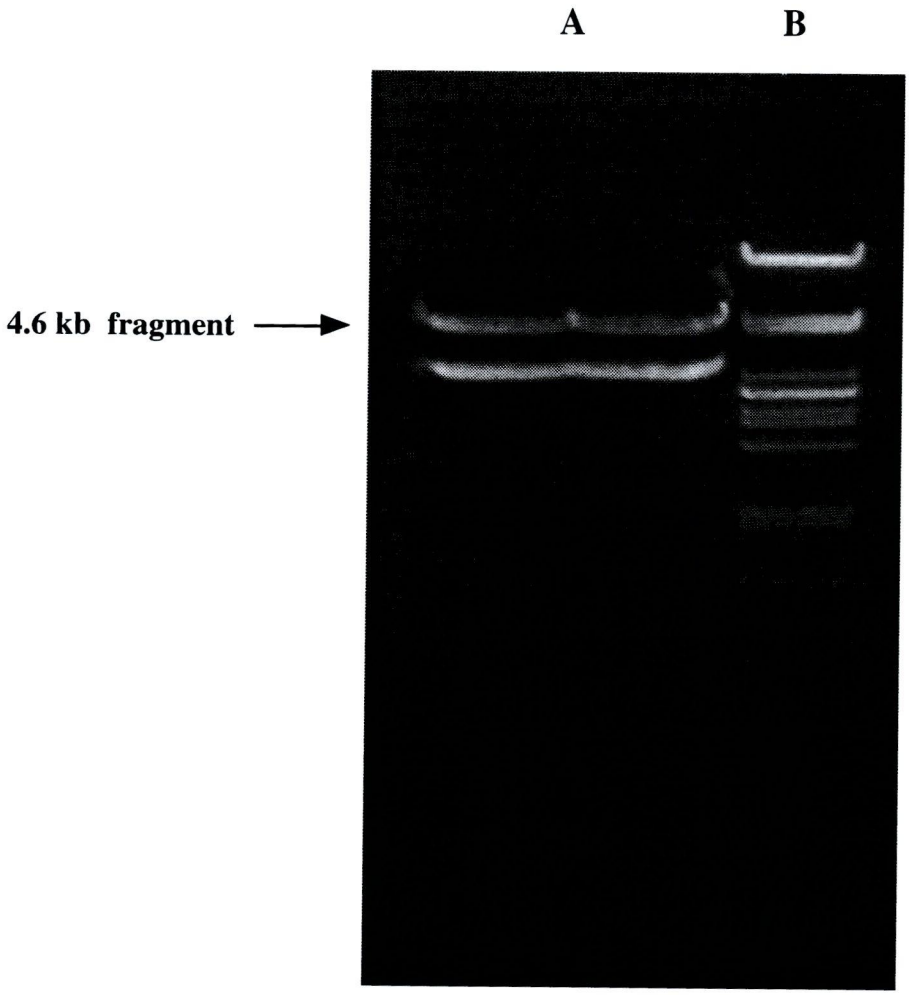

Fig .4.3. Restriction analysis of pECY2.
Lane A. pECY2 digested with EcoRI.
Lane B. λPstI size markers.

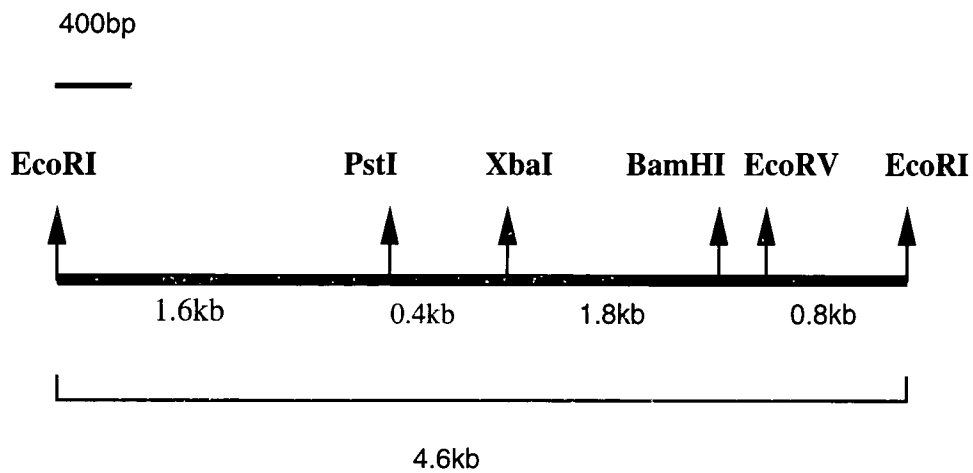

Fig 4.4. Restriction map of the pECY2 insert.

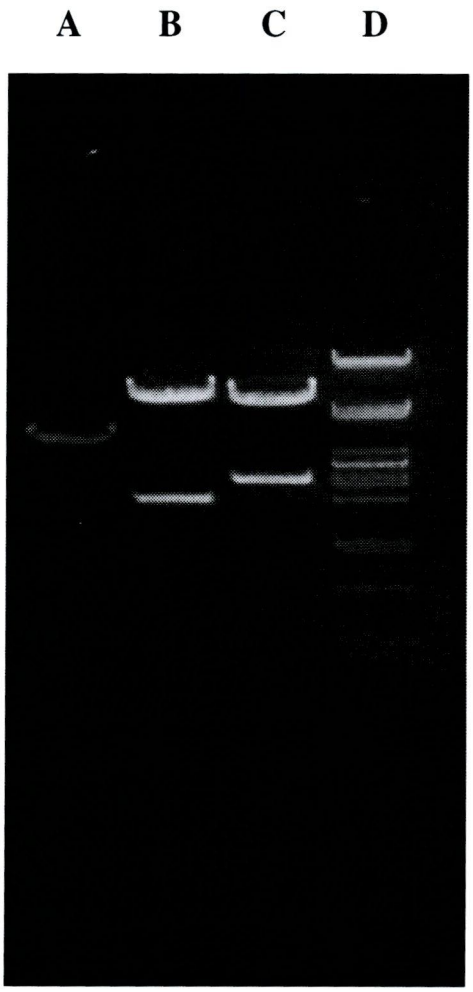

Fig.4.5. Restriction digests of pECY2

Lane A. Digestion with BamHI.
Lane B. Digestion with PstI.
Lane C. Digestion with XbaI.
Lane D. λ PstI size marker.

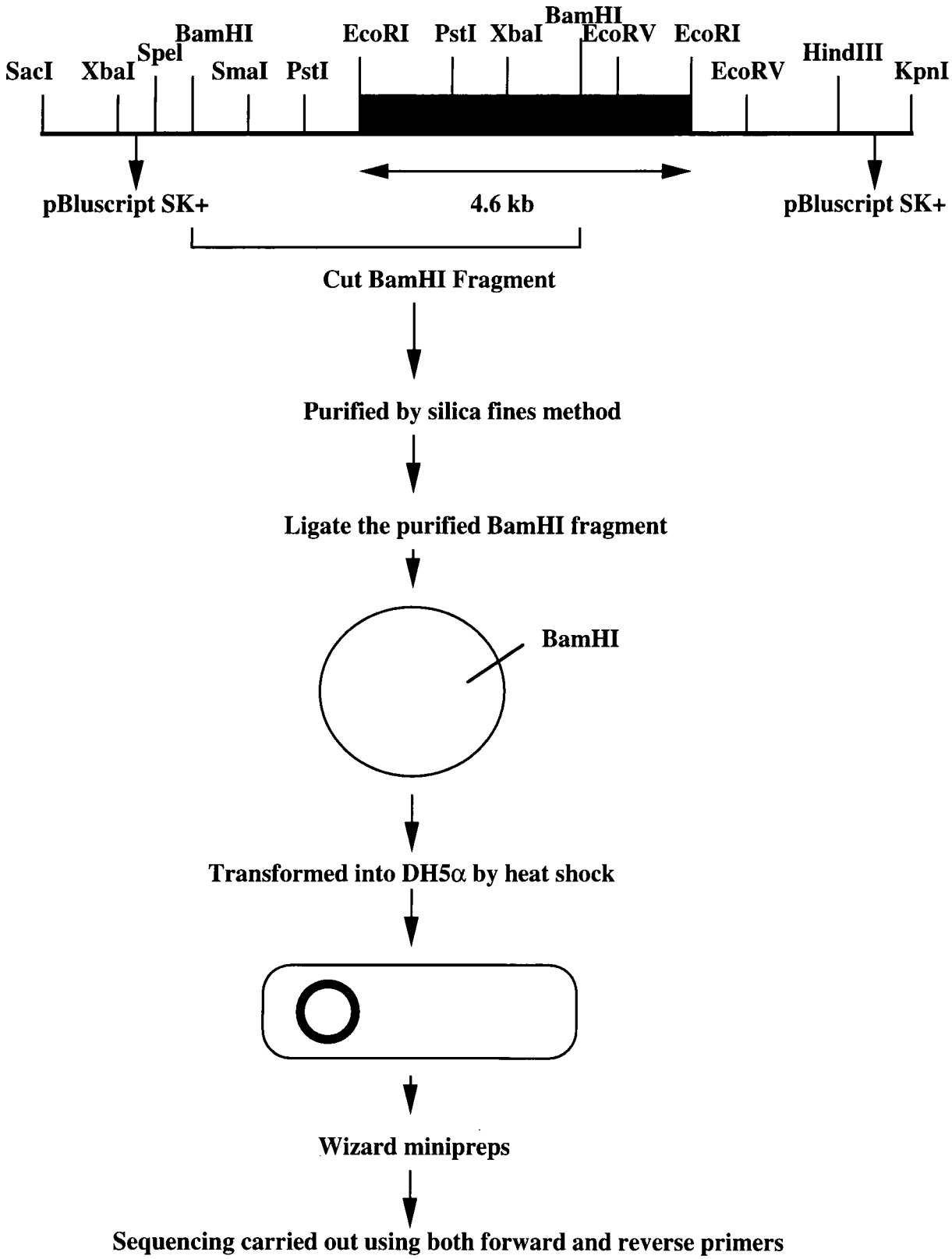

Fig 4.6. Isolation, purification and recloning of the BamHI fragment of pECY2

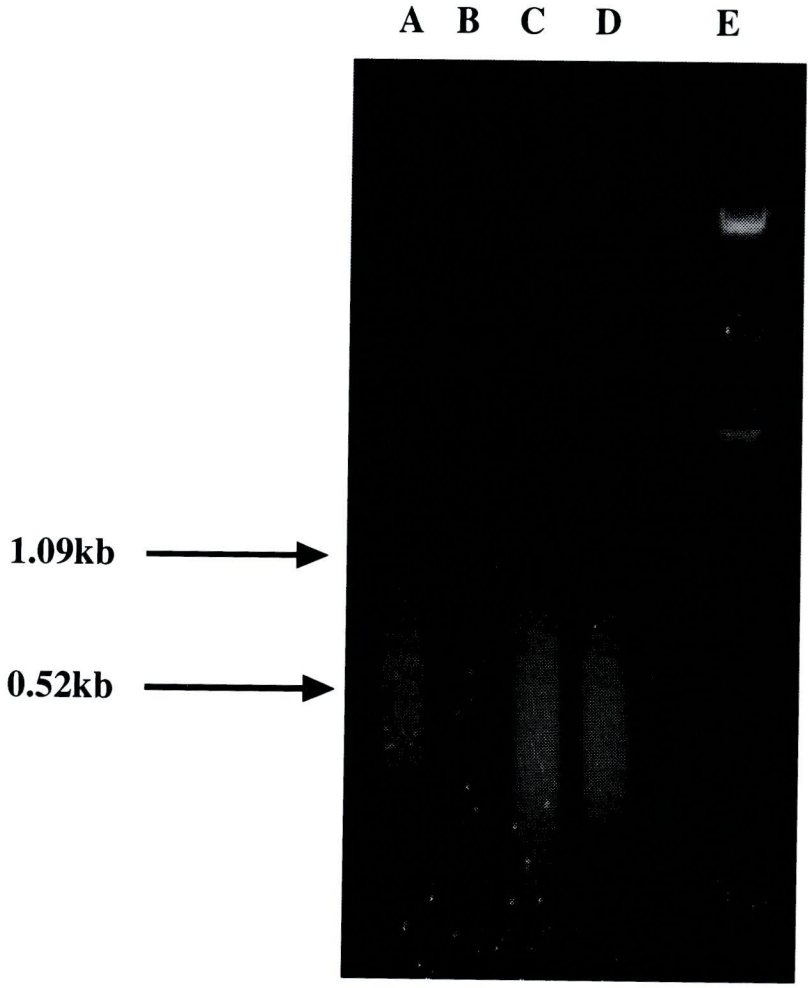

Fig 4.7. Sonication of pECY2 plasmid DNA.
Lane A-D. Sonicated DNA for 10, 20, 30 and 40 seconds respectively.
Lane E. λ PstI size marker.

The site nearest to the fragment should have either a 5' protruding or a blunt end, whereas the distal site must have an exonuclease III resistant 3' protruding end.

pECY2 has the 4.6 kb EcoRI fragment cloned into Bluescript pSK+. This vector has been specifically designed for the generation of nested-deletions through exonuclease III digestion. Unfortunately the right-hand end of the fragment (as shown in Fig 4.6) had a lack of suitable restriction sites. This could be remedied by the simple removal of the small EcoRV fragment and religation of the remainder. pECY2 DNA was cut with EcoRV in order to isolate the 7.1kb fragment of interest (Fig 4.8). After purification the fragment was treated with ligase in order to recircularise it and then transformed into DH5α. Four transformants were selected and minipreps of the plasmid DNA carried out. The plasmid DNA was restricted by separately by EcoRI, EcoRV and BamHI (Fig 4.9) to make sure that the EcoRV fragment had been deleted. Correct deletions will have lost one of the two EcoRI sites and be linearised upon EcoRI digestion (Fig 4.9 B). BamHI digestion of pECY2 generates two fragments of identical size (See fig 4.5 Track A). Correct deletions will now generate two clearly separable bands(Fig 4.9 C). All four transformants have plasmid DNA that conforms to the predicted pattern for the correct deletion. One of these was selected and the plasmid named pECY2D. This plasmid was sequenced using both forward and reverse standard primers. Pairs of enzymes were selected for the generation of linearised pECY2D suitable for exnucleaseIII digestion. For the generation of "rightward" deletion (See Fig 4.6) SacI and EcoRI were used. For the generation of "leftward" deletions KpnI and EcoRV were used.

After linearising the plasmid DNA in order to create one end susceptible to exonuclease III degradation (EcoRI or EcoRV) and an end resistant to exonuclease III degradation (SacI or KpnI), the DNA was digested with exonuclease III. The digestions were carried at 37°C in the presence of 75mM NaCI. By taking time samples every 2.5 minutes deletions of 300bp steps should be generated. 19 timed samples were taken. The single-stranded DNA was removed by treatment with Mung Bean Nuclease and the remaining DNA recircularised by ligation.

After transformation into DH5α, colonies were purified and plasmid DNA extracted. Intact plasmid DNA was electrophoresed on 0.7% agarose gels to determine the extent of the deletions (Fig 4.10). Plasmids with suitable sized deletions were then sequenced with either the forward or reverse primers according to the direction of the deletion.

4.2.5 Compilation of sequences of pECY2 (4.6kb).

The separate DNA sequences were assembled and edited into a single contig by the program Sequencher. Fig4.11 shows the assembled contig. In total 62 overlapping

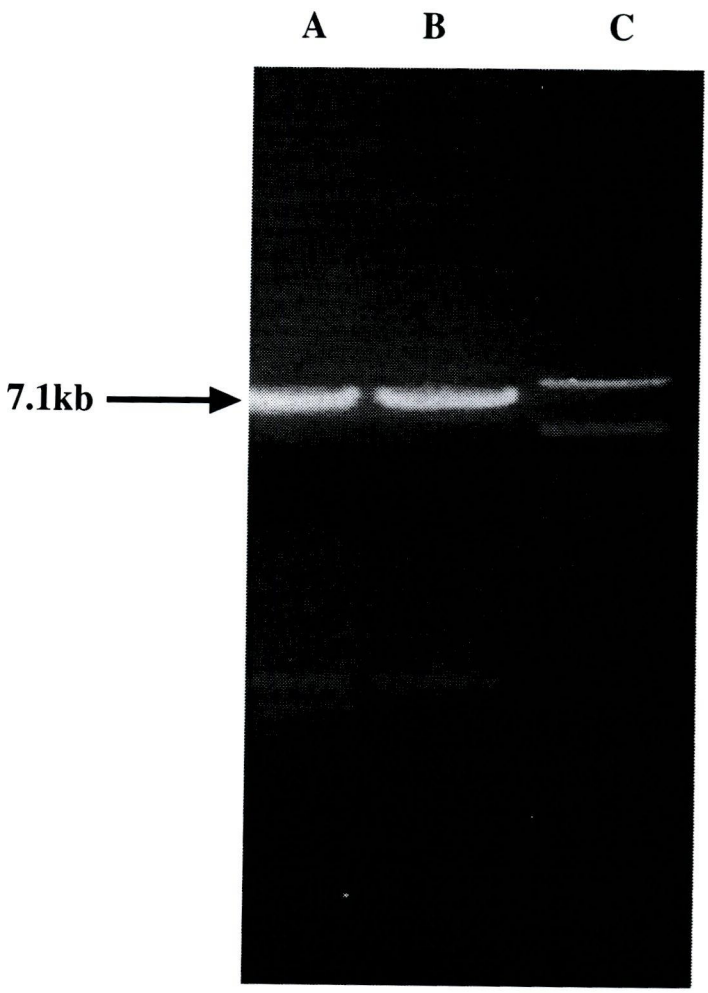

Fig 4.8. EcoRV digestion of pECY2.
Lanes A and B. EcoRV digestion of pECY2.
Lane C. λ PstI size marker.

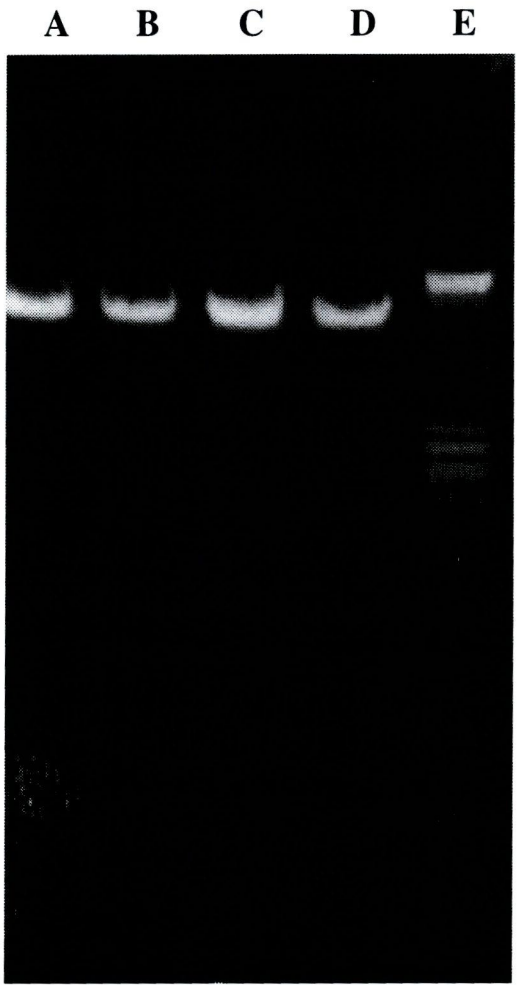

Fig 4.9A. Restriction analysis of EcoRV deletion derivatives of pECY2.

Lanes A to D. EcoRV digestion of miniprep DNA from different isolates of the deletion derivatives.

Lane E. λ PstI size marker.

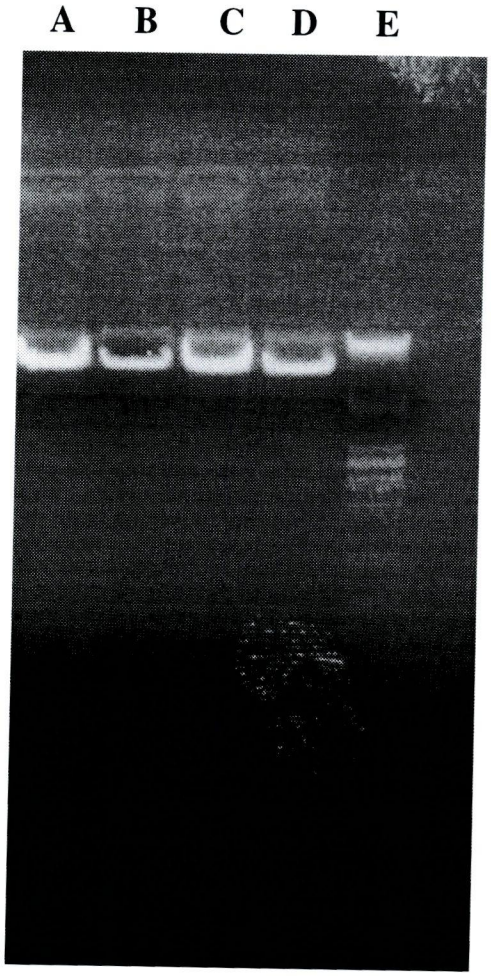

Fig 4.9B . Restriction analysis of EcoRV deletion derivatives of pECY2.

Lanes A to D. EcoRI digestion of miniprep DNA from different isolates of the deletion derivatives.

Lane E. λ PstI size marker.

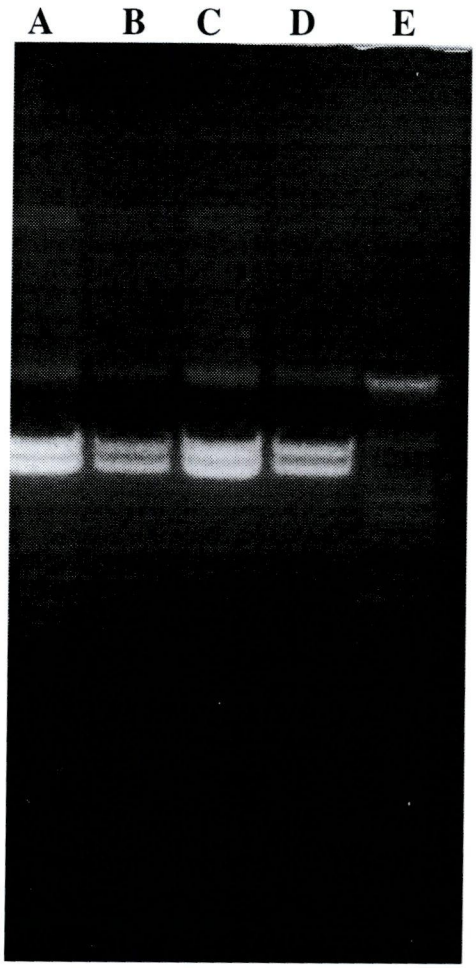

Fig 4.9C. Restriction analysis of EcoRV deletion derivatives of pECY2.

Lanes A to D. BamHI digestion of miniprep DNA from different isolates of the deletion derivatives.

Lane E. λ PstI size marker.

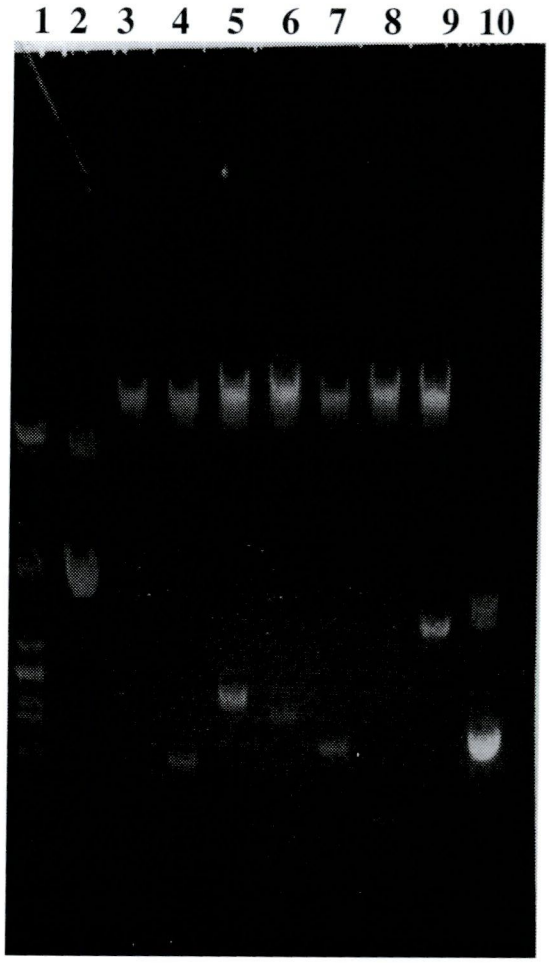

Fig 4.10. Nested deletions of pECY2D.

Lanes 3-9 undigested minprep DNA from different nested deletion isolates of pECY2D.

Lane 1. λ PstI size marker.

Lane 2. Undigested pECY2D DNA.

Lane 10. Undigested Bluescript plasmid DNA.

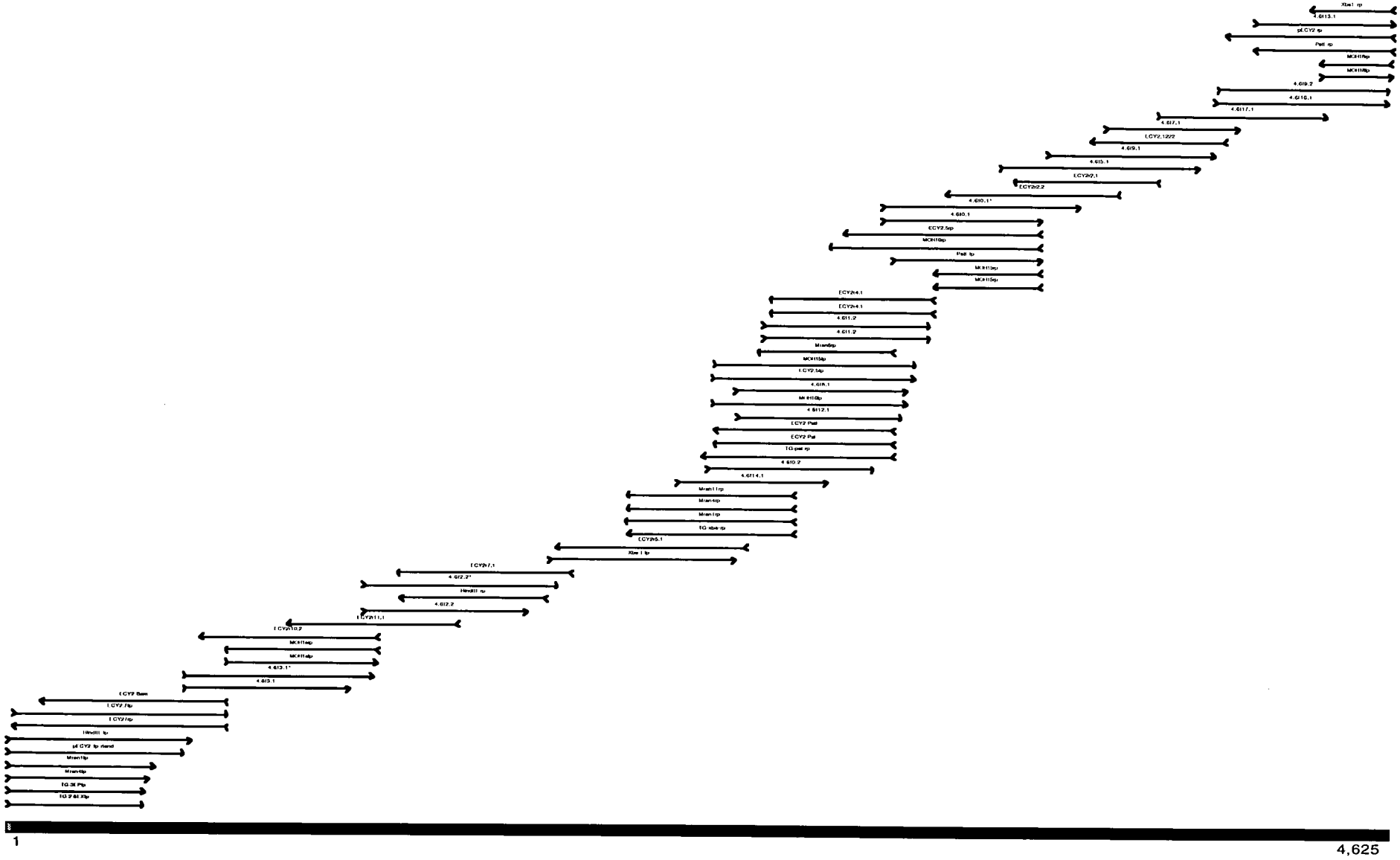

Fig 4.11. Compilation of all the overlapping sequencing runs of the 4.6kb EcoRI fragment.

fragments were sequenced to determine completely the 4625bp of the pECY2 insert on both strands.

4.3 Sequencing of 9.2kb EcoRI fragment.

4.3.1 Subcloning of the 9.2kb fragment.

Cosmid pEGH344 DNA was purified and a large scale digestion with EcoRI carried out. The resultant fragments were separated by agarose gel electrophoresis (see Fig 4.2). The slowest migrating band corresponds to the 9.2kb fragment plus also the 8.1 kb fragment of the vector pWE15. These two co-migrating bands were purified from the gel and ligated into EcoRI digested Bluescript pSK$^+$. After overnight ligation the DNA was transformed into DH5α and plated onto L-Amp+Xgal plates. Although several white colonies appeared, upon analysis none ever contained the 9.2kb fragment (Data not shown). Other strategies were tried, for example releasing the cosmid insert from within pEGH344 by NotII digestion, purifying the insert free from pWE15 vector, and then subsequent EcoRI digestion and ligation as described above. None of these strategies ever resulted in a suitable clone carrying the 9.2kb fragment.

4.3.2 Directed Subcloning of pEGH344.

To overcome the problem of being unable to subclone the 9.2kb EcoRI fragment an alternative subcloning strategy was attempted. pEGH344 was digested separately with BamHI, PstI, XbaI and HindIII. The digested DNA was then electrophoresed on an agarose gel (Fig 4.12) and then transferred to a nylon membrane for Southern blotting. The probe was DIG-labelled 9.2kb EcoRI fragment purified as described in section 4.3.1. Bands that hydridised to the probe were excised from the gel, purified and ligated into the appropriately cut Bluescript pSK$^+$. The ligation mixes were transformed into DH5α and then plated onto L-Amp plus X-gal . White colonies were patched onto duplicate fresh L-Amp plates and grown overnight. One set of plates was then subjected to colony hybridisation using the same probe as before. Only BamHI and PstI derived colonies were positive in these tests (Data not shown). Minipreps were made from the positive colonies and restricted with either BamHI or PstI to confirm the size of the inserts. The BamHI clone, sized 4.4kb was named pAI2 and the PstI clone, containing a 1.7kb insert, was named pAI56. (The purification of the restriction fragments, ligation and screening of the putative colonies was carried out by Ms Aisha Ibrahim as part of an undergraduate project).

4.3.3 Sequence determination of pAI56.

Plasmid pAI56 was cut with HindIII in order to generate two small fragments for further subcloning. The indicated fragments are 0.7kb and 0.4kb in size (Fig 4.13). The two fragments were excised, purified and ligated into pUC19 cut with HindIII. The

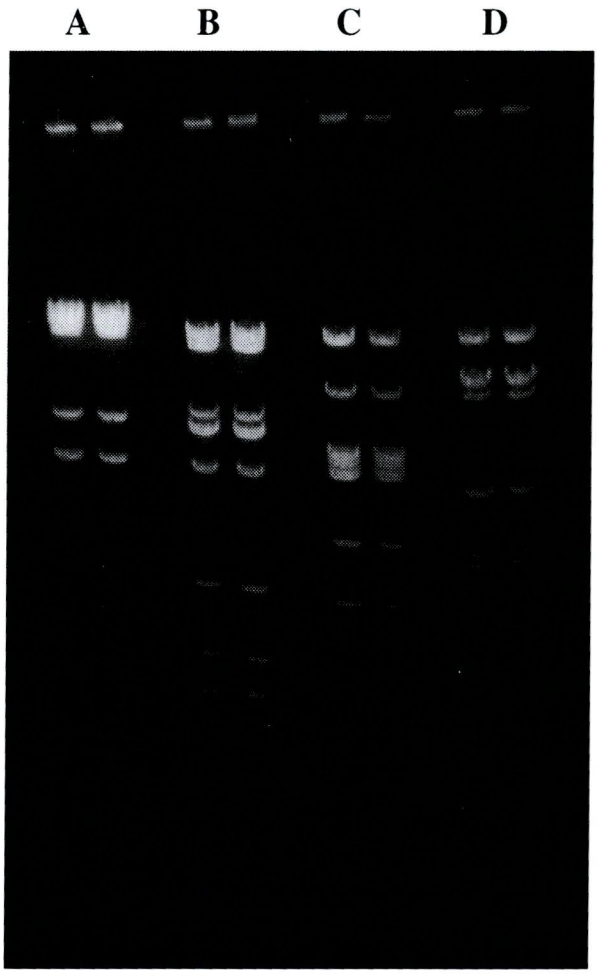

Fig 4.12. Restriction analysis of cosmid pEGH344.

Lane A. BamHI digested DNA.
Lane B. XbaI digested DNA.
Lane C. HindIII digested DNA.
Lane D. PstI digested DNA.

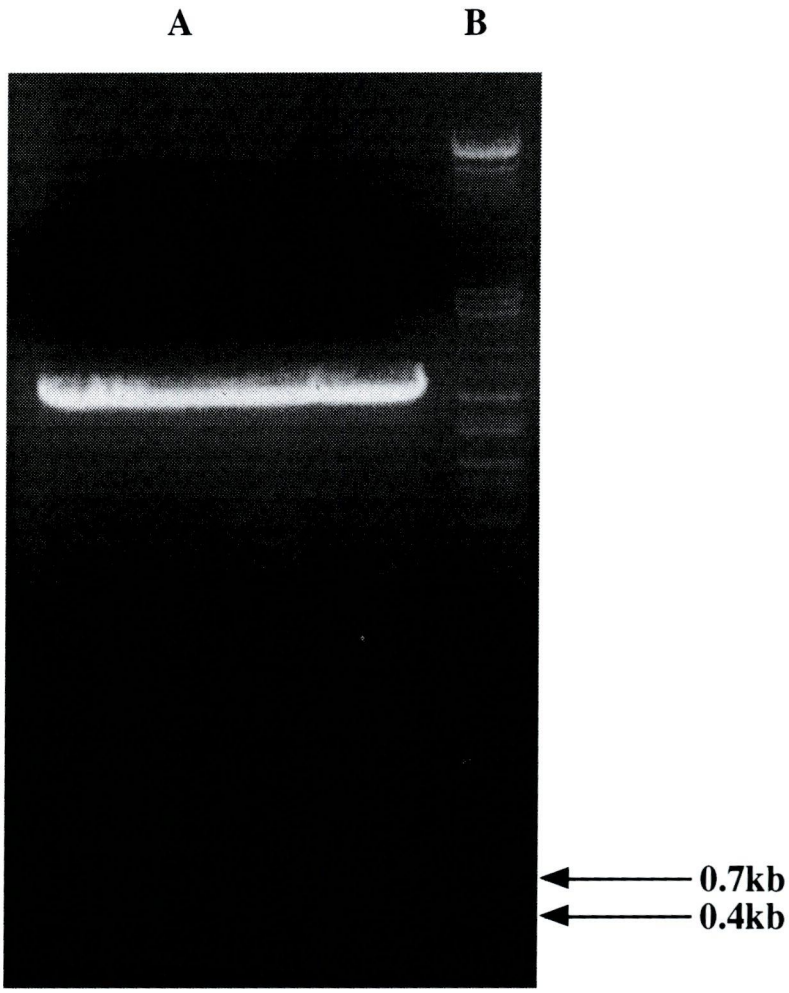

Fig 4.13. Fragment isolation from pAI56 digests.
Lane A. pAI56 digested with HindIII.
Lane B. λ PstI size marker

remaining vector was also excised and recircularised by self-ligation. The ligation mixtures were then transformed separately into DH5α and plated onto L-Amp plus X-gal. White colonies were picked and purified. Plasmid minipreps were carried out and restriction digests confirmed the presence of the correct insert. Plasmid pAI56, the 0.7 and 0.4 kb HindIII subclones and the religated HindIII cut remnant of pAI56 were sequenced using both forward and reverse standard sequencing primers (see Fig 4.14).

Preliminary restriction mapping of pAI56 revealed the presence of two SacI sites one of which must be in the cloned insert. pAI56 was digested with SacI and the two generated fragments separated by agarose gel electrophoresis excised and purified. The larger fragment (consisting of vector plus insert fragment) was self-ligated. The smaller fragment was ligated into SacI cut Bluescript pSK^+. After transformation into DH5α, several colonies were picked and purified. Plasmid minipreps were made and samples digested with SacI. Agarose gel electrophoresis of the digests alongside SacI digested pAI56, confirmed the correct subclones had been obtained (Fig 4.15). The religated SacI digested pAI56 was called pECY6 and the subcloned SacI fragment named pECY7. These two plasmids were subjected to automated DNA sequencing using forward and reverse primers.

The 0.4kb HindIII fragment (MAI56H3x.4 in Fig 4.14) sequences overlapped the right flanking sequence of pAI56 (pAI56-56rp), pECY6 and the known short sequence 500bp from the right end of cosmid pEGH452 (EGH452int). (This is the overlapping cosmid to the left of pEGH344). This latter result immediately confirms that the 9.2kb EcoRI fragment is the one that spans both pEGH452 and pEGH344 cosmids. (Volckaert and Tettelin, personal communication). The 0.7kb HindIII fragment sequences overlapped with pECY7 and the known right hand end of pEGH452 (AI56-prim2) and a sequence obtained from pEGH344 using this border sequence as a primer (EGH344-2). The remnant of pAI56 (MAI56H3rp) overlapped with the left hand end of pAI56 itself. To join all of these fragments together oligonucleotide primers were designed to extend the sequence beyond that already determined. These primers (Designated 1223-1226 in Fig 4.14) all used pAI56 as a template. The sequences obtained using these primers was sufficient to assemble all of pAI56 into a complete contig sequenced on both strands.

4.3.4. Construction of pECY8 and pECY9.

The isolation of pAI56 and pAI2 showed that although a major proportion of the 9.2kb EcoRI fragment (f 9.2) had been subcloned these was still some more to be isolated. pAI56 is an internal BamHI fragment of f9.2. The aim of this section was to subclone the flanking BamHI-EcoRI fragments such that all of f9.2 was available. Cosmid pEGH344 was digested with EcoRI restriction enzyme in order to isolate f 9.2 by agarose gel electrophoresis (see Fig 4.2). The fragment purified from the gel contains f9.2

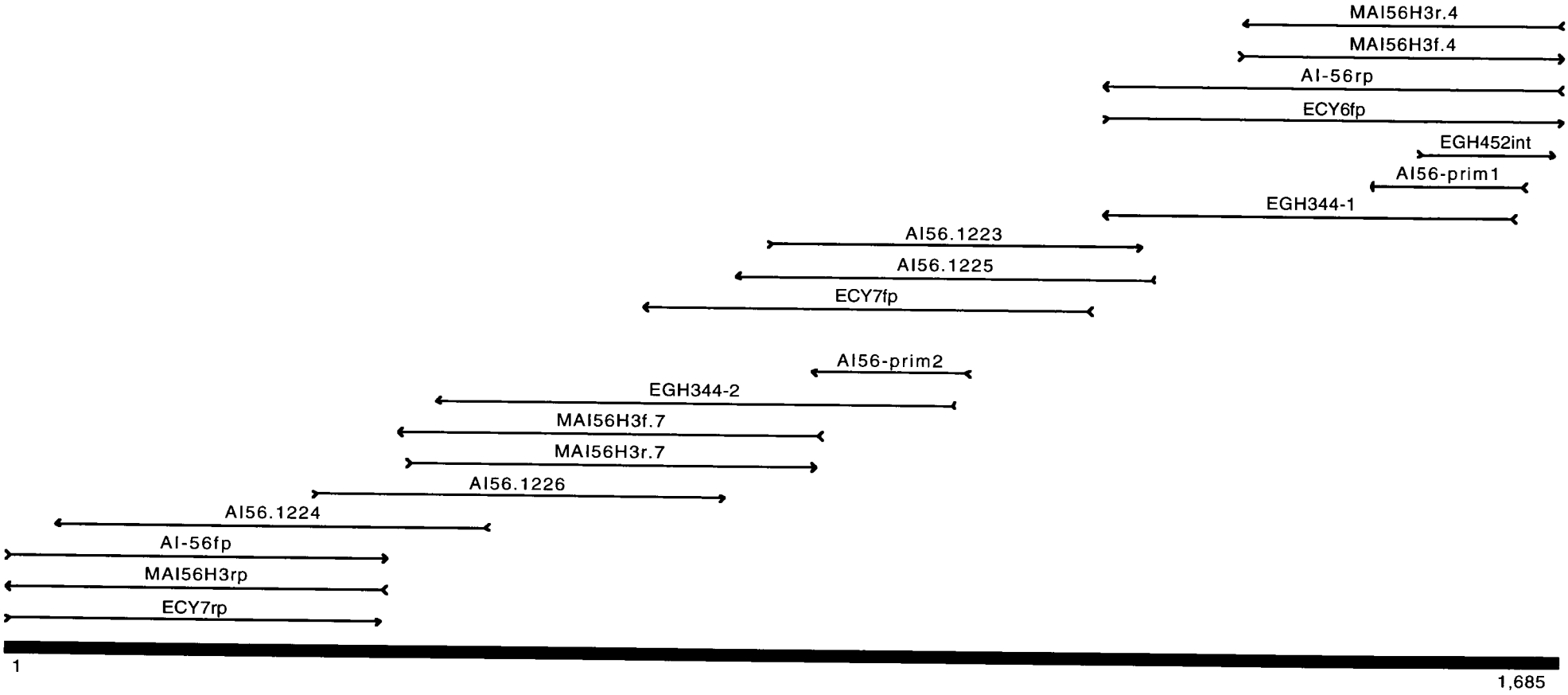

Fig 4.14 Compilation of the sequencing runs from plasmid pAI56 and its subclones.

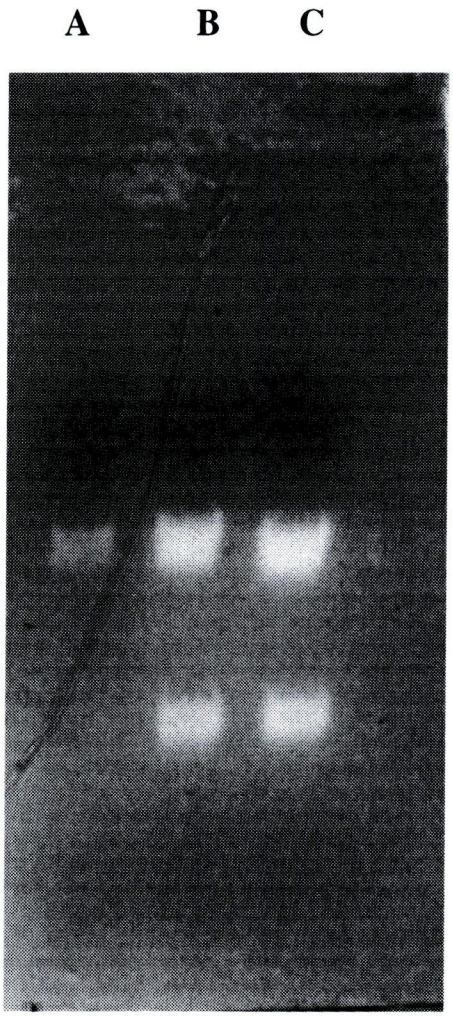

Fig 4.15 . Subcloning of SacI fragments from pAI56.
Lane A. pECY6 digested with SacI.
Lane B. pECY7 digested with SacI.
Lane C. pAI56 digested with SacI.

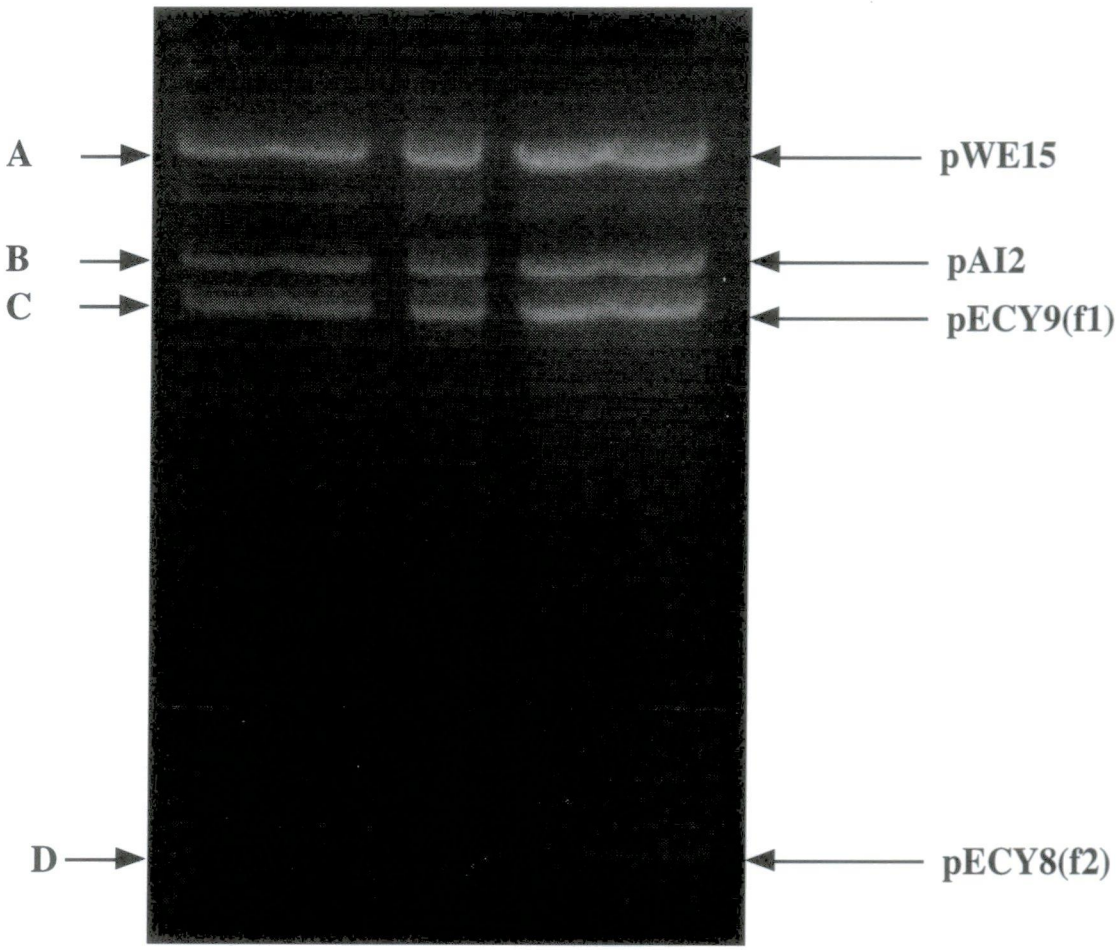

Fig 4.16. Restriction of mixed 9.2kb EcoRI fragment plus vector pWE15 with BamHI.

Band A. pWE15 not cut with BamHI.
Bands B-D. Resulting fragments of f9.2 digestion with BamHI.
Band B. Identical to the BamHI fragment in pAI2.
Band C. BamHI-EcoRI fragment labelled f1, purified and sub-cloned to give pECY9.
Band D. BamHI-EcoRI fragment labelled f2, purified and sub-cloned to give pECY8.

and also pWE15 vector. This largest band was excised, purified and restricted with BamHI. This generates four bands (Fig 4.16). The largest fragment is pWE15 which dose not contain a BamHI site. The second band is identical to the BamHI fragment in pAI2. The third band represents one of the EcoRI-BamHI fragments, named here f1 (Fig 4.17). The fourth and smallest band is the other BamHI-EcoRI fragment, named here f2 (Fig 4.17). f1 and f2 were purified and ligated separated into EcoRI-BamHI cut pUC19 and then transformed into DH5α. White colonies were picked and patched. Crude minipreps were carried out by phenol extraction and the intact plasmid analysed.(Data not shown). This showed that minipreps Nos 2, 4 and 6 from f1 and No 3 from f2 were considered promising. Full 'Wizard' minipreps of these colonies were produced and the DNA restricted with BamHI plus EcoRI. The results in Fig 4.18 show that f1 isolate No 4 has a real insertion, while f2 isolate No 3 also shows a good insertion. These were checked against authentic f1 and f2. The f1 isolate 4 was named pECY9 and the f 2 isolate 3 named pECY8.

pECY9 should contain within it the PstI fragment found in pAI56. PstI digestion of pECY9 and pAI56 shows that they have a common band of 1.2 kb thus confirming the nature of pECY9. pECY8 having only a small insert was completely sequenced on both strands by use of standard forward and reverse primers.

4.3.5 Sequencing of pECY9.

pECY9 DNA was sonicated (2.5.5) and then subjected to agarose gel electrophoresis (Fig 4.19). DNA fragments ranging in size from 1.0 to 1.8 kb were purified and repaired with T4 and Klenow DNA polymerases (2.5.11). The DNA fragments were ligated with SmaI digested pUC19. The ligation mix was transformed into DH5α and plated onto LB agar supplemented with ampicillin and X-gal. Correct subcloned colonies were selected by colony hybridization using the BamHI-EcoRI insert of pECY9 as a probe. Plasmid DNA was purified from positive colonies using "Wizard" miniprep kits. All of the positive colonies were subjected to DNA sequencing using the standard forward and reverse primers. Most of the cloned random fragments overlapped pAI56 (Fig 4.20). However, some extended the pAI56 sequence "rightwards" to overlap that obtained from the "right" (BamHI) end of pECY9. Not all of the pECY9 sequence was obtained, particularly that from the "left" (EcoRI) end. This end of pECY9 is also found in cosmid pEGH452 which had been sequenced by Volckaert. It was thus not characterised further.

4.3.6 Sequencing of pAI2.

pAI2 was a suitable construct for sequencing using nested-deletions. The general strategy for this is outlined in section 4.2.4. The pairs of restriction enzymes that create a 5' overhang or blunt end plus a distal 3' overhanging end are PstI/XbaI and SacI/ EcoRI (Fig 4.21). pAI2 was digested with these pairs of enzymes and subjected to exonuclease

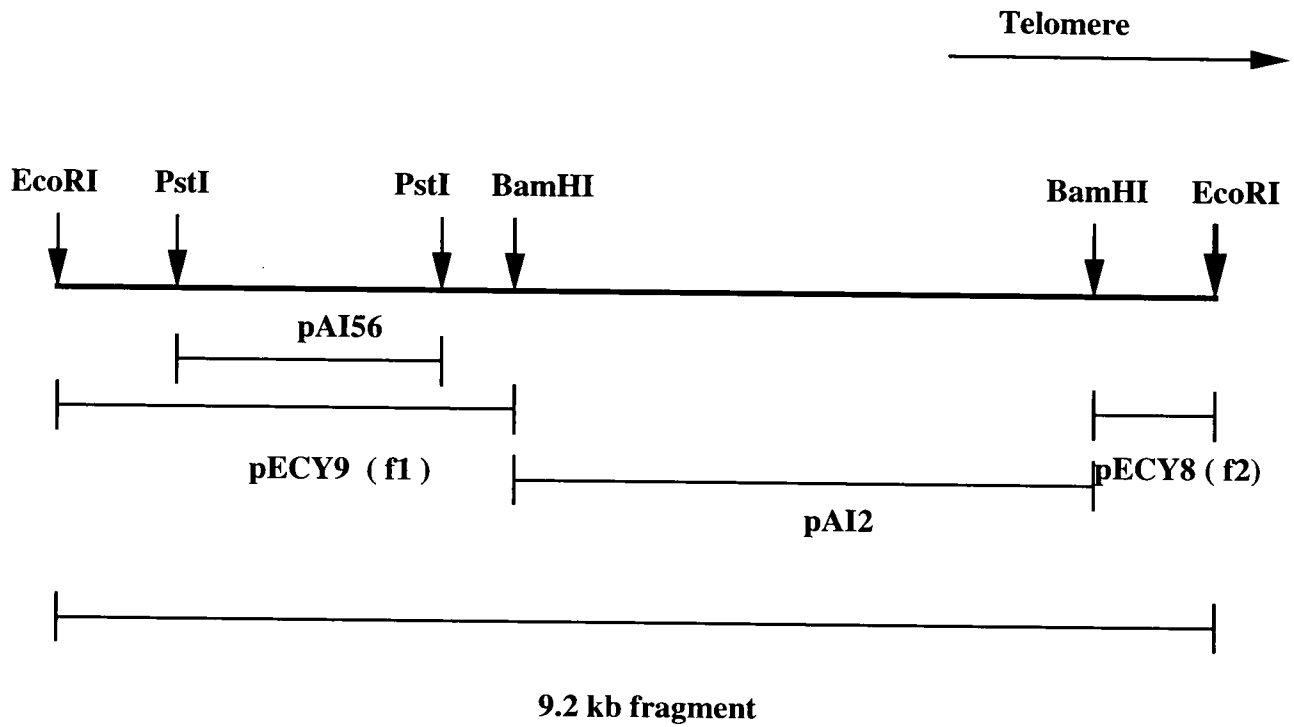

Fig 4.17. Restriction map of the 9.2kb EcoRI fragment showing the positions of the inserts subcloned into pECY9 (f1) and pECY8 (f2).

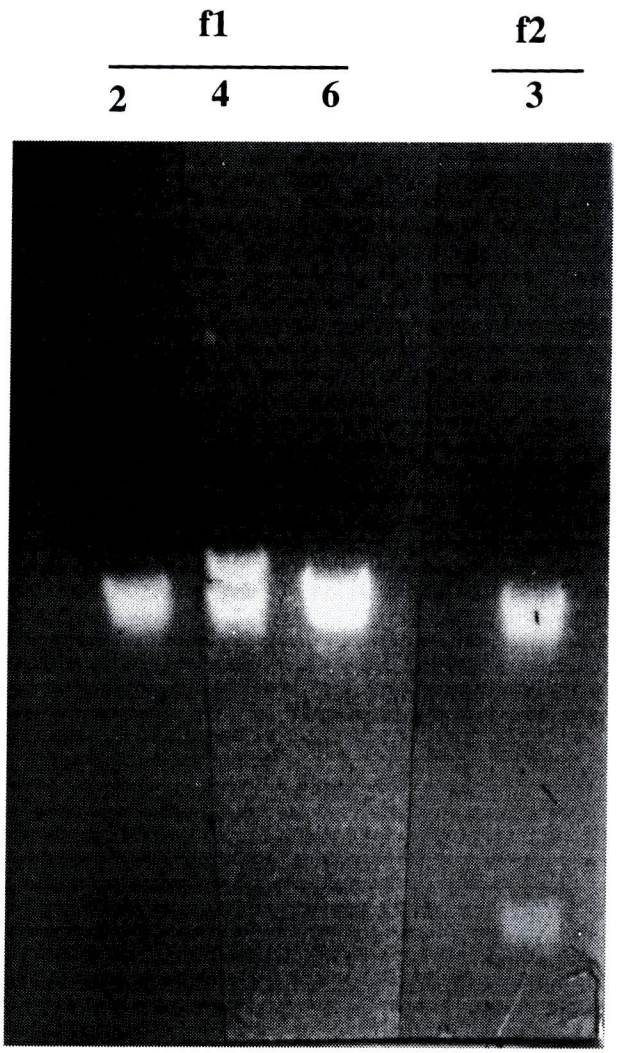

Fig 4.18. Restriction analysis of different f9.2 subclone isolates.

Lanes 2, 4 and 6. Miniprep DNA from isolates 2, 4 and 6 of f1 subclones digested with BamHI and EcoRI.
Lane 3. Miniprep DNA from isolate3 of f2 subclones digested with BamHI and EcoRI.

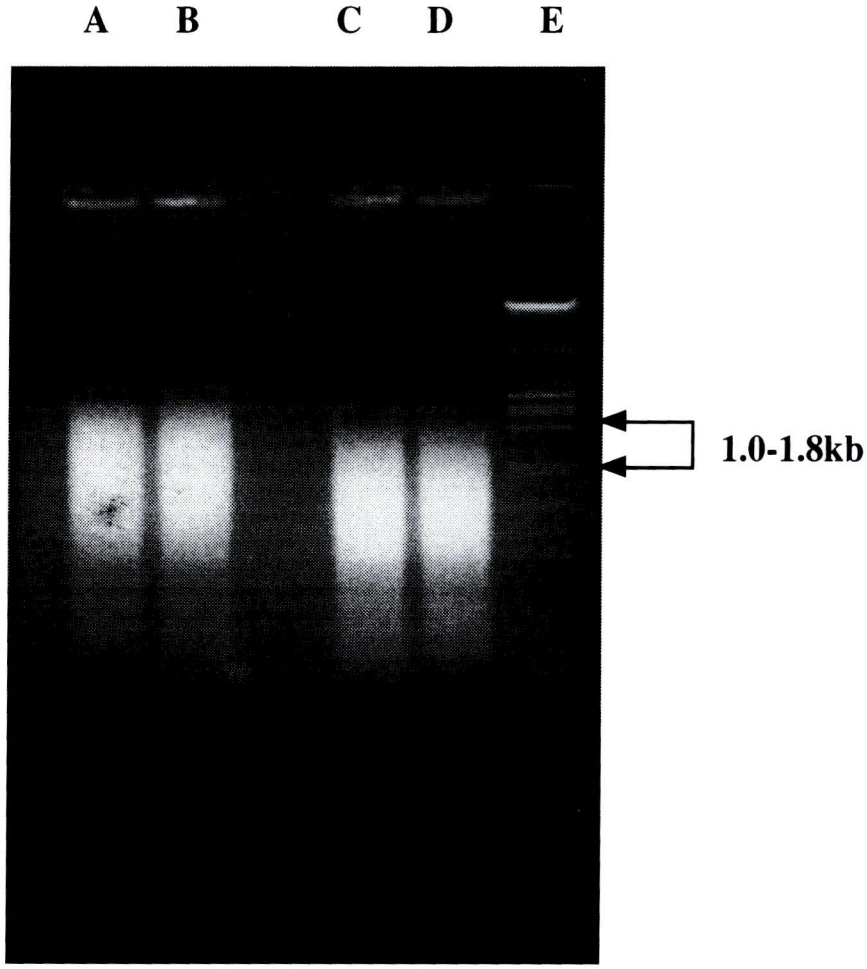

Fig 4.19. Sonication of plasmid pECY9 DNA.
Lanes A-D. Sonicated pECY9.
Lane E. λ PstI size marker.

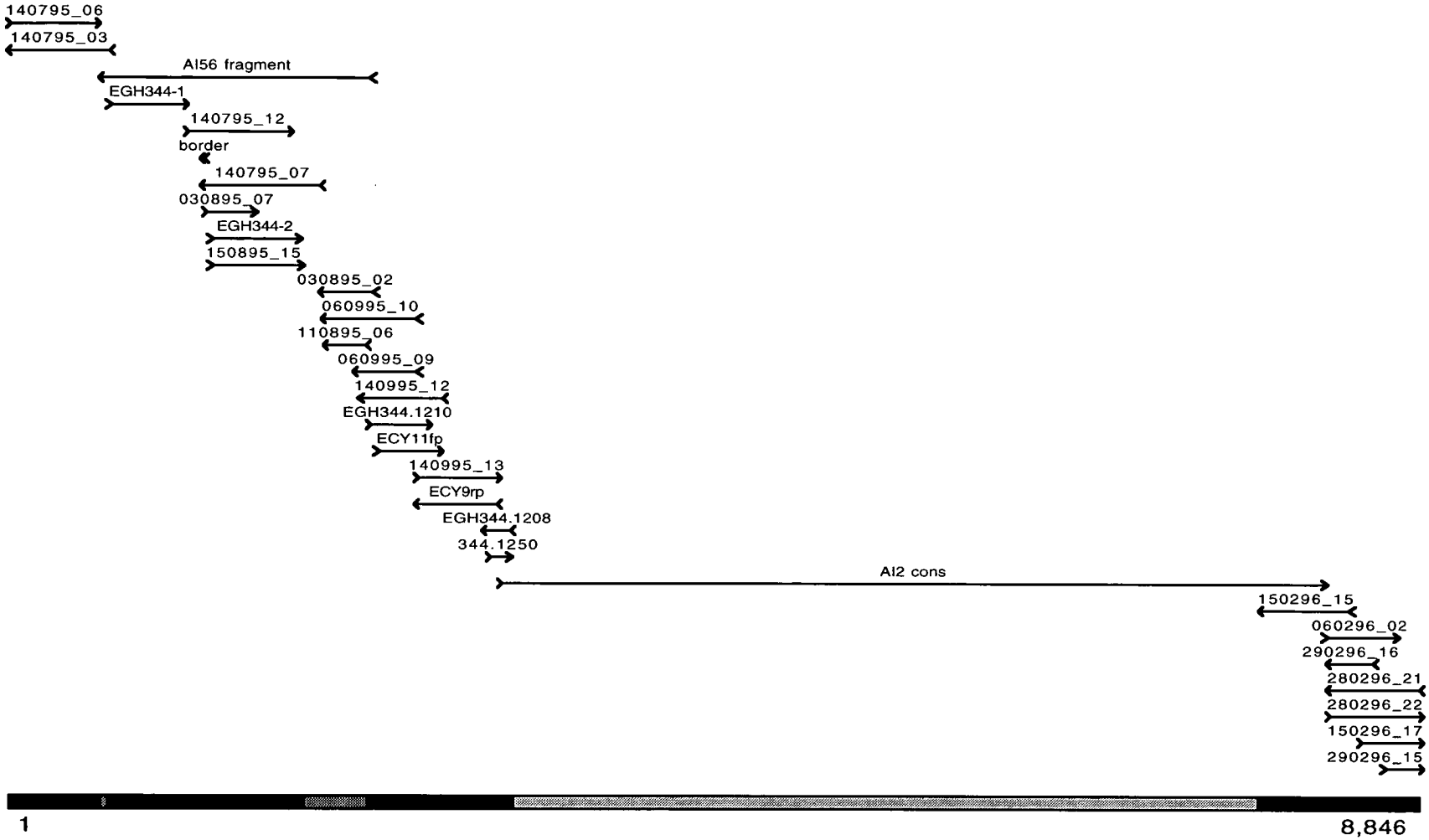

Fig.4.20. The complete contig of the 9.2kb EcoRI fragment, showing the individual runs of pECY9 (to the left) and sequences that extend beyond the right hand end.

Fig 4.21. The restriction sites in pAI2 used in the generation of nested deletions.

III / mung bean nuclease digestion. Timed samples were taken religated and transformed into DH5α. Minipreps were made and intact plasmid DNA sized by electrophoresis on agarose gels (Figs 4.22.A and4.22.B). Suitable sized deletions were sequenced using the appropriate forward or reverse primers.

Assembly of the sequence data showed that nearly all of pAI2 had been sequenced in both directions. However, there were a number of gaps or regions sequenced in only one direction. These were filled in by designing suitable primers based on the available sequence data. The primers were used to sequence from pAI2 as a template. The complete contig is shown in Fig 4.23.

4.3.7 Assembly of fragment 9.2kb sequence.

The sequence of f 9.2 was in three adjacent contigs of the inserts found in pECY9, pAI2 and pECY8. These were joined by designing oligonucleotide primers to sequence part the end points of these contigs using pEGH344 as a template. pECY9 and pAI2 were joined by sequences EGH344.1208 and 344.1250 in Fig 4.20.
pAI2 and pECY8 were joined by sequence EGH344.1209 in Fig 4.23.

4.4 Joining of f9.2 and f4.6.

The restriction map of pEGH344 provided by H. Tettelin showed that f4.6 and f9.2 were adjacent to each other and at the right hand end of cosmid pEGH344. Sequencing of the ends of f4.6 showed that one end was adjacent to the cloning site of the vector pWE15. The left end of f9.2 had been shown to overlap with cosmid pEGH452. Thus the right hand of f9.2 should be adjacent to f4.6. Primers were designed to determine the overlapping sequence using pEGH344 as template. The sequences obtained going leftwards from f4.6 (not shown) did not overlap with f9.2. Likewise the rightwards sequences from f9.2 (fig 4.20) did not overlap with f4.6. A further small fragment to the right of f9.2 had been missed by Tettelin. The right-hand end at this fragment contained the cloning site sequences of vector pWE15. Thus f4.6 and f9.2 are not adjacent but rather the left and right ends respectively of pEGH344. This was confirmed by Guido Volckaert (personal communication) who compared the sequence of f4.6 with his sequence of pEGH452. The two completely overlap.

4.5 Sequence analysis of f4.6 and f9.2.

The complete yeast genome sequence is available from MIPS, Martinreid, Germany via its WWW server (http://speedy.mips.biochem.mpg.de/mips/yeast/index.htmlx)
Potential open reading frames (ORFs) were sought by use of the computer program DNA Strider. f4.6 has a large ORF of 1073 amino acids between bases 293 and 3515 in reading frame 2 of the figure 4.24. Comparison of this ORF with the Gen Bank database shows that is identical to the yeast gene *YOR1*.

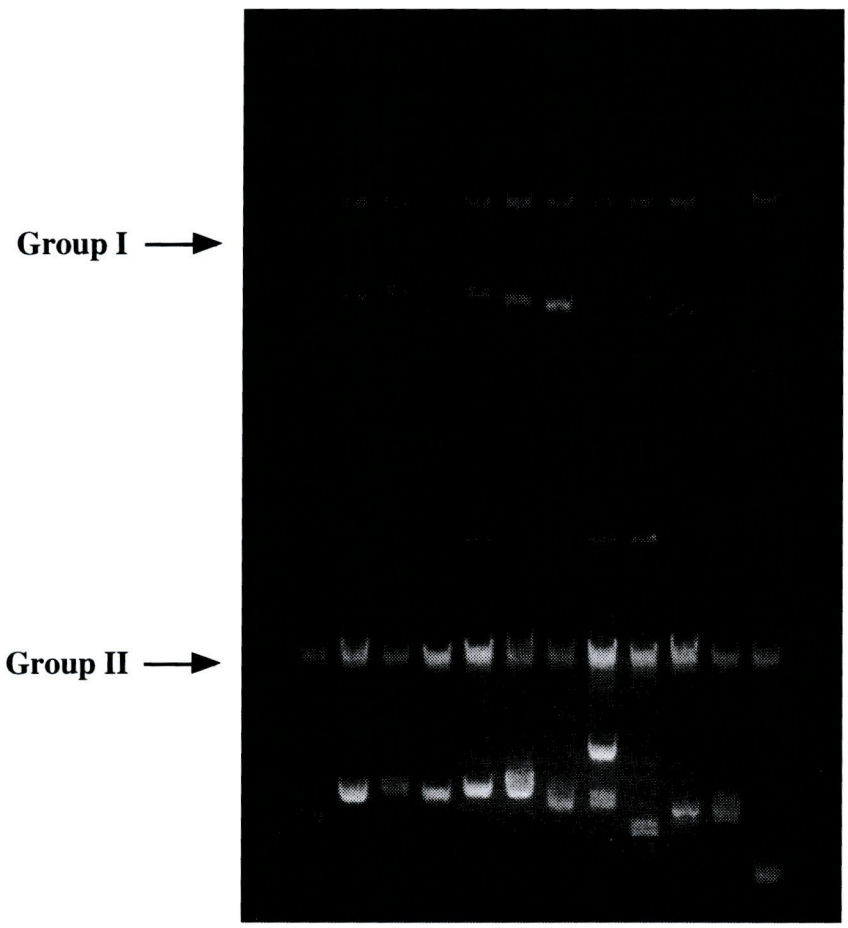

Fig . 4.22A. Analysis of isolates produced by nested deletions of pAI2.

Group 1. Clones produced from site 1 (fig. 4.21)
Group II. Clones produced from site 2 (fig. 4.21)

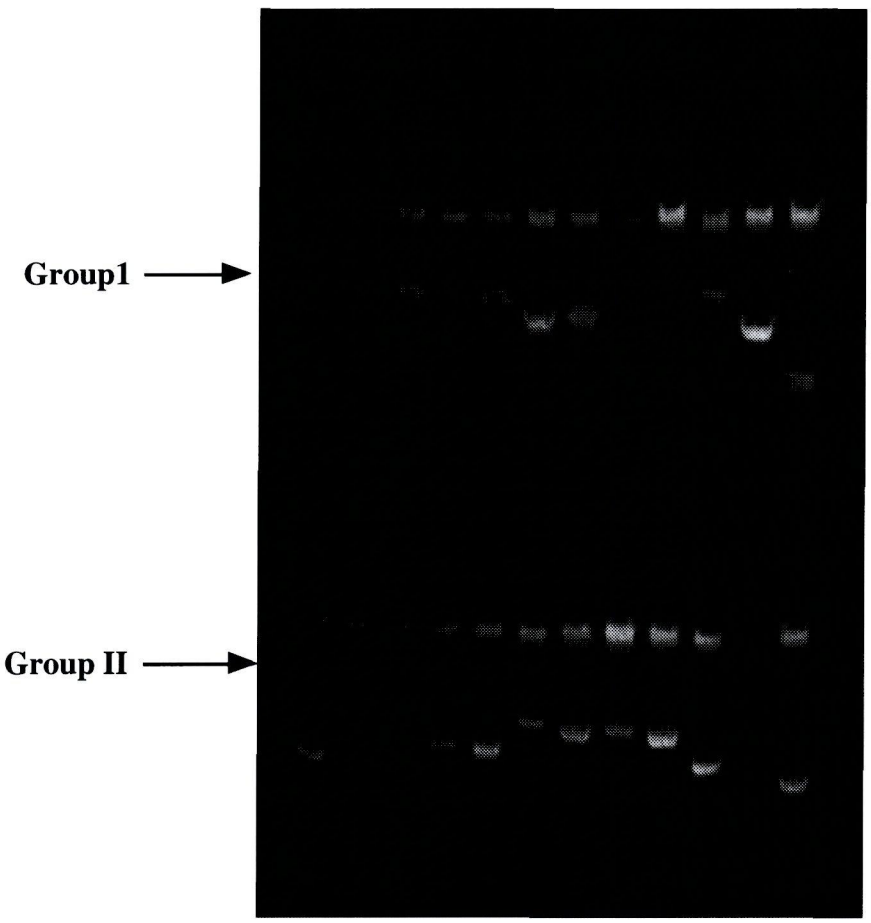

Fig . 4.22B. Analysis of isolates produced by nested deletions of pAI2.

Group 1. Clones produced from site 1 (fig. 4.21)

Group II. Clones produced from site 2 (fig. 4.21)

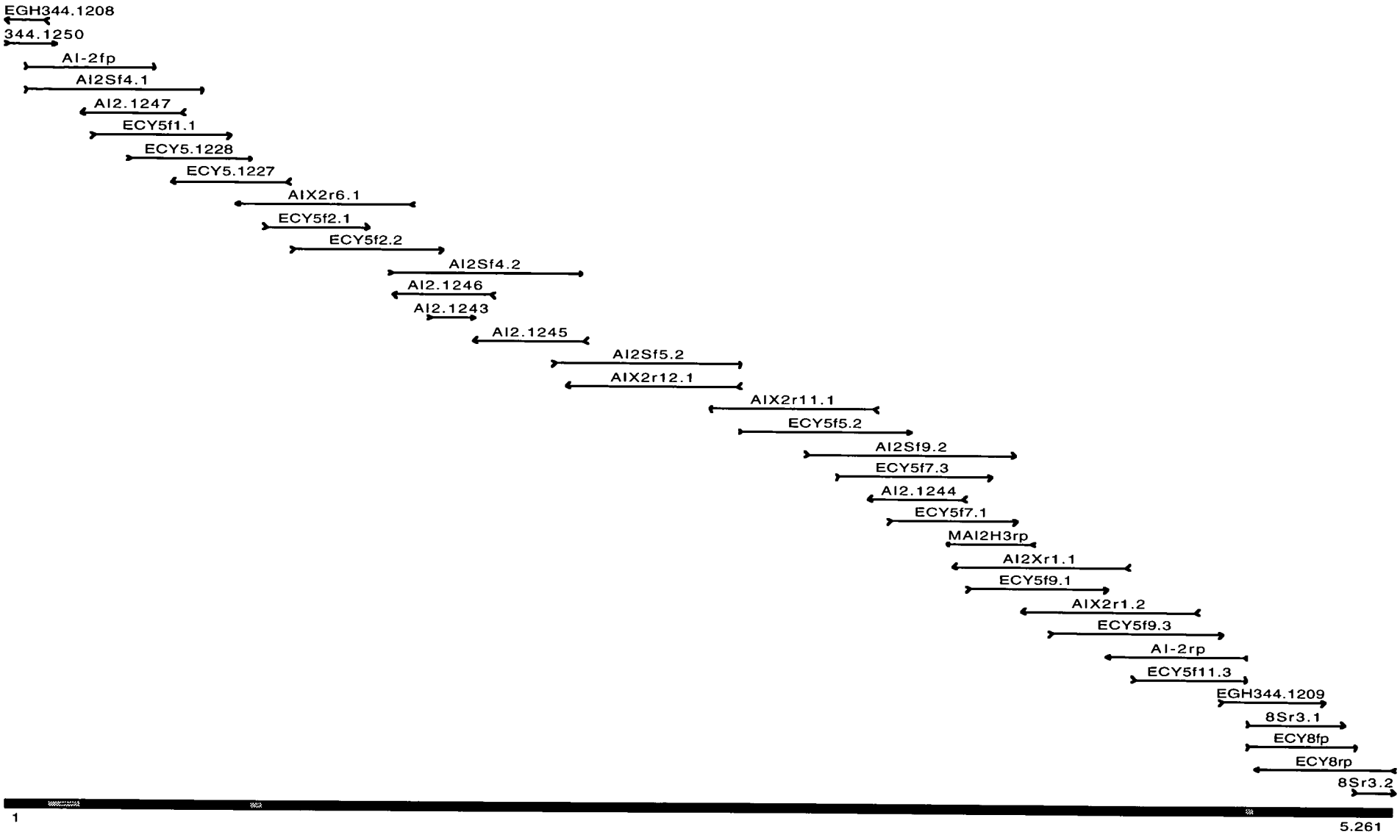

Fig 4.23. The complete contig from sequencing pAI2.

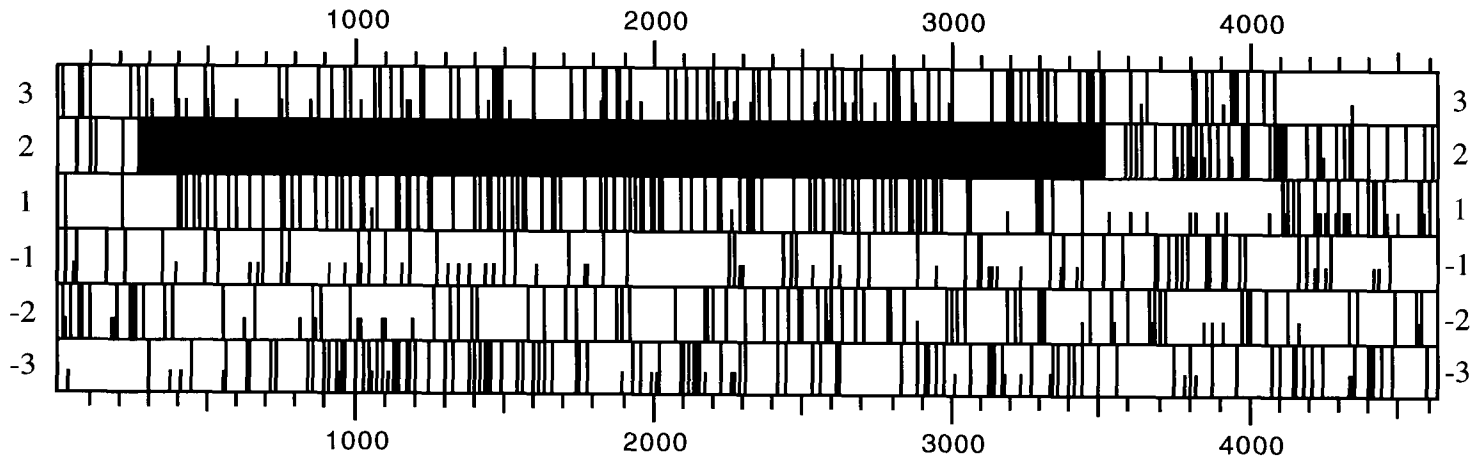

Fig 4.24. Potential open reading frames within f4.6

Analysis of the f9.2 sequence with DNA Strider indicates at least three potential ORFs (Fig 4.25). The first is in reading frame 2 and lies between bases 29 and 66. It encodes a protein of 120 amino acids that shows similarity to the SrplP/ Tiplp proteins. The second, which in this work is called ORF1, is in reading frame -2 and lies between bases 2805 to 1660. It encodes a potential protein of 381 amino acids. The last potential ORF is in reading frame 1 and lies between bases 5281 and 8245 (the end at the sequence). In this work this is called ORF2 and it encodes a potential protein of greater than 988 amino acids. ORF1 and ORF2 are analysed further in the next chapter.

4.6 Discussion.

This chapter describes the sequence determination of two fragments of DNA from the sub-telomeric region of chromosome VII right. The two EcoRI fragments of 4.6kb and 9.2kb were originally determined to be adjacent within the cosmid pEGH344. This was based on two pieces of information. The 4.6kb fragment contains vector sequences at one end. Neither fragment was found in digests of the overlapping cosmid pEGH344 (Tettelin, personal communication). This conclusion was incorrect. f4.6 was not found in pEGH344 EcoRI digests because it is one of the flanking sequences in pEGH344. The lack of flanking sequence in f9.2 is because of the presence of a small EcoRI fragment to the right of f9.2. This fragment was missed in the initial analysis of pEGH344.

DNA sequence determination of small (<10kb) fragments should optimally be obtained by using a nested-deletion strategy. In practice the commercially available kits are unreliable on a number of grounds.

Firstly suitable pairs of restriction sites, one with a 5' or blunt end and the other generating a 3' overhang cut, are not always available. The susceptibility of different restriction cuts to exonuclease III digestion is somewhat variable. The rate of exonuclease III digestion is also difficult to control. When this technique works well, as with its use with f4.6, it is simple and convenient. When it is does not works well as with pAI2, it takes a lot of optimisation. This leads to the conclusion that with small fragments primer-walking is probably the method of choice. This can be made more efficient by producing a number of start points. This is accomplished by sequence determination of a number of sub-clones produced by restriction digests. Primer-walking is expensive and wasteful in oligonucleotide synthesis, however, it is efficient in that there is little redundancy in sequence coverage.

Sequencing of large fragments is best accomplished by a shot-gun approach. The limiting factor is the quality of the library of sub-clones produced. In this work random

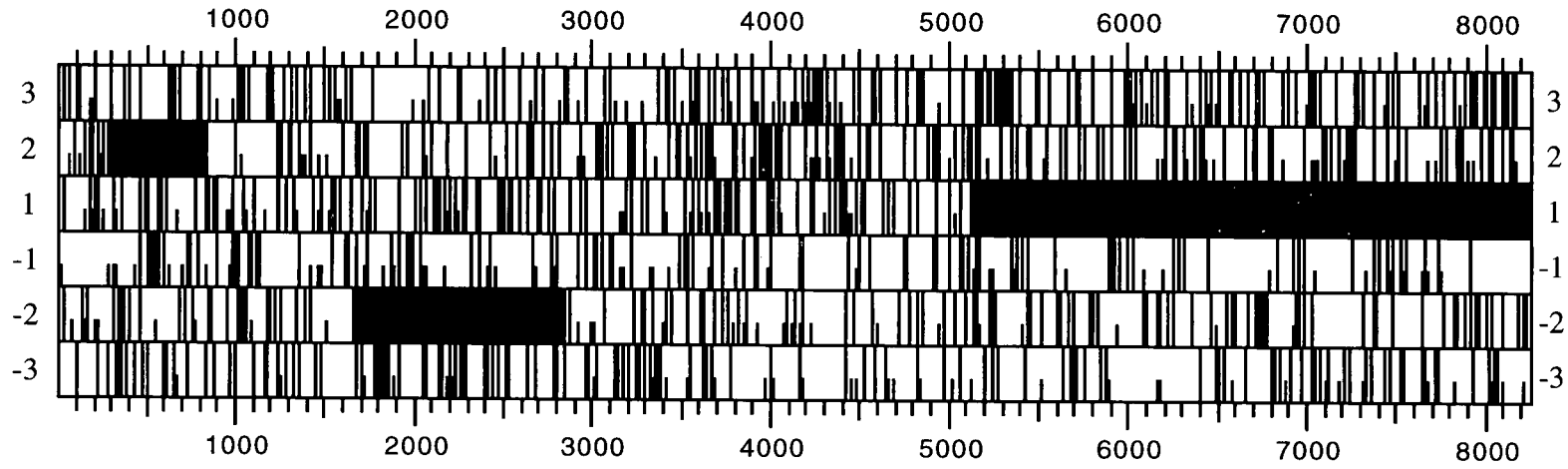

Fig 4.25. Potential open reading frames within f9.2

fragments were produced by sonication. This was successful but is difficult to control. Consequently large quantities of DNA are needed in order to make trial experiments and timed samples. Better control for the production of random fragments can be achieved by using a nebulizer (Pohl and Maier,1995). This produces fragments within a narrow size-range, thus needing less input DNA. After purification of fragments in the desired size range (usually 800-1500bp) ends are repaired and the fragments subcloned. Another problem with shot-gun cloning is contamination with *E.coli* DNA. This is a problem that was encountered in this work. Many of the sub-clones that were produced did not hybridise to yeast DNA. This problem can be alleviated by purification of plasmid DNA through multiple cycles of CsCl/ Ethidium Bromide centrifugation. A newer method uses commercial enzymes that degrade linear (contamination) DNA leaving intact pure plasmid. This methodology is now used by all major DNA sequencing laboratories engaged in genome research.

A 100kb BAC (bacterial artificial chromosome) can be characterised by sequencing in one direction only 1800 clones with 800bp inserts. This can be accomplished using one automatic sequencer in a matter of two months (T. Pohl, personnel communication).

The *YORI* gene was identified during the sequencing of cosmid pEGH452. It was shown by computer searching of databases to have homology to ATP-binding cassette (ABC) transporter proteins. Disruption of the gene results in sensitivity to oligomycin although the cells are viable (Katzmann et al, 1995). *YORI* is a member of a large family of proteins with similar properties. It is functionally most related to the yeast Snq2p. This protein is found in the plasma membrane. Disruption of the gene results in sensitivity to phenanthroline, staurosporin and fluorphenazine (Servos et al 1993; Decottignies et al,1995). Yorlp is structurally most related to mammalian MrpI with 33% identity and ycflp with 32% identity. It shows 28% identity to the cystic fibrosis transmembrane conductance regulation (CTFR) protein, (Yeast Protein Database). YorIp is believed to be a plasma membrane protein and is predicted to have a potential trans-membrane spanning domains.

ORF YG2294W encodes a protein named Pau2p in the Swiss-Prot database. Pau2p is a member of the serine-rich protein superfamily which has 23 members in yeast. All of these proteins are stress regulated. Typical of the family is Tirlp which is found in the plasma membrane and has 8 serine-rich tandem repeats of 12 amino acids each (Marguet et al,1988). Expression of *TIRl* is induced by glucose, cold-shock and anaerobiosis (Donzeau et al,1996). Pau2p is a member of this gene family but lacks the serine-rich motifs. It is thus another of the sub-family of seripauperins, serine-poor members of the serine-rich family. Expression of *PAU2* is not found under starvation and stress conditions (Viswanathan et at,1994).

CHAPTER 5

FUNCTIONAL ANALYSIS

5.1 Introduction.

The systematic sequencing of the *Saccharomyces cerevisiae* genome has revealed a number of Open Reading Frames (ORFs). ORFs are defined as a potential coding sequence for a gene and contain a stretch of at least 100 amino acids without any interrupting termination codon . These sequences are preceded by a potential promoter and a start codon. The analysis of the complete nucleotide sequence of the right sub-telomeric end of chromosome VII by DNA Strider™ revealed 3 potential open reading frames . ORF1 is 1142bp in length and found between position 1700 and 2900 in the sequence shown in Fig 5.1. This sequence comprises most of the 9.2kb EcoRI fragment and sequences extending from here to the right end of the cosmid pEGH344 insert. ORF2 is greater than 4625bp in length and starts at position 5200 and extends beyond the end of the determined sequence.

The aim of this chapter is to begin a functional analysis of ORF1 and ORF2 by gene disruption.

5.2. Strategy for disruption of ORF1.

5.2.1. Overall strategy.

The overall strategy for the disruption is shown in Fig 5.2. 5' and 3' flanking sequences of ORF1 are amplified by PCR and cloned. The PCR primers incorporate suitable restriction enzymes to facilitate subsequent manipulations. The 5' flanking sequence has a 5' PstI site and a 3' BamHI site. The 3' flanking sequence has a 5' BamHI site and a 3' EcoRI site. These two PCR products are joined together to create a PstI-EcoRI fragment with a central BamHI site. Into this site the *LEU2* selectable marker is cloned. This creates the disruption cassette. The entire cassette is isolated by PCR amplification and then transformed into diploid wild-type yeast.

5.2.2. Amplification of The 5' flanking region.

Two primers were designed to amplifying the 5' flanking region of ORF1. The 5' primers corresponds to nucleotides at position 670 to 687 upstream the initation codon shown in Fig 5.3. The 3' primer incorporates a BamHI site and extends from positions 995 to 979 upstream from the initiation codon. Use of these primers generates a

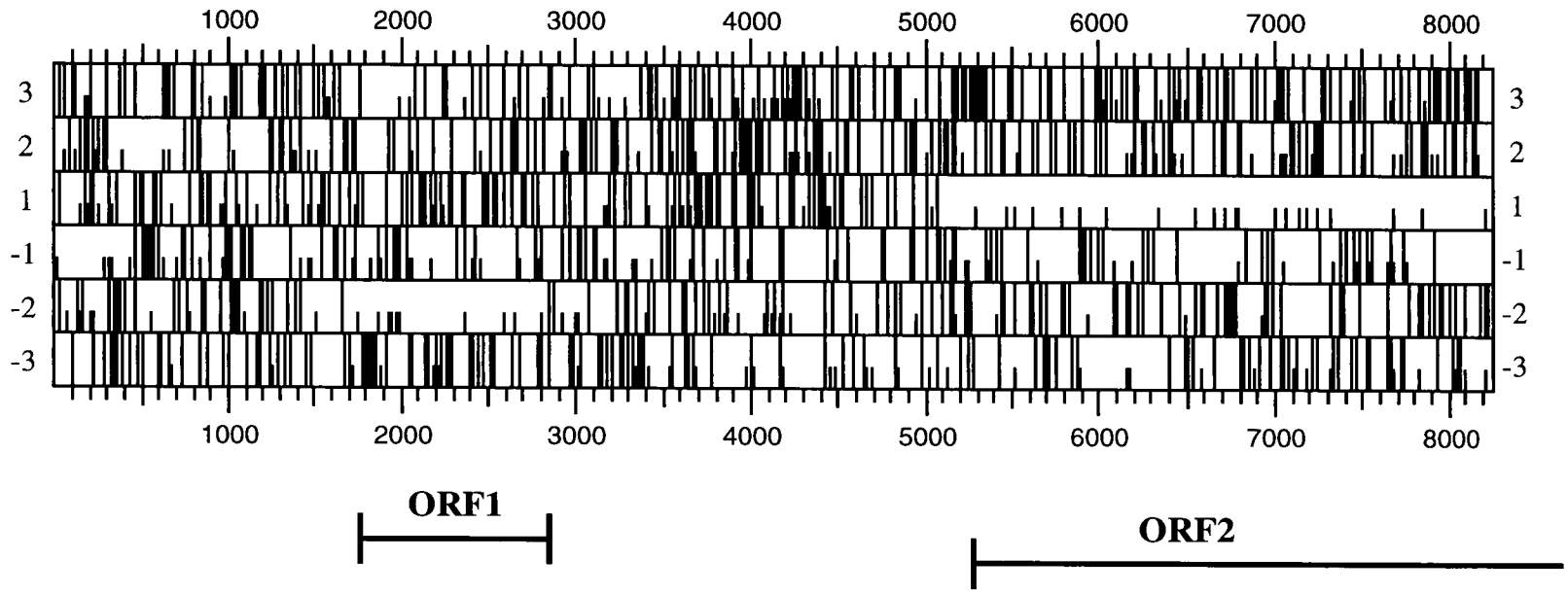

Fig 5.1. Translation of all six reading frames of the 9.2kb EcoRI fragment.
The positions of ORF1 in reading frame 1 and ORF2 in reading frame -2 are indicated.

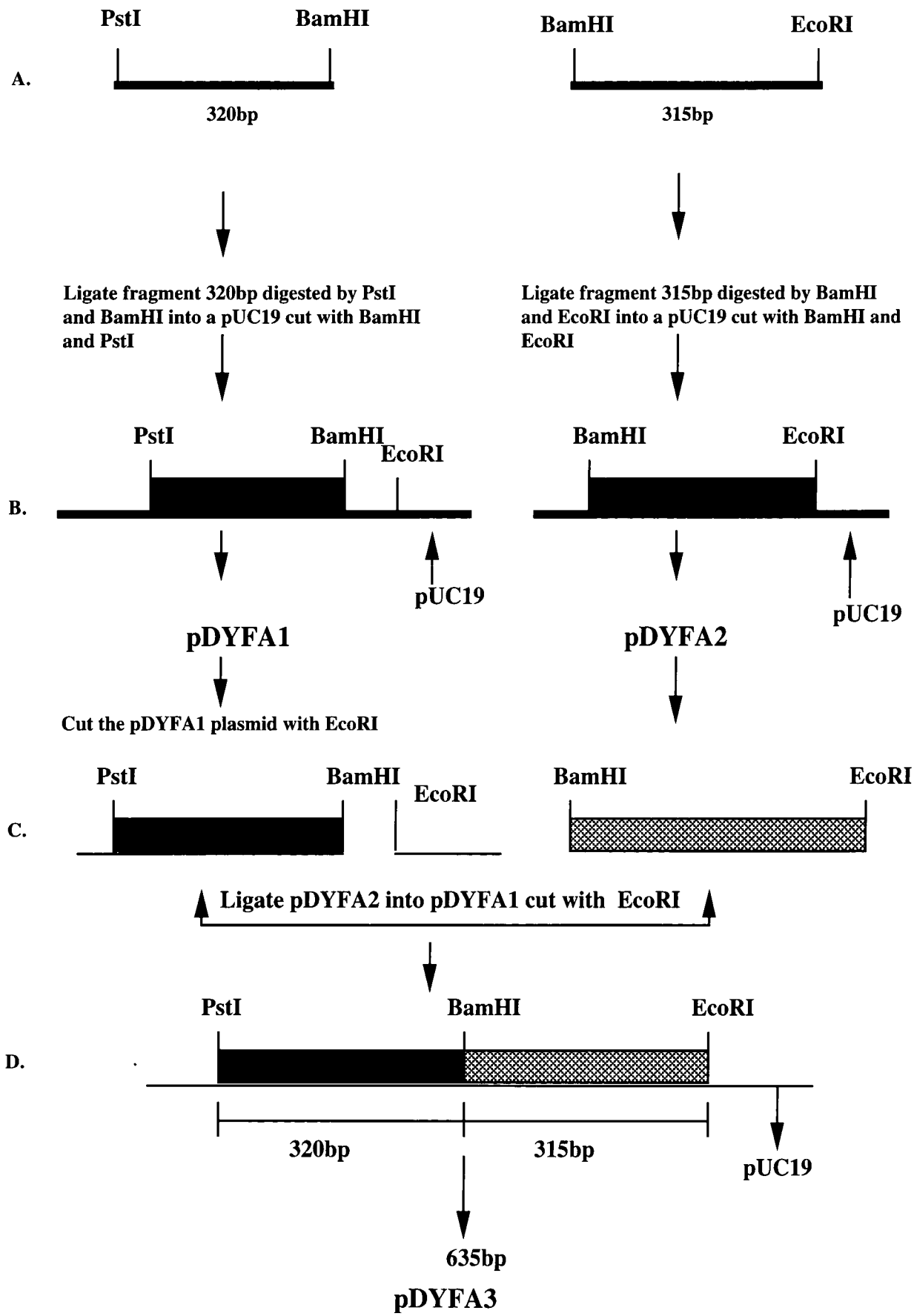

Fig 5.2. Strategy for the disruption of ORF1 (continued on next page)

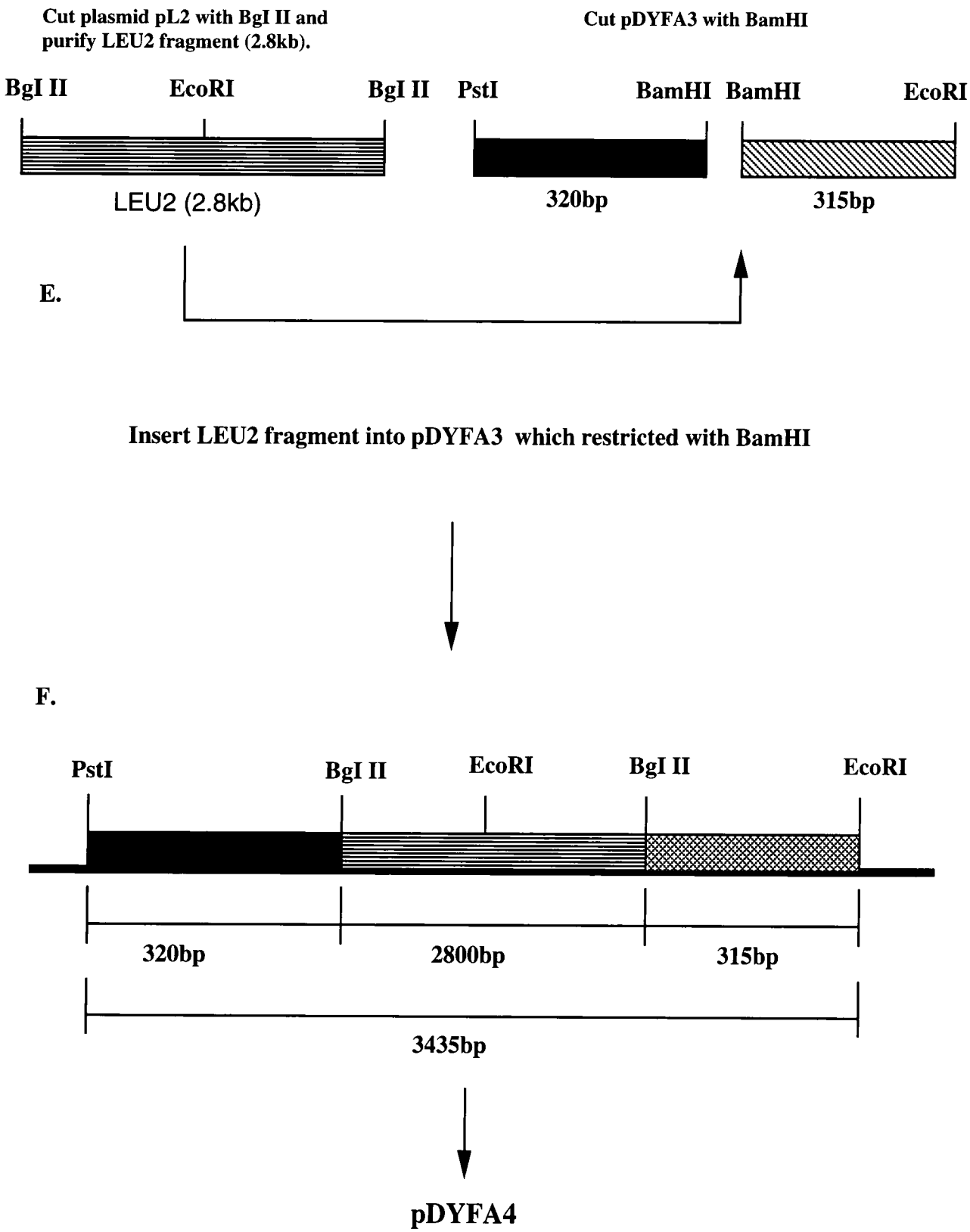

Fig 5.2 (continued). Strategy for the disruption of ORF1

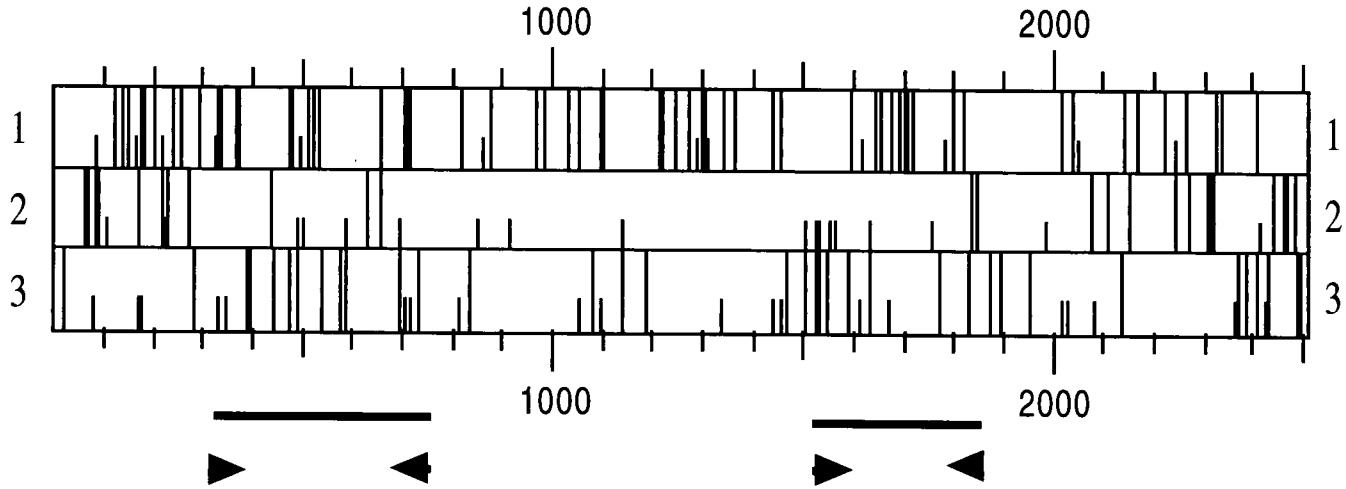

Fig 5.3 ORF1 showing the 5' and 3' flanking sequences amplified by PCR.

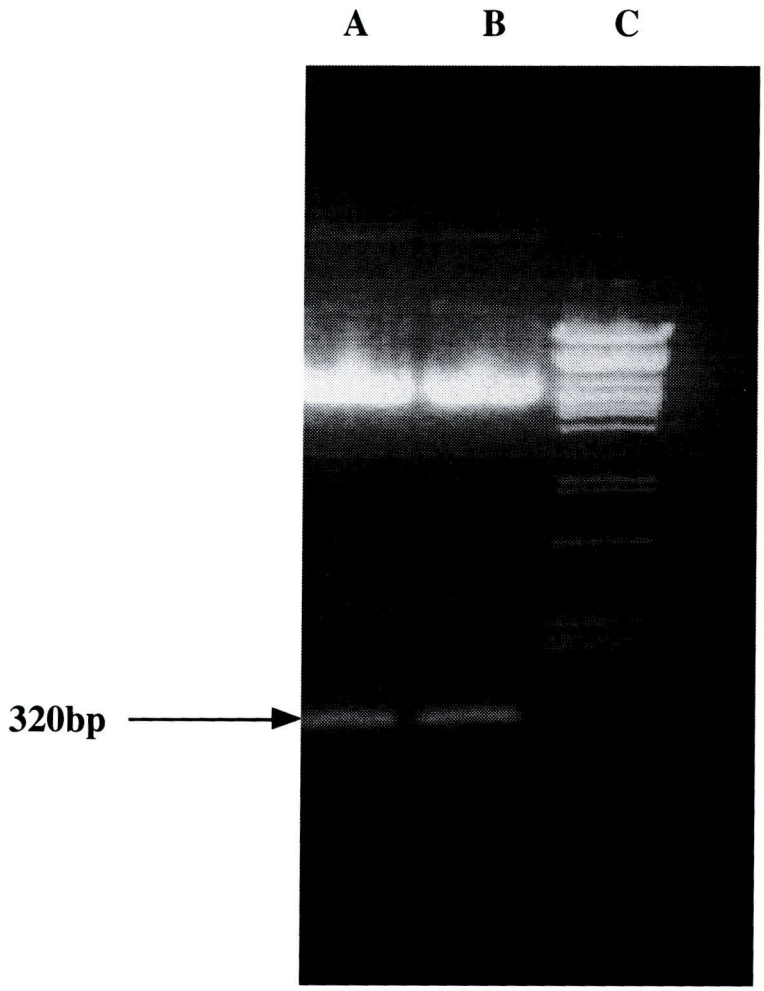

Fig 5.4. Cloning of the ORF1 5' flanking region in pDYFA1.
Lanes A and B show pDYFA1 digested with BamHI plus PstI. Lane C.λ PstI size marker.
This liberates the 320 bp flanking sequence.

fragment of 320bp in length. The primers are shown below. The BamHI site in the 3' primer is underlined. Included in the PCR product adjacent to the 5' end is a naturally occurring PstI site.

5'Primer No 1391 GGACTCCTCACTGCAGGA

3'Primer No 1390 AAAGGGATCCATGACGAGAGATTTCCGG.

The 5' flanking region was amplified from pECY9 as a template using the following conditions. 2 minutes at 94°C initial denaturation. Then 30 cycles of 2 minutes at 94°C, 2 minutes at 55°C, 2.5 minutes at 72°C. Then a final elongation step of 5 minutes at 72°C. Amplification the PCR product was restricted with BamHI and PstI. After agarose gel electrophoresis the fragment was excised, purified and ligated with BamHI-PstI cut pUC19 vector, DH5α cells were transformed with the ligation mixture. The transformed cells were plated onto L- agar plus ampicillin and X-gal. A few white colonies were picked and used to inoculate 10 ml LB broth plus ampicillin cultures. After incubation at 37°C overnight with continuous shaking, minipreps were carried out in order to isolate the plasmid DNA. This was then mixed with BamHI and PstI, incubated for 3-4 hours at 37°C and then mixed with loading dye and analysed by 1.5% agarose electrophoresis (Fig 5.4). The results have the correct 320bp BamHI-PstI fragment. This plasmid was named pDYFA1.

5.2.3 Amplification of the 3' flanking region.

The strategy for the amplification of the 3' region was essentially the same as for the 5' flanking region. Two primers were designed that allowed amplification of a 315bp fragment. The 5' primers (No 1389) starts at a position 1445-1463bp from the termination codon of ORF1. This is close to a naturally occurring BamHI site that will be included in the amplification product. The 3' primer (No 1388) incorporates an EcoRI restriction site. It starts from a position 1757-1740bp from the termination codon. The sequences of the primers are shown below. The EcoRI site in the 3' primer is underlined.

5'Primer No 1389 TCATGAGGAATCCGAACTTG.

3'Primer No 1388 AAGGAATTCGTCAAACAGCTCGAATCCC.

The PCR conditions were identical to that in section 5.2.2 for the amplification of the 5' flanking region, except that pEGH344 was used as a template.

After the amplification of pEGH344. the PCR product was exposed to restriction by

BamHI and EcoRI in order to isolate the 315bp fragment. The BamHI-EcoRI fragment was excised, purified and ligated with BamHI-EcoRI cut pUC19 vector. DH5α cells were transformed with the ligation mixture and plated onto L-agar plus ampicillin and X-gal. A few white colonies were formed, picked and used to inoculate 10ml LB broth plus ampicillin cultures. After incubation at 37°C minipreps were carried out in order to isolate the plasmid DNA. Samples from each minipreps were digested with BamHI and EcoRI, incubated for 3 hours at 37°C and then mixed with loading dye and analysed by 1.5% agarose gel electrophoresis (Fig 5.5). All plasmids contained the correct insert. One of these was retained and named pDYFA2.

5.2.4 Joining of the 5' and 3' flanking regions.

Plasmid pDYFA1, the 5' flanking PstI-BamHI fragment, was digested with BamHI and EcoRI. The linearised fragment was electrophoresed on an agarose gel, excised and purified. The BamHI and EcoRI sites are adjacent to each other and form part of multiple cloning plasmid pDYFA2, the 3' flanking BamHI-EcoRI fragment, was cut with these enzymes and the insert purified after agarose gel electrophoresis. The linearised pDYFA1 and the 315bp insert from pDYFA2 were ligated together, transformed into DH5α and plated onto L-agar plus ampicillin. Five colonies were purified and plasmid minipreps carried out. Digestion of the plasmid DNA with PstI plus EcoRI resulted in the generation of a 635bp fragment. All five colonies contained plasmid with this pattern (Fig 5.6). This is the predicted result of joining the inserts of pDYFA1 and pDYFA2. This new plasmid is named pDYFA3.

5.2.5 Construction of the Disruption Cassette.

The selectable marker for use in making the gene disruptions is *LEU2*. This available on a plasmid pL2 (Fig 5.7). This plasmid carries the yeast *LEU2* gene flanked by pairs of unique restriction sites within the plasmid pUC12 (Raymond and Stevens, personal communication).

Plasmid pDYFA3 was linearised with BamHI. Plasmid pL2 was cut with BgI II and electrophoresed on a agarose gel (Fig 5.8). This liberates a 2.8kb fragment carrying the *LEU2* gene. This fragment was excised from the gel and purified. The linearised pDYFA3 and the *LEU2* fragment were ligated together then transformed into *E. coli* JA221. The transformed mixture was plated onto M9 minimal media lacking leucine. JA221 is a *leuB* auxotroph which can be complemented by the yeast *LEU2* gene. Colonies were purified and plasmid minipreps made. The plasmid DNA was restricted with PstI plus EcoRI (Fig 5.9). This should generate three bands on an agarose gel. the vector and two insert fragments as *LEU2* has a single EcoRI site within it (see Fig 5.7).

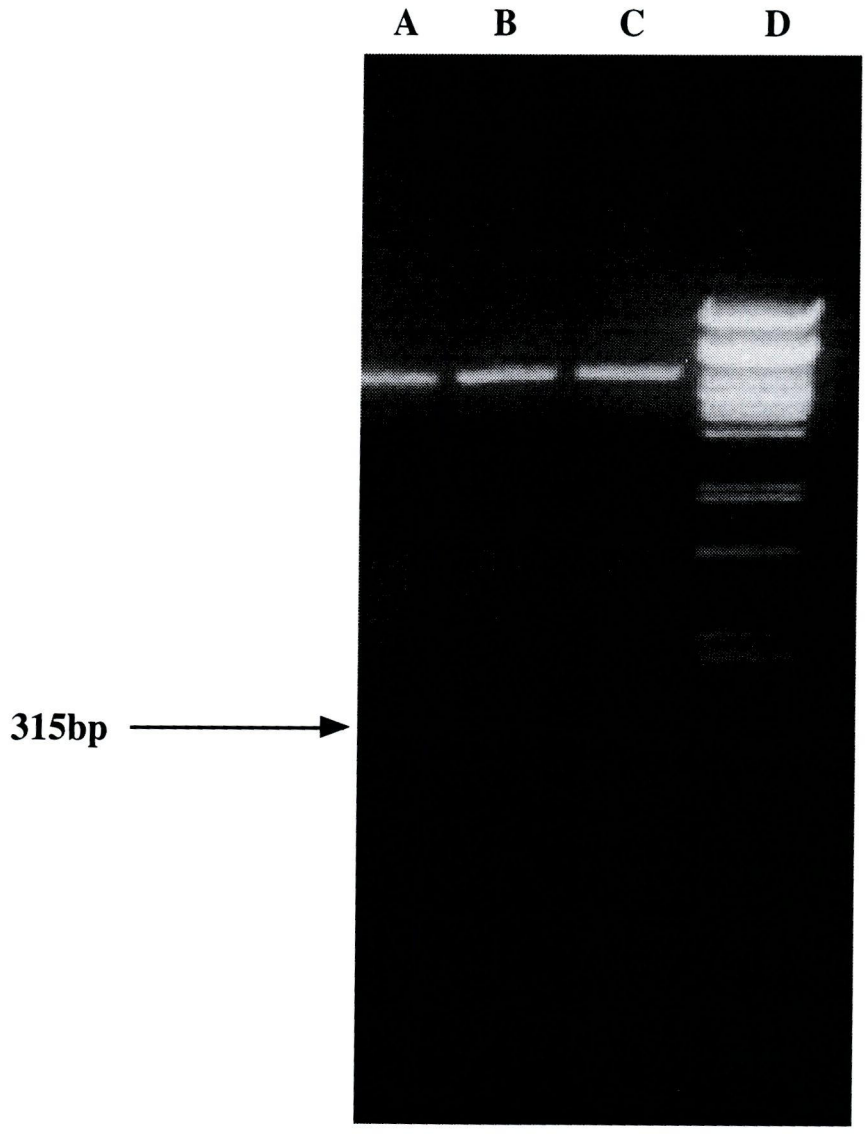

Fig 5.5. Cloning of the ORF1 3' flanking region in pDYFA2. Lanes A, B and C show pDYFA2 digested with BamHI plus EcoRI. This liberates the 315bp flanking sequence. Lane D. λ PstI size marker.

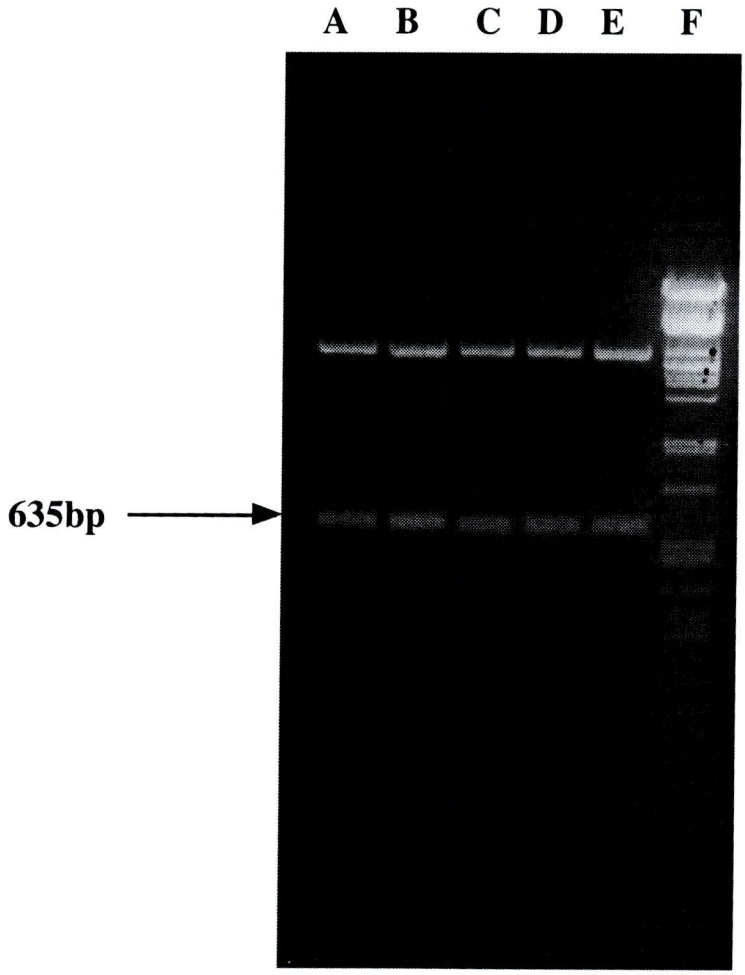

Fig 5.6. Restriction analysis of pDYFA3.

Lanes A to E. pDYFA3 digested with EcoRI plus PstI. This liberates the 635bp combined 5' and 3' flanking sequences. Lane F. λ PstI size markers.

PLASMID pL2

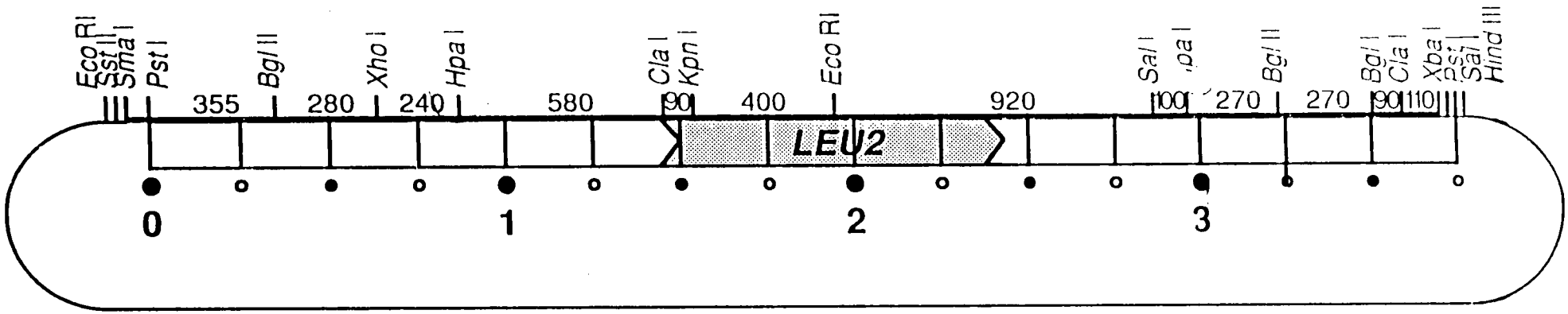

(pUC12)

Fig. 5.7 Restriction map of pL2

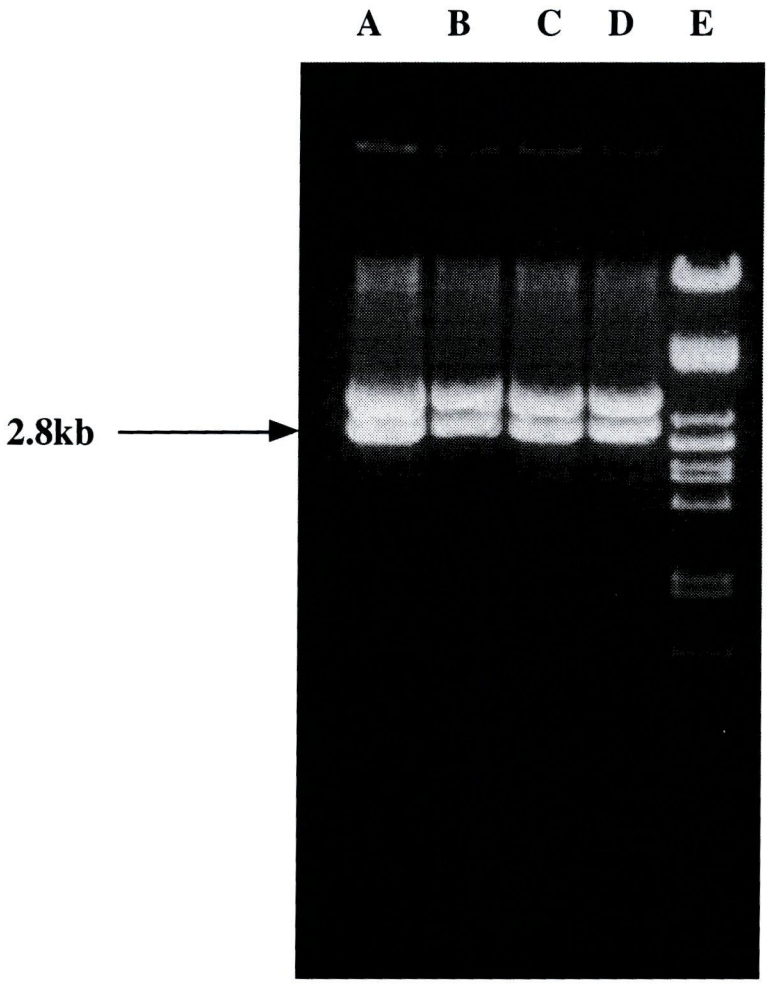

Fig 5.8. Isolation of the *LEU2* fragment.
Lanes A to D show pL2 digested with BglII.
Lane E. λ PstI size marker.